Forschungszentrum Jülich

IBG-2: Plant Sciences

Nutrient remediation from wastewater by Algal Turf Scrubber (ATS) and evaluation of ATS biomass as fertilizer

Dissertation

zur Erlangung des Grades

Doktorin der Agrarwissenschaften (Dr. agr.)

der Landwirtschaftlichen Fakultät

der Rheinischen Friedrich-Wilhelms-Universität Bonn

von

Xinyu Gan

aus

Henan, China

Bonn, 2024

Referent: Prof. Dr. Wulf Amelung

Korreferent: Prof. Dr. Uwe Rascher

Tag der mündlichen Prüfung: 27.09.2024

Angefertigt mit Genehmigung der Landwirtschaftlichen Fakultät der Rheinischen

Friedrich-Wilhelms-Universität Bonn

Abstract

The increasing discharge of nutrient-rich wastewater into natural water bodies poses a severe environmental challenge, demanding innovative and cost-effective solutions for efficient nutrient removal and recovery. This study first aims to validate the hypothesis that the Algal Turf Scrubber (ATS) system, an advanced algal biofilm reactor, can effectively remove and recover nutrients from wastewater under diverse environmental conditions. Rigorous evaluations were conducted, including laboratory-scale tests varying total inorganic carbon, nitrogen-to-phosphorous (N:P) ratio, and light intensity (Chapter 3), and continuous operation of technical-scale ATS systems in a greenhouse, analyzing their nutrient removal and recovery under different temperature and light conditions (Chapter 4). Mathematical modeling elucidated the system's responses. The findings reveal that the ATS system exhibits rapid and effective removal of phosphorus and nitrogen from wastewaters while simultaneously generating nutrient-rich biomass. Furthermore, the ATS system demonstrates robust performance across a wide range of temperature and light intensity conditions. Notably, the ATS system offers a cost advantage, with the biomass production cost being only 18% of that associated with conventional tubular photobioreactors. Overall, the results demonstrate the cost-effectiveness and versatility of ATS system as a technology for efficient nutrient removal and recovery from wastewaters, making it suitable for various regions.

To test the hypothesis that the ATS system provides a viable pathway for recovering nutrients from wastewater and ultimately promote plant growth, we used biomass harvested from the ATS system as an organic phosphorus fertilizer in subsequent greenhouse pot experiments to evaluate its effectiveness on plant performance and phosphorus uptake by wheat (Chapter 5). The results indicate that phosphorus derived from algal biofilms is as accessible in similar rate as from mineral fertilizer, highlighting the potential of algal biofilms as organic nutrient sources for wheat cultivation.

In summary, ATS systems emerge as potent tools for achieving efficient nutrient removal and recovery in various environments. In addition, the harvested biomass holds promise as a robust organic fertilizer, thus reinforcing advocacy for sustainable agricultural practices and marking a significant advance in environmentally friendly wastewater management practices.

Zusammenfassung

Die zunehmende Einleitung von nährstoffreichen Abwässern in natürliche Gewässer stellt eine große Herausforderung für die Umwelt dar und erfordert innovative und kostengünstige Lösungen für eine effiziente Nährstoffentfernung und -rückgewinnung. Diese Studie zielt zunächst darauf ab, die Hypothese zu validieren, dass das Algal Turf Scrubber (ATS)-System, ein fortschrittlicher Algen-Biofilmreaktor, unter verschiedenen Umweltbedingungen effektiv Nährstoffe aus dem Abwasser entfernen und zurückgewinnen kann. Es wurden strenge Bewertungen durchgeführt, darunter Tests im Labormaßstab, bei denen der gesamte anorganische Kohlenstoff, das Stickstoff-Phosphor-Verhältnis (N:P) und die Lichtintensität variiert wurden (Kapitel 3), sowie der Dauerbetrieb von ATS-Systemen im technischen Maßstab in einem Gewächshaus, bei dem die Nährstoffentfernung und -rückgewinnung unter verschiedenen Temperatur- und Lichtbedingungen analysiert wurde (Kapitel 4). Durch mathematische Modellierung wurden die Reaktionen des Systems erläutert. Die Ergebnisse zeigen, dass das ATS-System schnell und effektiv Phosphor und Stickstoff aus dem Abwasser entfernt und gleichzeitig nährstoffreiche Biomasse erzeugt. Darüber hinaus zeigt das ATS-System eine robuste Leistung in einem breiten Spektrum von Temperatur- und Lichtintensitätsbedingungen. Vor allem bietet das ATS-System einen Kostenvorteil: Die Kosten für die Biomasseproduktion betragen nur 18 % der Kosten, die bei herkömmlichen röhrenförmigen Photobioreaktoren anfallen. Insgesamt zeigen die Ergebnisse die Kosteneffizienz und Vielseitigkeit des ATS-Systems als Technologie zur effizienten Nährstoffentfernung und -rückgewinnung aus Abwässern, wodurch es für verschiedene Regionen geeignet ist.

Um die Hypothese zu testen, dass das ATS-System einen gangbaren Weg zur Rückgewinnung von Nährstoffen aus dem Abwasser bietet und letztlich das Pflanzenwachstum fördert, haben wir die aus dem ATS-System geerntete Biomasse als organischen Phosphordünger in anschließenden Gewächshaustopfversuchen verwendet, um ihre Wirksamkeit auf die Pflanzenleistung und die Phosphoraufnahme durch Weizen zu bewerten (Kapitel 5). Die Ergebnisse zeigen, dass Phosphor aus Algenbiofilmen in ähnlichem Maße zugänglich ist wie aus Mineraldünger, was das Potenzial von Algenbiofilmen als organische Nährstoffquellen für den Weizenanbau unterstreicht.

Zusammenfassend lässt sich sagen, dass sich ATS-Systeme als wirksame Instrumente für eine effiziente Nährstoffentfernung und -rückgewinnung in verschiedenen Umgebungen erweisen. Darüber hinaus ist die geerntete Biomasse ein vielversprechender, robuster organischer Dünger, der die Befürwortung nachhaltiger landwirtschaftlicher Praktiken stärkt und einen bedeutenden Fortschritt in der umweltfreundlichen Abwasserentsorgung darstellt.

Graphical abstract

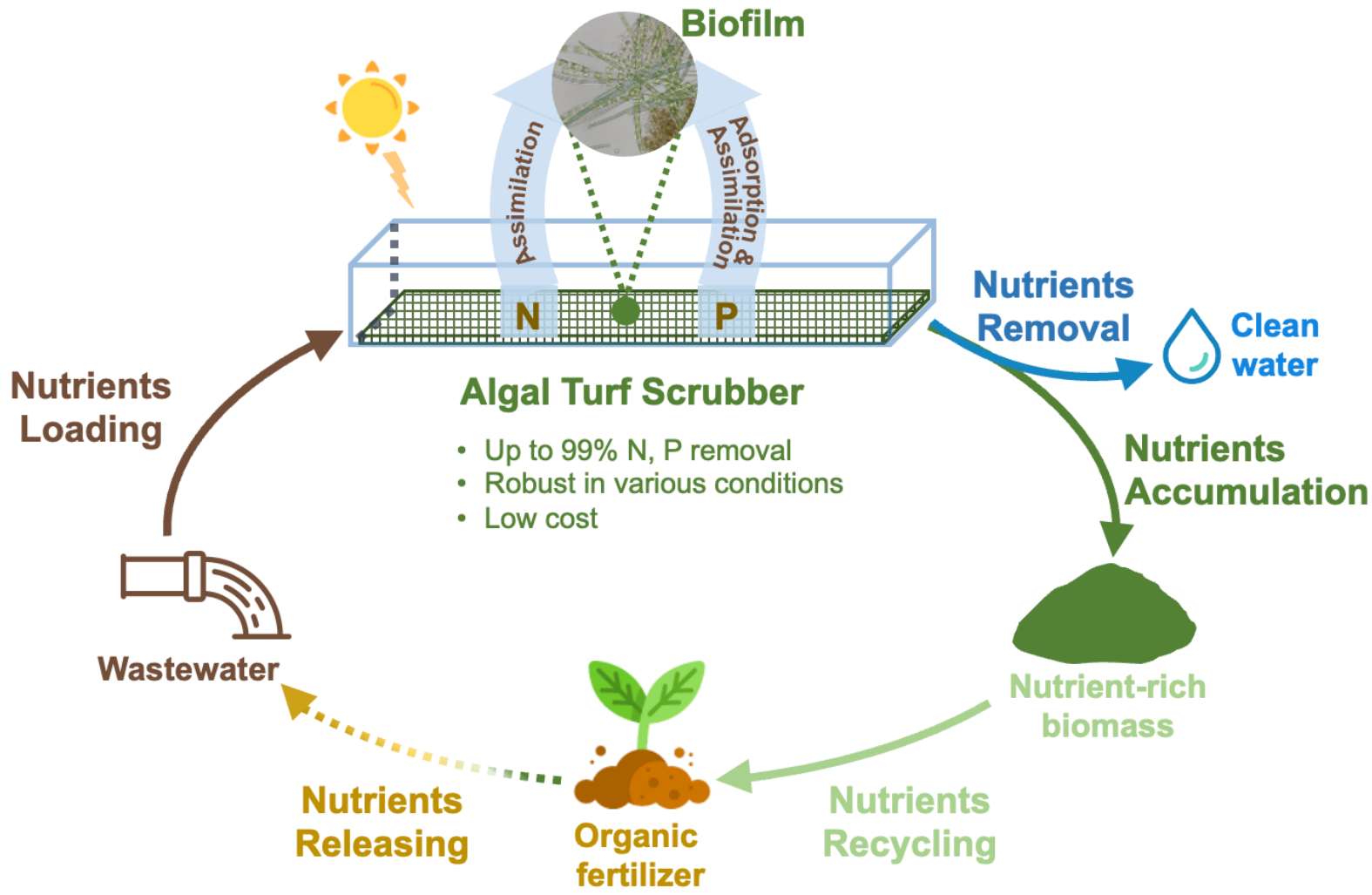

Table of Contents

List of Figures

List of Tables

List of Abbreviations

a.P.	Adequate precision
ABF	Algal biofilms
AIC	Akaike's Information Criteria
AMF	Arbuscular mycorrhizal fungi
ANOVA	Analyses of variance
ATS	Algal Turf Scrubber
BBD	Box-Behnken design
BIC	Bayesian Information Criterion
CapEx	Capital cost
CAZymes	Carbohydrate-active enzymes
CV	Coefficient of variation
DHA	Docosahexaenoic acid
DO	Dissolved oxygen
DOE	Design of Experiment
DW	Dry weight
EPA	Eicosapentaenoic acid
EPS	Extracellular substances
HRAP	High rate algal pond
OpEx	Operating cost
P	Phosphorus
PBs	Photobioreactors
PDW	Plant dry weight
PER	Percentage prediction error
PI	Prediction interval
P_i	Inorganic phosphorus
P_o	Organic phosphorus
PUFA	Polyunsaturated fatty acids
RDW	Root dry weight
RMSE	Root Mean Squared Error
RSM	Response Surface Methodology

SD	Standard deviation
SDW	Shoot dry weight
SE	Standard error
TIC	Total inorganic carbon
TN	Total nitrogen
TP	Total phosphorus
TSP	Triple super phosphate
WW	Wastewater
WWTP	Wastewater treatment plant

1 Background and aims of the study

1.1 Background

Rapid population growth and human actions release more wastewater into natural water bodies. This has caused serious environmental issue a called eutrophication, which harms ecosystems and results in economic losses (Daud et al. 2015, Pittman et al. 2011). To address this, effective wastewater treatment is needed to remove excess nutrients before they enter aquatic environments. However, traditional wastewater treatment plants (WWTPs) have their drawbacks, including high energy use, large sludge production, and limited nutrient recovery (Chae and Kang 2013, Plappally 2012, Wan et al. 2016).

Algae-based wastewater treatment has emerged as a promising alternative due to its remarkable nutrient removal efficiency, coupled with a modest land footprint (Chae and Kang 2013, Plappally 2012, Wan et al. 2016). Besides nutrient uptake and accumulation via photosynthesis, algae exhibit remarkable efficiency in the removal of pollutants through non-metabolic mechanisms like ion exchange, complexation, chelation, and precipitation (Su et al. 2011, Xu et al. 2014). In addition, photosynthesis significantly aids comprehensive remediation by raising pH above 9 and increasing dissolved oxygen (Nurdogan and Oswald 1995, Sañudo-Wilhelmy et al. 2004). This synergistic effect leads to the precipitation of phosphorus and the disinfection of treated water, enhancing the overall remediation capacity of these algae. Furthermore, algae possess an impressive capacity for photosynthesis, allowing them to capture atmospheric CO_2 and convert solar energy into valuable storage compounds like lipids, carbohydrates, and proteins (Li et al. 2008, Stiefvatter et al. 2022, Wang et al. 2015). These compounds serve as versatile feedstock for biofuel and animal feed production, showcasing algae's diverse applications in wastewater treatment. Additionally, when cultivated in wastewater, algae can efficiently absorb and concentrate nutrients within their biomass, potentially offering an eco-friendly fertilizer solution (Adey et al. 2013, Coppens et al. 2016a, Walter et al. 2008).

Within the realm of algal wastewater treatment, various system configurations have been explored to explore the potential of light, nutrients, and pollutants across diverse wastewater sources. However, optimizing these systems for maximum efficiency and versatility remains a crucial challenge. Algal wastewater treatment systems mainly fall into three major categories based on the immobilization state of the algae: suspended, immobilized, and attached systems

(Mohsenpour et al. 2021, Wang et al. 2018a). Suspended systems are common but face challenges in biomass harvesting, which contributes significantly to production costs (Posadas et al. 2015, Uduman et al. 2010). Immobilized systems are less common due to stability and production time issues (Mallick 2002, Wang et al. 2018a). Attached algal systems, such as Algal Turf Scrubber (ATS), offer a solution with easier biomass harvesting and have been used for decades in various pollution remediation applications. ATS relies on algal biofilms submerged in wastewater and is subject to operational and environmental variables such as CO_2 concentration, nutrient levels, pH, water flow rate, temperature, and light (Adey et al. 2013, D'Aiuto et al. 2015, Higgins 2011, Mulbry et al. 2008, Ray et al. 2015, Walter et al. 2008). Understanding the relationships between these factors and ATS performance is critical for optimizing nutrient removal.

Previous studies have often focused on individual variables affecting ATS performance, but industrial-scale systems require the consideration and simultaneous optimization of multiple variables and their interactive effects. Water temperature and light intensity are particularly crucial, making it essential to comprehend their interplay in ATS systems.

Furthermore, excessive mineral fertilizer use in agriculture can contribute to nutrient pollution. Algal biomass has been proposed as a slow-release fertilizer, but the release rate, efficiency of algal biofilms, and the potential for combining algae with mycorrhizal fungi as a phosphorus fertilizer remain areas requiring further investigation.

1.2 Thesis Objectives

The main objective of this PhD thesis is to establish a viable pathway for the recovery of nutrients from wastewater, traversing through the algae treatment system (ATS), and culminating in the enhancement of plant growth. This research is divided into two core aspects: the first focuses on the removal and recovery of nutrients from wastewater, while the second revolves around the use of ATS biomass as an effective fertilizer, thus facilitating the cycling of nutrients from the ATS biomass to the soil and ultimately to the plants. Specific research questions are:

- : How can the efficiency of nutrient removal in ATS systems be improved?
- : What are the independent and interdependent effects of water temperature and light intensity on biomass composition, nutrient removal, and recovery in ATS systems?
- : What is the potential of algae biomass, including nutrient release rates and the use of mycorrhizal fungi, as a sustainable fertilizer to mitigate excessive mineral fertilizer use in agriculture?

In order to address the above questions, the following work-tasks were addressed.

1. Optimizing nutrient removal and biomass production of the Algal Turf Scrubber (ATS) under variable cultivation conditions by using Response Surface Methodology (Chapter 3)

A simple low-cost ATS system was used to test it nutrient remediation efficiency under three cultivation variables—total inorganic carbon, nitrogen-to-phosphorous (N:P) ratio, and light intensity. The total nitrogen and total phosphorus removal rate were monitored. The biomass productivity and the processes of N and P accumulation into biomass were observed. All above data were analyzed via response surface methodology (RSM) to offer novel insights into system optimization.

2. Stable year-round nutrients removal and recovery from wastewater by technical-scale Algal Turf Scrubber (Chapter 4)

Three technical-scale ATS systems were continuously operated in a greenhouse over one year to evaluate the nutrient removal and recovery ability. The independent and interdependent effects of water temperature and light intensity on dependent variables, such as

nutrient removal and recovery, and biomass productivity were identified via mathematical modelling. The economic potential of ATS system were based on the calculation of the capital and annual operating costs.

3. Synergistic effects of arbuscular mycorrhizal fungi and Sebacina vermifera on wheat growth and phosphorus uptake from algal biofilms produced on municipal wastewater effluent (Chapter 5)

Wheat plants were fertilized with P provided either by ATS biomass or by mineral fertilizer, and inoculated with mycorrhiza and *Sebacina vermifera*, in single and dual inoculations. Comprehensive analyses encompass plant performance parameters, mycorrhization status, and P-uptake assessments conducted within a controlled greenhouse environment.

These research endeavors collectively contribute to advancing our understanding of ATS-based nutrient recovery and its implications for sustainable wastewater treatment and nutrient recycling.

2 General introduction

2.1 Water pollution

2.1.1 Current status

The rapid growth of human population and activities has contributed to the generation of significant amounts of wastewater from urban, agricultural and industrial sources. This has led to the release of nutrients such as nitrogen and phosphorus into natural water bodies, resulting in harmful algal blooms, eutrophication, and dead zones, which have negative environmental and economic impacts (Cai et al. 2013, Conley et al. 2009, Daud et al. 2015, Dodds and Smith 2016, Pittman et al. 2011, Qin 2009). It's essential to treat wastewater properly to eliminate excessive nutrients before it's released into water bodies. However, the nutrient recovery rates for nitrogen and phosphorus are only 35.8% and 35.7% (2.05×10^5 and 2.94×10^4 t a^{-1}) for municipal wastewater in China, respectively (Li et al. 2019c, Sun et al. 2016). These low recovery rates underscore the urgent need to enhance nutrient recovery in wastewater treatment.

2.1.2 Wastewater treatment plant (WWTP)

Water treatment is a vital process that involves converting contaminated wastewater into clean water that is safe for release into the environment. This is accomplished by eliminating contaminants such as organic matter, heavy metals, and pathogens as well as controlling levels of nutrients like nitrogen and phosphorus to meet the legal requirements (Grady Jr et al. 2011, Gray 2004). In Germany, public wastewater treatment plants process around 9.4 billion cubic meters of wastewater every year from households, businesses, and industry (BMUV). The process involves three stages of purification: *primary*, *secondary*, and *tertiary*, which are explained shortly below.

- In the primary stage, floating and settable materials in the raw wastewater are mainly settled and removed by physical processes, sometimes with the support of chemical precipitation. (Tchobanoglus et al. 2003). Wastewater still contains high levels of organic carbon, nutrients and other pollutants after primary treatment, which requires further treatment.
- In the secondary stage, organic matters are decomposed into carbon dioxide by making use of the bacteria in it. This stage results in the removal of about 90% of

the organic matter (EPA 2004). The biological treatments used in the secondary stage are mainly divided into three different systems (Naidoo and Olaniran 2014). Following secondary treatment, the effluent should flow to a second clarifier to remove any remaining bacteria by settling before being discharged.

- ✓ First is waste stabilization ponds, where the bacteria responsible for decomposing waste remain within the pond, such as in anaerobic ponds, facultative ponds, and polishing ponds.
- ✓ Second is suspended growth systems, where the bacteria are suspended in the wastewater under aerobic conditions, including activated sludge, batch reactor, and aerated lagoons.
- ✓ Third is fixed film systems, where the bacteria grow on the certain surface. Conventional biofilters, rotating biological contactors, and biological aerated filters are the three major types of fixed film systems.

- In the tertiary or advanced stages, specific nutrients or pollutants will be eliminated by additional purification processes such as filtration, carbon adsorption, chemical precipitation, biological phosphorus removal, autotrophic nitrification and heterotrophic denitrification, and distillation.

Following these purification stage, effluents from WWTP could be reused for recreational, agricultural and industrial purposes.

However, recent concerns have arisen regarding the economic and environmental feasibility of traditional WWTPs (IPCC 2007, Mohsenpour et al. 2021). The primary concerns involve the high energy consumption resulting from intensive aeration, excessive waste sludge discharge, and significant greenhouse gas emissions, predominantly CO_2, nitrous oxide, methane, and hydrogen sulphide (Chae and Kang 2013, Plappally 2012, Wan et al. 2016). In particular, the nitrogen and phosphorus remediation processes require excessive energy consumption (Grady Jr et al. 2011). Therefore, to establish a more sustainable future, it is crucial to develop novel wastewater treatment processes that curtail energy consumption, sludge production, and enhance waste disposal, predominantly nutrient recovery.

2.2 Wastewater treatment with algae

2.2.1 Algae

Algae, originating from the Latin word for seaweed, signify a diverse group of organisms that have evolved over 3.5 billion years, resulting in a wide genetic diversity that underpins their robustness and adaptability (Bellinger and Sigee 2015, Webster 1981). Taxonomically, algae are classified into diverse phyla, including Cyanophyta, Chlorophyta, Euglenophyta, and others, encompassing both prokaryotes and eukaryotes (Bellinger and Sigee 2015). Inhabiting a broad spectrum of environments globally, algae are not confined to traditional habitats but are found in fresh and brackish water, wastewaters, plants, soils, and rocks, showcasing their ecological resilience (Barsanti and Gualtieri 2005). Beyond their ecological significance, algae are crucial contributors to the world's oxygen supply, generating nearly 50% of the annual oxygen (Barsanti and Gualtieri 2005, Bellinger and Sigee 2015, Su 2020). Moreover, their metabolic flexibility, transitioning from phototrophy to heterotrophy, finds contemporary applications in innovative systems like Algal Turf Scrubbers (ATS). This adaptability makes them invaluable components in wastewater treatment and environmental remediation, emphasizing their historical importance and enduring relevance in diverse fields.(Barsanti and Gualtieri 2005, Pfandl et al. 2009).

2.2.2 Algal wastewater treatment

Algae have shown promising results in treating various types of wastewater, including municipal (pre-treated and secondary treatment effluent), agricultural (from dairy, poultry, swine and cattle feedlot), industrial (such as textile, winery, tannery, olive mill and paper mill), and even anaerobic digestion effluent (including dairy and poultry manure, sewage sludge, and food waste). This is due to their large capacity of nutrient removal and little land requirements (Cai et al. 2013, Li et al. 2019c, Su 2020). To maximize nutrient removal efficiency, brief mechanisms of nutrient removal by algae are outlined here, and these are roughly categorized by elemental composition.

- *Carbon*: algae are able to uptake both CO_2 and HCO_3^- from environments and then convert them to organic matter through photosynthesis. Nevertheless, it's crucial to understand that HCO_3^- is more abundant in natural environments due to the slower diffusion rate of CO_2 in water versus air (Raven et al. 2008, Su 2020). t

Additionally, many algae can also uptake organic carbon in the form of sugars, alcohols, and acids, at a lower metabolic cost than inorganic carbon (Perez-Garcia et al. 2011).

- *Nitrogen*: the energy-dependent nitrogen assimilation process is a key factor for algae in converting inorganic nitrogen (mostly NO_3^-, NO_2^- and NH_4^+) into protein, ribonucleic acid (RNA), and deoxyribonucleic acid (DNA) (Perez-Garcia et al. 2011). Algae stepwise reduce NO_3^- to NO_2^- and NH_4^+ in their cytosol and chloroplasts before further assimilation, therefore, NH_4^+ is preferred over NO_2^- and NO_3^- in inorganic nitrogen sources because of the fewer energy requirements (Sanz-Luque et al. 2015, Su 2020). In addition, dissolved organic nitrogen and atmospheric nitrogen can also be fixed by algae (Antia et al. 1991, Cai et al. 2013, Chen and Chen 2006). Depending on the nitrogen quantity and quality and the algal specie, the major enzymes in the nitrogen fixation are glutamate dehydrogenase, glutamate ammonia ligase and glutamine oxoglutarate aminotransferase (Nurdogan and Oswald 1995, Sañudo-Wilhelmy et al. 2004, Su et al. 2011). Additionally, ammonia will be volatilized at high pH conditions since algae produce OH^- during photosynthesis when taking CO_2 or HCO_3^- (Chi et al. 2011, Perez-Garcia et al. 2011, Xie et al. 2017).
- *Phosphorus*: similar to nitrogen, it is a fundamental macronutrient to algae. Algae prefer inorganic P (PO_4^{3-}, HPO_4^{2-} and $H_2PO_4^-$ depending on pH) to synthesize nucleic acids (e.g. RNA and DNA) and ATP and phospholipids for their growth and metabolism (Dyhrman 2016). The main group of enzymes in phosphorous recovery are the alkaline phosphatases (Perez-Garcia et al. 2011, Xie et al. 2017). In addition to assimilation, precipitation and adsorption are the main mechanisms by which algae remove P from water (Su et al. 2011, Xu et al. 2014). At optimal pH values between 9 and 11, the P-adsorption to the algal cell wall and precipitation with cations can occur within minutes (Nurdogan and Oswald 1995, Sañudo-Wilhelmy et al. 2004).
- *Heavy metals*: algae are capable of removing heavy metals (cadmium, nickel, zinc, copper, mercury, arsenic, chromium and lead) from aqueous solutions through two major mechanisms: bioaccumulation and biosorption (Goswami et al. 2022, Salama et al. 2019). Bioaccumulation is a metabolism-dependent process in

which heavy metals enter algal cells through active and/or passive transport (Mantzorou et al. 2018). Biosorption can be classified as 1) a non-metabolic process in which heavy metals are attached to functional groups on the surface of algal cells due to ion exchange, complexation, chelation and precipitation (Park et al. 2016, Salama et al. 2019); 2) a metabolic process in which high pH caused by photosynthetic growth of microalgae promotes flocculation and precipitation of heavy metals (Munoz 2005).

In brief, biological removal through algal uptake and abiotic removal through algal photosynthesis due to environmental changes are the two main mechanisms by which algae remove pollutants from wastewater (Gan et al. 2022, Su 2020).

2.3 Algal cultivation systems in wastewater treatment

Algal wastewater treatment systems have been designed and configured in different ways to optimize the use of light and nutrients or pollutants from different sources of wastewater. As a result, higher biomass and pollutant removal efficiencies have been achieved (Li et al. 2019c, Mohsenpour et al. 2021, Wang et al. 2018b). In addition, cost- and energy-efficient systems are flourishing in large-scale applications (Gan et al. 2023, Leong et al. 2021, Wang et al. 2018a).

Algal wastewater treatment systems can be categorized into three major types based on the mobility of the algal cells in: (a) suspended, (b) immobilized, and (c) attached systems, including the Algal Turf Scrubber, as depicted in Fig. 2-1 (Mohsenpour et al. 2021, Wang et al. 2018a). Each type has its own advantages and disadvantages, which will be discussed in the following sections.

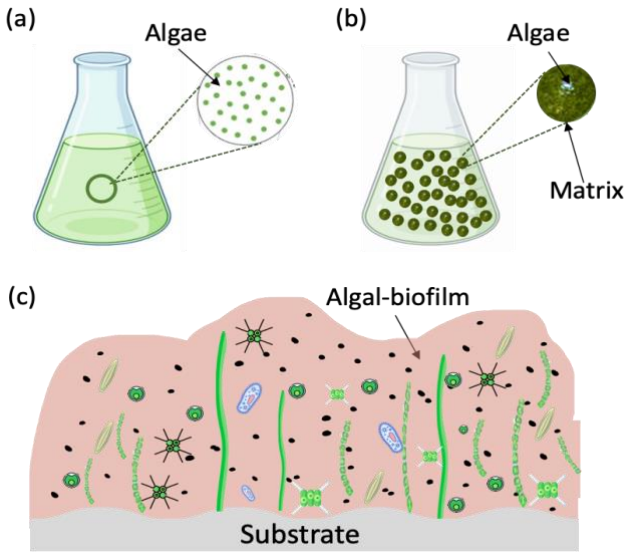

Figure 2-1 Schematic illustration of (a) suspended; (b) immobilized; and (c) attached algal systems for wastewater treatment.

2.3.1 Suspended algal systems

Fig. 2-1a shows that suspended algal cultivation systems involve the use of a liquid nutritious medium in which the microalgae freely float. The two main subtypes of suspended systems are the open raceway ponds and the closed tubular or plate photobioreactors (PBRs). Both, are well-established systems and frequently employed in commercial biomass production and wastewater treatment (Li et al. 2019c, Mohsenpour et al. 2021).

2.3.1.1 High rate algal pond

The high rate algal pond (HRAP) was first applied in industrial-scale wastewater treatment by Oswald and Gotaas (1957). It is now one the most commercialized algae wastewater treatment systems used to treat agriculture, domestic and industry wastewater due to the low capital and operation cost (Buchanan et al. 2018, Leong et al. 2021, Posadas et al. 2015). As shown in Fig. 2-2, HRAP is an open channel system and there is no problem of preventing light from entering the algae with covering materials (Park et al. 2011b, Wang et al. 2018b). The water depth is usually designed to 0.2-1 m to get better light penetration depending on wastewater clarity (Craggs et al. 2014). Depending on soil conditions, HRAPs could be either unlined or lined with PVC, asphalt or concrete to reduce infiltration into surrounding soil and further into groundwater (Leong et al. 2021, Park et al. 2011b). Paddlewheels or other mechanical devices are used to keep the algae in suspension and ensure

that they receive sunlight throughout the day (Leong et al. 2021, Posadas et al. 2015, Wang et al. 2018b). The horizontal water velocities are recommended controlled between 0.09 and 0.3 m s^{-1} (Garcia et al. 2000). HRAP could be built on non-arable lands to avoid competition with commercial crops or close to industries to get fuel gas to better recycle energy and CO_2 or close to wastewater treatment plants to easily assess nutrients (Cai et al. 2013). On the industrial-scale, the area of HRAPs ranges from 1000-50000 m^2 (Craggs et al. 2012).

Open ponds offer economic benefits, but they also have significant drawbacks that must be taken into account. One major issue is water loss due to evaporation, which can range from 3-10 L m^{-2} d^{-1} in HRAPs depending on the climate. While turbulence control can help to reduce evaporation, it only offers a partial solution (Cai et al. 2013, Posadas et al. 2015). Another problem is that suspended algae in open ponds have poor settling capacity and relatively low cell density, which makes it difficult and expensive to separate them from the treated wastewater (Posadas et al. 2015, Uduman et al. 2010). Different treatment methods such as chemical flocculation, physical methods like centrifugation, filtration, ultrasonic separation and gravity sedimentation, and biological methods like bioflocculation have been employed to harvest algal biomass from HRAPs (Uduman et al. 2010). Finally, controlling algal contamination is a persistent challenge in HRAPs, as algae are difficult to control in open ponds (Park et al. 2011a).

Figure 2-2 An outdoors pilot scale high rate algal pond (Marín et al. 2018).

2.3.1.2 Closed algal photobioreactor

Photobioreactors (PBs) are enclosed suspended algae culture systems that use transparent plastic or glass materials to contain the algae and growth medium (Mohsenpour et al. 2021, Vo et al. 2019). PBs offer several advantages over HRAPs in wastewater treatment. They provide superior control over algae growth conditions, leading to faster and more efficient pollutant removal, and reduce the risk of contamination and evaporation (Molinuevo-Salces et al. 2010, Vo et al. 2019, Wang et al. 2018b). Additionally, the high surface area to volume ratio of PBs improve the light utilization of the algae and further increased the photosynthetic rate and cell density of the algae (Jung et al. 2014, Sun et al. 2016). However, the high cost of materials, construction, operation, maintenance, and harvesting should be considered, and the high biomass concentration can lead to shading and light attenuation, reducing overall process efficiency (Kesaano and Sims 2014, Vo et al. 2019, Wang et al. 2018a, Wang et al. 2018b).

There are different types of PBs used in wastewater treatment, including

- Flat plate PBs (Fig. 2-3 a) with a high surface area-to-volume ratio, yielding 5-10 times more biomass than other PBs (Huang et al. 2016, Lee et al. 2014). Airlift flat PBs improve growth rates and pollutant removal efficiency through efficient mixing and aeration (Issarapayup et al. 2011).
- Column PBs (Fig. 2-3 b) with different shapes, such as X-shape, H-shape, and serial column, maximize sunlight captured by algae and are scalable by connecting modules (Lee et al. 2014, López-Rosales et al. 2016, Vo et al. 2019).
- Tubular PBs, both vertical and horizontal (Fig. 2-3 c and d), are also used, but the former saves footprint and increases biomass productivity (Henrard et al. 2011, Slegers et al. 2013). However, they are rarely used in wastewater treatment due to the high energy consumption required to mix media in long continuous pipes (Vo et al. 2019).
- Finally, soft frame PBs (Fig. 2-3 e) made of flexible, foldable, replaceable, and mobile materials are a viable alternative, although their high maintenance needs and easily damaged materials may hinder their applications (Hom-Diaz et al. 2017, Schreiber et al. 2017).

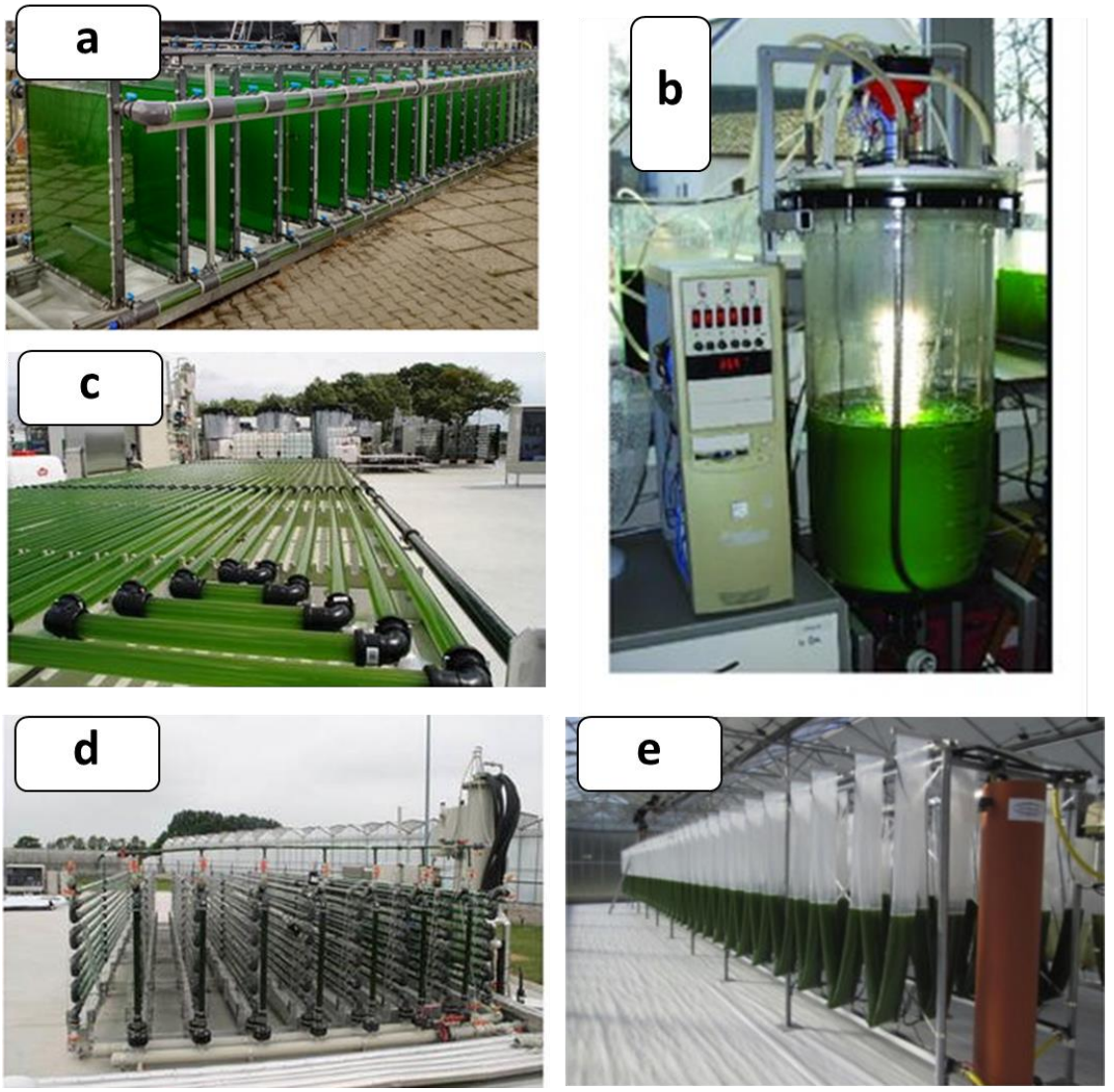

Figure 2-3 Examples of enclosed algal PBs. (a) Flat plate PB (Lindblad et al. 2019); (b) Column PB (Masojídek and Torzillo 2008); (c) Horizontal tubular PB (De Vree et al. 2015); (d) Vertical PB (De Vree et al. 2015); (e) Soft frame PB (Schreiber et al. 2017).

2.3.2 Immobilized algal systems

According to Demirbas (2010), the harvesting process in suspended culture systems may contribute to 20-30% of the total production cost. To address this issue, immobilized algal systems have been suggested as an alternative approach. In these systems, algae are immobilized or trapped in a 3-4 mm natural or synthetic polymeric gel matrix (Fig. 2-1 b) such as carrageenan, alginate, or acrylamide, with the help of flocculants or chemical agents (De-Bashan and Bashan 2010, Mallick 2002, Mohsenpour et al. 2021). Compared to suspended systems, immobilized systems greatly reduce the costs associated with harvesting

and achieve higher algal concentrations by easily separating algal biomass from treated water (Christenson and Sims 2011, Moreno-Garrido 2008). However, their potential for wider application is limited by issues such as leakage of algae from the immobilized systems, toxicity of polymeric materials to algae and the surrounding environment, and long lag time required for entrained algae in immobilized systems (Mallick 2002, Wang et al. 2018a).

2.3.3 Attached algal systems

Another approach to address the issues of suspended systems is to develop attached algal systems, so-called biofilm systems that allow for easy biomass harvesting (Christenson and Sims 2011). It should be noted that it is essentially impossible to maintain a bioreactor in an axenic state and therefore the attached algae are attached algal biofilms. Algal biofilm constitutes an environmental mesocosm of bacteria, pro-and eukaryotic algae, fungi, and protozoa attached to a bedding substrate, and particularly or completely submerged in wastewater to facilitate biofilm development (Fig. 2-1 c and Fig. 2-4) (Adey et al. 2013, Kangas et al. 2017, Kebede-westhead et al. 2003, Kesaano and Sims 2014, Liu et al. 2016, Mulbry and Wilkie 2001).

The thickness of the algal biofilm ranges from 0.052 to 2 mm and the high surface area to volume ratio of algal biofilms help to optimize the use of light and CO_2 for optimal performance (Boelee et al. 2014, Irving and Allen 2011, Mohsenpour et al. 2021). The solids content in algal biofilms is notably higher than that in suspended systems, ranging from 12-16% in comparison to the 0.5% found in suspended systems, moreover, the straightforward scraping harvesting method helps reduce energy consumption, with a 99.7% reduction in dewatering energy requirements compared to open ponds (Christenson and Sims 2012, Gan et al. 2023, Ozkan et al. 2012). Algal biofilms not only offer higher biomass productivity but also have the added advantage of adsorbing, precipitating, and assimilating pollutants from the ambient liquid medium, which improves overall pollutant removal efficiency (Gan et al. 2022, 2023, Wang et al. 2018a). Although these benefits are evident, it is essential to acknowledge and tackle the potential drawbacks associated with the need for an extensive footprint and the shedding of microorganisms from the biofilm (Boelee et al. 2011).

2.3.3.1 Mechanism of algae attachment

The formation of algal biofilms begins when algal and bacterial cells adhere to the substrate through physical (gravitational or hydrodynamic) and chemical (cationic, inorganic

and organic adhesion) reactions (Schnurr and Allen 2015, Wang et al. 2018a). Once attached, the microorganisms secrete extracellular substances (EPS) such as polysaccharides, proteins, phospholipids, and more (Czaczyk and Myszka 2007). EPS not only enhance cell adhesion but also assist in capturing and concentrating nutrients from the ambient liquid medium to facilitate better growth (Czaczyk and Myszka 2007, Shen et al. 2014). After successful initial adhesion, the algal biofilm thickens through microbial colonization, and more EPS is produced to strengthen the adhesion between cells (Schnurr and Allen 2015, Xiao and Zheng 2016). The different growth stages of algal biofilm are shown in Fig. 2-4.

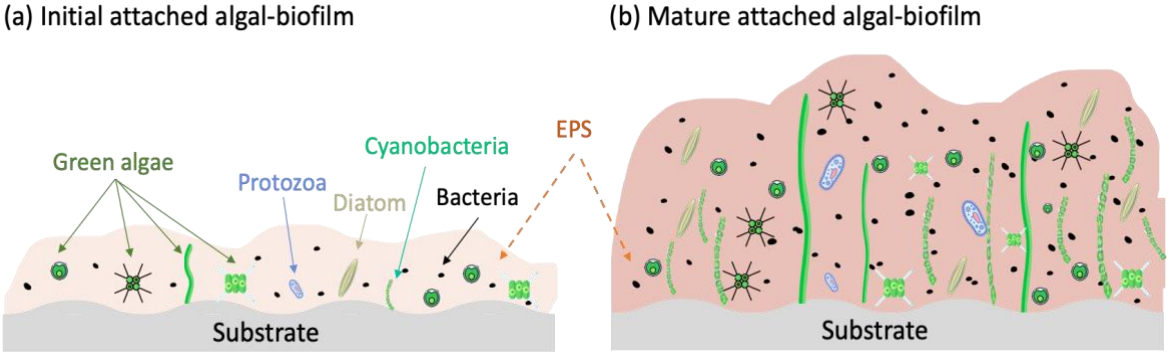

Figure 2-4 Initial (a) and mature (b) stages of attached algal biofilm. EPS: Extracellular polymeric substance.

2.3.3.2 Substrate materials

The selection of a suitable substrate is crucial for attached algal systems, as it can significantly impact the initial adhesion, attachment strength, and growth dynamics of cells through its hydrophobic and topographic properties (Karimi et al. 2021, Zhou et al. 2021). Several materials, including polyethylene, polystyrene, polyurethane, loofah, nylon sponge, cardboard, cotton, and stainless steel, have been found to support algal biofilm growth (Cao et al. 2009, Ozkan and Berberoglu 2011, Shen et al. 2014). Synthetic plastic materials are promising as they provide good attachment surfaces that can enhance biomass productivity and pollutant removal efficiency. However, the release of microplastics must be taken into consideration to prevent secondary contamination (Smith et al. 2021, Venable and Podbielski 2019).

2.3.3.3 Algal Turf Scrubber (ATS)

The classification of attached algal biofilm systems as either stationary or mobile depends on the movement of the substrate materials (Wang et al. 2018b). Similarly, the stationary systems can be categorized as either horizontal or vertical depending on the orientation of the substrate (Wang et al. 2018a). One example of a horizontal stationary attached algal system is the ATS, which has been utilized for over 40 years to purify various sources of pollution such as agricultural drainage, manure wastewater, and urban wastewater (Adey et al. 2013, D'Aiuto et al. 2015, Higgins 2011, Mulbry et al. 2008, Ray et al. 2015, Walter et al. 2008).

As shown in Fig. 2-5, Fig. 3-1 and Fig. 4-1, the ATS system comprises four main components: the flow-way, the substrate for biofilm attachment, the tipping bucket, and the pump. The flow-way, which can be made of acrylic, wood, steel, or other materials, is placed horizontally with a slope of 0.5-2% and can have a surface area ranging from 0.05-1000 m^2 (Craggs et al. 1996, Gan et al. 2022, 2023, Leong et al. 2021, Liu et al. 2016) The substrate covers the flow-way, providing a growth surface for the biofilm (for more information on the substrate, see section 1.3.3.2). The submersible pump is used to deliver wastewater to the flow-way, with water flow rates ranging from 0.3-750 L min^{-1} depending on the size of the flow-way (Craggs et al. 1996, Kangas et al. 2017, Mulbry et al. 2008, Sandefur et al. 2011). The tipping bucket distributes the water in waves, increasing the contact surface area of the biofilm with air and reducing diffusional resistance (Blersch et al. 2013, D'Aiuto et al. 2015, Wilkie and Mulbry 2002). However, this wave-like distribution may not be necessary for all ATS systems, particularly those with freshwater algae species that have already adapted to constant flow conditions (Craggs 2001, Sindelar et al. 2015).

Figure 2-5 Front view of a pilot-scale ATS.

The ATS biomass is harvested by scraping when the biofilm matrix becomes mature or thick enough to shade the underlying biofilm. Depending on the growth and operational conditions, the ATS biomass is typically harvested at intervals of 4-21 days, with biomass productivity ranging from 2-39 g DW m^{-2} d^{-1} (Chen et al. 2015, Gan et al. 2022, Kebede‐westhead et al. 2003, Marella et al. 2019). ATS biomass is rich in nutrients (N and P contents: 0.8-7.2% and 0.1-3.2%) or other organic matter, which can be utilized as fresh or dried fertilizer, soil conditioner, or biogas substrate (Cheenakula et al., 2022; Gray, 2021; Marella et al., 2019; Pizarro et al., 2006; Ray et al., 2015; Schreiber et al., 2018). Several factors, including operational conditions (CO_2 and nutrient concentration, pH, water flow rate, pulsing condition, harvesting frequency) and environmental conditions (temperature, light intensity, light/dark period), affect the performance of ATS biofilms and, consequently, the nutrient removal efficiency of ATS (Adey et al. 2013, D'Aiuto et al. 2015, Leong et al. 2021, Liu et al. 2016).

2.4 Algal biomass utilization

2.4.1 Algal biomass composition

Algae are a rich source of carbohydrates, lipids, proteins, pigments, and vitamins and are therefore a valuable feedstock for cosmetics, biofuels, and food and feed supplements (Li et al. 2008, Stiefvatter et al. 2022, Wang et al. 2015). Moreover, the algae cultured in wastewater could remove and then concentrate nutrients inside algal biomass (Mulbry et al. 2008), but the nutrient concentrations in algae vary a lot under different culture conditions (Adey et al. 2013, Coppens et al. 2016a, Walter et al. 2008).

2.4.2 Algal biomass as biofuel

Algae possess the remarkable ability to utilize photosynthesis, capturing atmospheric CO_2 and harnessing energy from sunlight to convert them into valuable storage substances like lipids and carbohydrates (Li et al. 2008). These lipids and carbohydrates derived from algae serve as a versatile feedstock for the production of various biofuels, including biodiesel, bioethanol, and biobutanol (Gan et al. 2016, Gao et al. 2016, Ho et al. 2013). The utilization of algae as a biofuel source offers significant advantages, primarily attributed to its high lipid and carbohydrate contents, exceptional productivity, and lack of competition with arable land in contrast to terrestrial plants (Maity et al. 2014, Singh et al. 2011). Furthermore, the short life cycle of algae, typically spanning only a few days, further enhances its appeal as a sustainable biofuel solution (Chia et al. 2018). Using a validated algal growth model, Moody et al. (2014) determined that the maximum global algal lipid production is 24 to 27 $m^3\ ha^{-1}\ year^{-1}$ (13-15 $g\ m^{-2}\ d^{-1}$ algal biomass production). This potential could supplement about 30% of fuel consumption through microalgae, especially using non-arable land in various regions. Mussatto et al. (2010) summarized that microalgae could potentially produce approximately 46,760-140,270 $L^{-1}\ ha^{-1}\ year^{-1}$ of ethanol. This yield is significantly higher than the yields obtained from various plants, such as corn (3460-4020 $L^{-1}\ ha^{-1}\ year^{-1}$), sugarcane (6190-7500 $L^{-1}\ ha^{-1}\ year^{-1}$), and switchgrass (10760 $L^{-1}\ ha^{-1}\ year^{-1}$). To achieve commercial-scale production of algal biofuels, numerous techniques have been employed to further enhance the lipid and carbohydrate contents of algae. These methods include optimizing cultivation conditions such as light intensity, temperature, and CO_2 concentration, applying nutritional stresses, manipulating genes, and selecting superior algal species (Chen et al. 2013, Chia et al. 2018, Daud et al. 2015, Gao et al. 2016, Radakovits et al. 2010). With these optimization

techniques, algal lipid content and carbohydrate content can reach impressive levels of 50-70% and 40-70%, respectively (Chia et al. 2018). However, despite these promising characteristics, the widespread adoption of algal biofuels still faces limitations due to the high costs associated with cultivation, harvesting, and extraction of valuable products (Pittman et al. 2011).

2.4.3 Algal biomass as food and feed supplements

2.4.3.1 Direct utilization of algae

Microalgae, renowned for their abundant nutrient content, particularly proteins, vitamins B12, C, and D, are globally consumed and marketed as dietary supplements (Colla et al. 2007, Enzing et al. 2014, Wells et al. 2017). The market size of algae protein was estimated to be approximately EUR 928 million in 2023, nearly doubling between 2016 and 2023 (Mendes et al. 2022). Algae are readily available in liquid form or as dried algae powder, pellets, or chips, requiring no additional processing (Priyadarshani and Rath 2012). Prominent commercially available algal species include the green algae *Chlorella*, *Haematococcus*, *Dunaliella*, and the Cyanobacterium *Arthospira platensis*, known as *Spirulina* (Chacón‐Lee and González‐Mariño 2010, Enzing et al. 2014). Furthermore, algae find application as feed in larval and juvenile shellfish and finfish aquaculture (Norambuena et al. 2015, Priyadarshani and Rath 2012).

2.4.3.2 Algal extracts

The commercial utilization of algae extends beyond whole organism sales, with a notable focus on high-value components. Current market trends emphasize pigments like astaxanthin, fucoxanthin, and ß-carotene, sourced primarily from *Haematococcus Pluvialis*, brown algae, and *Dunaliella* (Enzing et al. 2014, Wells et al. 2017). These pigments, highlighted for their antioxidant, anti-cancer, and anti-obesity properties, serve as pivotal food and feed additives (Foo et al. 2017, Kovač et al. 2013, Zorofchian Moghadamtousi et al. 2014). Polyunsaturated fatty acids *(PUFA)*, including eicosapentaenoic acid (EPA) and docosahexaenoic acid (DHA), are abundantly found in marine algae (Gladyshev et al. 2013). Originating from microalgae, these essential fatty acids play a crucial role in marine ecosystems and are vital for brain development in children and cardiovascular health, making them invaluable resources with promising applications (Gladyshev et al. 2013, Stiefvatter et al. 2022, Wells et al. 2017).

2.4.4 Algal biomass as fertilizer

Algae-based fertilizers can be classified into three major groups based on their fertilization action mechanisms: living bio-fertilizers, liquid foliar fertilizers, and organic fertilizers.

2.4.4.1 Live bio-fertilizer

Living algae bio-fertilizers refer specifically to non-toxic nitrogen-fixing cyanobacteria fertilizers (Dhar et al. 2015, Lu and Xiao 2022, Zou et al. 2021). It is important to note that not all cyanobacteria can directly fix nitrogen from the atmosphere (Tomitani et al. 2006). Two cyanobacteria species, *Microcystis aeruginosa* and *Anabaena* sp. PCC 7120, have been tested and found to be beneficial for the growth, development, and metabolic activity of corn seedlings (Dhar et al. 2015).These nitrogen-fixing cyanobacteria effectively act as fertilizers using a variety of strategies, including:

- Enhancing soil fertility by fixing nitrogen from the atmosphere and transferring it into the soil to support plant growth (Li et al. 2022, Singh et al. 2014).
- Fostering the formation of biological crusts by producing extracellular polymeric substances (Chamizo et al. 2018, Zhang et al. 2018). These crusts play a crucial role in stabilizing soil structure, preventing erosion, and promoting overall soil health (Chamizo et al. 2018).
- Promoting plant growth, crop yield and plant vigor by secreting plant growth promoting substances (Li et al. 2019b).
- Enhancing the biodiversity of soil microorganisms (Bidyarani et al. 2016).

2.4.4.2 Liquid foliar fertilizer

Liquid foliar fertilizer derived from algae is obtained through the breakdown of algal cells, resulting in an algal extract that is could subsequently applied to plant leaves (Lu and Xiao 2022, Zou et al. 2021). This extract is enriched with nutrients and small-molecular-weight components derived from the degradation of larger molecular-weight compounds (Ramya et al. 2015). Furthermore, the direct application of this liquid fertilizer onto crops, allows for rapid absorption through leaf pores, minimizing nutrient loss after irrigation (Zou et al. 2021). The unique attributes of algal-based liquid foliar fertilizer contribute to its

remarkable capacity for enhancing both the quantity and quality of plants (Grzesik et al. 2017).

2.4.4.3 Organic-fertilizer

Algae-based organic fertilizer refers to the desiccated form of algae utilized for soil application. Upon application, the algae undergoes microbial decomposition, leading to the release of essential macro-nutrients (carbon, nitrogen, phosphorus, potassium) and micro-nutrients (zinc, magnesium, calcium, iron, copper) that were previously assimilated from water sources (Lu and Xiao 2022, Zou et al. 2021). The decomposition process is intricately linked to factors such as microbial profile and abundance, as well as soil moisture and temperature conditions (Adl 2003). Subsequently, the liberated nutrients become available for plant assimilation, thereby fostering plant growth and enhancing soil fertility by elevating the levels of plant-available nutrients in the soil (Coppens et al. 2016a, Schreiber et al. 2018). It should be notice that the efficacy of algae organic fertilizer compared to inorganic fertilizers varies. Some studies show no significant difference between the two, while others find inorganic fertilizers to be more beneficial (Chan et al. 2021, Lu and Xiao 2022, Nkebiwe et al. 2016).

2.4.4.4 Co-application of mycorrhiza and algal biomass

The combined application of organic and bio or chemical fertilizers have proven to be a better approach to increase and sustain soil fertility and crop yields than the application of chemical or organic fertilizers alone (Han et al. 2016, Sun et al. 2015). And application of biofertilizer - mycorrhizae produces better root systems which combat root rotting and soil-borne pathogens and then help plants absorb many nutrients, particularly the less available mineral nutrients such as phosphorus, zinc, molybdenum and copper through hyphae (Chen 2006, Gerdemann 1968).

Mycorrhizal fungi hold great promise as biofertilizers in sustainable agricultural practices due to their ability to supply essential mineral nutrients to host plants and protect them from biotic and abiotic stress factors (Meena et al. 2018, Shi et al. 2023). Furthermore, the combined application of organic and bio or chemical fertilizers has been empirically established as a superior approach for enhancing soil fertility and sustaining crop yields compared to using chemical or organic fertilizers alone (Oyetunji et al. 2022). Notably, co-applying organic fertilizer and mycorrhizae optimizes soil fertility, fosters robust crop growth,

and advances sustainability by promoting the development of improved root systems. These root systems effectively combat root rot and soil-borne pathogens while facilitating the enhanced absorption of various nutrients, particularly those that are less readily available in the soil, such as phosphorus, zinc, molybdenum, and copper, through their hyphae (Amaya-Carpio et al. 2009, Bargaz et al. 2018)

3 Optimizing nutrient removal and biomass production of the Algal Turf Scrubber (ATS) under variable cultivation conditions by using Response Surface Methodology

Based on a journal article published as Gan, X., Klose, H. and Reinecke, D., 2022. Optimizing nutrient removal and biomass production of the Algal Turf Scrubber (ATS) under variable cultivation conditions by using Response Surface Methodology. *Frontiers in Bioengineering and Biotechnology, 10*. https://doi.org/10.3389/fbioe.2022.962719

Contribution: Design 70%, Experimentation 100%, Analysis 90%, Publication work 80%

3.1 Graphical abstract

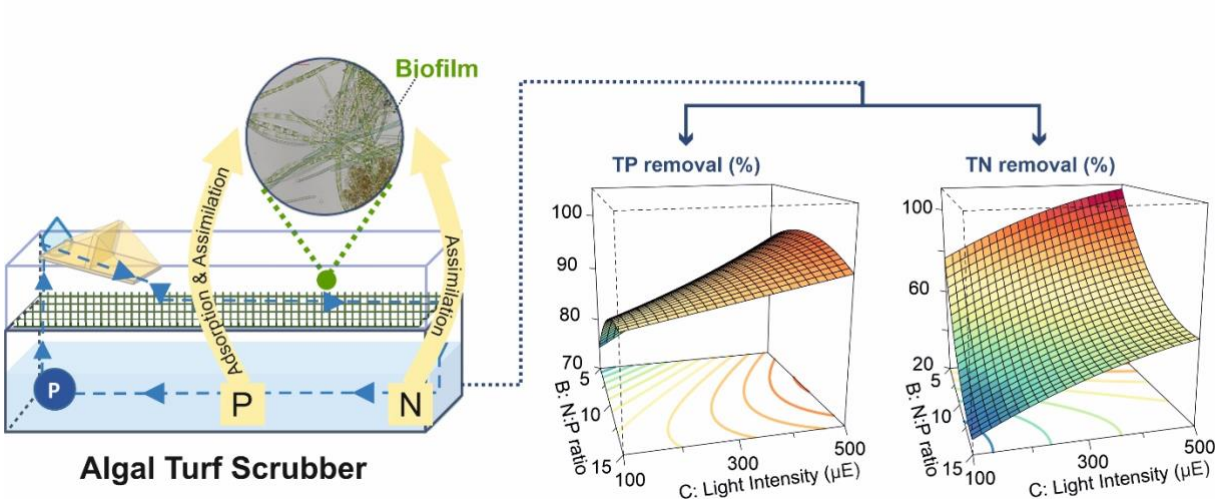

3.2 Introduction

The vast quantity of nutrient-rich urban, agricultural, and industrial wastewater generated by an ever-increasing human population and its activities pose a threat to natural bodies of water (Daud et al. 2015, Pittman et al. 2011). Eutrophication is one of the most striking effects of nutrient release, and is associated with the development of harmful algal blooms and anoxic zones (Dodds and Smith 2016, Qin 2009). Nitrogen leakage into drinking water can negatively affect human health (Wegahita et al. 2020), while mining and the depletion of finite phosphorous ores can cause complex environmental and political issues (Barquet et al. 2020). Therefore, wastewater (WW) treatment and nutrient recovery are essential for healthy ecosystems and human populations.

Among the numerous physical and chemical WW treatment methods, biological remediation technologies based on algae are particularly attractive due to their high nutrient removal efficiency and comparatively low land requirements (Li et al. 2019c, Wang et al. 2018b). Furthermore, algal biomass can serve as an intermediate nutrient carrier between the WW and crop production. However, harvesting algal biomass of suspended cultures, such as open ponds and tubular photobioreactors, is time- and labor-intensive (Richardson et al. 2012). According to the literature, harvesting processes can account for as much as 20- 30% of the total production costs in suspended culture systems (Demirbas 2010). In contrast, algal biofilm reactors are more cost-effective due to the higher biomass density and easier down-stream processing. In algal biofilm reactors, the biofilm constitutes an environmental

mesocosm of bacteria, pro-and eukaryotic algae, fungi, and protozoa attached to a matrix, and submerged in WW. The biofilm is harvested by scraping off the biomass. This process is illustrated in Fig. 3-1 (Christenson and Sims 2011). One of these systems, the Algal Turf Scrubber (ATS), has been successfully employed in the treatment of manure, agricultural drainage, and urban wastewater (D'Aiuto et al. 2015, Higgins and Kendall 2011, Mulbry et al. 2008, Ray et al. 2015, Walter et al. 2008). The system offers ecological benefits such as purification and oxygenation of water as well as CO_2 fixation by the algae. The ATS biomass can be used either as a long-term fertilizer and soil conditioner, or as animal feed (carbohydrates, proteins, and lipids) (Gray 2021, Marella et al. 2019, Ray et al. 2015, Schreiber et al. 2018).

In ATS biofilms, the various algal species employ a broad range of up-take and turn-over mechanisms to meet their macro- and micronutrient requirements. Additionally, essential macronutrient, such as phosphorous, can be precipitated and assimilated as reserves at pH 9-11. Depending on the nutrient quantity and quality and the algal specie, the major enzymes in the nitrogen fixation are the glutamate dehydrogenase, glutamate ammonia ligase and glutamine oxoglutarate aminotransferase. The main group of enzymes in the phosphorous recovery are the alkaline phosphatases (Nurdogan and Oswald 1995, Sañudo-Wilhelmy et al. 2004, Su et al. 2011, Xu et al. 2014). Furthermore, the efficiency of nutrient removal by algal cultures, including ATS biofilms, is strongly effected by the culture conditions. These conditions include osmolarity, shear force, retention time, temperature, light quantity and quality as well as biotic factors (D'Aiuto et al. 2015, Liu et al. 2016). To improve the efficiency and economics of nutrient removal in ATS systems, it is critical to investigate the relationship between these culture conditions and ATS performance. Although ATS systems have been used in WW treatment for 40 years, there remains a need for further systematic studies to optimize the ATS system, Table 3-1.

Response Surface Methodology (RSM) is a collection of mathematical and statistical techniques for designing experiments, building models, evaluating the interdependence of variables, and obtaining the optimal response conditions with a limited number of planned experiments. One RSM is the Box-Behnken Design (BBD) (Ferreira et al. 2007). In short, the model has three levels for each variable and is built specifically to fit a quadratic model. Compared to the full factorial design, BBD largely reduces the number of necessary

experiments. RSM has been successfully used to model the growth of microalgae (Pandey et al. 2020a, Pandey et al. 2020b, Shen et al. 2014). In this study, we use this method to investigate the effect of culture conditions on nutrient removal efficiency and biomass productivity to optimize an ATS system. CO_2 and light are essential to algal photosynthesis. The N:P ratio has been reported to affect the biochemical composition of algal biomass. Therefore, three independent variables, TIC concentration, N:P ratio, and light intensity were chosen to test their independency and interactive effects on nutrient removal, water quality, biomass productivity, and composition in a lab-scale ATS, Fig. 3-1. The experimental ranges of TIC and N:P ratio were chosen based on previous studies (Li et al. 2019c, Liu and Vyverman 2015, Zhu et al. 2021). Temperature and light intensity were based on the local climatic conditions (N 50°54´20; E 6°25´4). The annual light intensity of the daily average and maxima were 125 and 359 µmol photons m^{-2} s^{-1}, respectively. Thus, the maximum light intensities were 500 and 333 µmol photons m^{-2} s^{-1} in 16 and 24 h, respectively.

Table 3-1 The settings and performances of reviewed ATS systems.

ATS System			Wastewater		Cultivation conditions			Effluent			Biomass		Reference
								Removal ($mg\ L^{-1}\ d^{-1}$)					
Size (m); Slope (%)	Flow rate ($L\ min^{-1}$); Intervals (min^{-1})	Replicates; Site	Source; Volume (L)	Nutrient concentration ($mg\ L^{-1}$)	pH-value	T (°C); Light intensity ($\mu mol\ photons\ m^{-2}\ s^{-1}$)	Harvest cycle (d)	P	N	pH-value	Biomass productivity ($g\ m^{-2}\ d^{-1}$)	Nutrient and Ash content (%)	
0.5 × 10; 1%	46.5; zero	Singlicate; Outdoor	Reservoir	TP: 0.002-0.108 TN: 1.9-3.3	7.01	15.0-26.9; N/A	3-9	18-49	161-214	7.42	17.6-25.4	P: 0.1-0.2 N: 0.8-1.3 Ash: 87.2	(Chen et al. 2015)
1 × 50; 2%	60-700 $L\ min^{-1}\ m^{-1}$; zero	6 flow-ways; Outdoor	Agricultural drainage; 1200	TP: <0.1 TN: <0.5	N/A	N/A; N/A	7	25 $mg\ m^{-2}\ d^{-1}$ or 50-69%	125 $mg\ m^{-2}\ d^{-1}$ or 53-72%	N/A	N/A	P: 0.21-0.26 N: 1.5-2.2 Ash: 60-70	(Kangas and Mulbry 2014)
0.3 × 90; 2%	60; 5-6	Singlicate; Outdoor	River	PO_4-P: 0.03-0.09 NO_3-N: 0.4-1.4	N/A	5-30; N/A	7-21	3-40 $mg\ m^{-2}\ d^{-1}$	30-450	N/A	11-18	P: 0.2 N: 2.5 Ash: 60-70	(Kangas et al. 2017)
1 × 1; N/A	110; 4	Singlicate; Indoor	Diluted manure effluent; 200	TN: 1.3-9.0	7-7.5	19-24; 160-460, 240-633	7	0.6-2.4 $mg\ L^{-1}\ d^{-1}$ loading	3.8-17.4 $mg\ L^{-1}\ d^{-1}$ loading	7-7.5 (CO_2 controlled)	5-9	P: 0.6-1.5 N: 3.6-7.1 Ash: 7-10	(Kebede-westhead et al. 2003)
0.39 × 2.5; 1%	2, 4, 6, 8; N/A	Triplicate; Outdoor	Horticultural drainage; 65	PO_4-P: 9-12 NO_3-N: 30 -50	7.0	N/A; N/A	7	0.6-1.2 or < 99%	1-3 or < 99%	> 8.5	2.0	P: 2.1-2.3 N: 6.2-6.8	(Liu et al. 2016)

0.1 × 0.75; 1%	65; zero	Singlicate with 3 cycles; Outdoor	Non-point source WW	TP: 3.7-4.4 TN: 51-69	8-8.8	20-32; 781-1147	15	0.4-1.25	1.3-2.5	N/A	20.7-38.9	P: 0.9-3.2 N: 5.0-6.4	(Marella et al. 2019)
1 × 30; 1 or 2%	93; 4-8	Duplicate; Outdoor	Diluted manure effluent; 3500	TP: 0.68-3.6 TN: 2.6-21.4	7.0	< 32; N/A	4-12	0.4	2500	9-10	2.5-24	P: < 1.0 N: < 6.8	(Mulbry et al. 2008)
3 × 30; 2%	750; 4	Singlicate; Outdoor	Stream	TP: 0.25 TN: 4.1	7.8	15-25; N/A	5-14	48%	12%	10.8	12-34	N/A	(Sandefur et al. 2011)
0.5 × 1; 0.5%	25; N/A	Triplicate; Outdoor	Diluted anaerobically digested food-waste concentrate	TP: 13 TN: 164	7.2	22-28; 6000-8000 μmol photons m^{-2}	7	0.02-0.18 g m^{-2} d^{-1}	0.27-1.65 g m^{-2} d^{-1}	9.3-10.1	20-25	P: 0.8-2.1 N: 8.0-9.9	(Sutherland et al. 2020)
0.1 × 0.52; 1%	0.3; 8-10	Triplicate; Indoor	Artificial WW; 5	TP: 10 TN: 50-150	7-7.2	22-24; 100, 300, 500	7	7.5-10.4 mg L^{-1} or < 99%	35.2-64.7 mg L^{-1} or < 100%	10.5-11.2	4.1-11.2	P: 1.1-1.9 N: 4.9-7.8 Ash: 6.3-9.4	Current study

Note: N/A means nothing was reported in the reference.

3.3 Materials and methods

3.3.1 Culture system

A lab-scale ATS system was designed and constructed using acrylic plates, Fig. 3-1. The 0.1 × 0.52 m flow-way was covered with nylon netting (white, 3.5 × 3.5 mm) serving as a growth substratum. The medium was continuously discharged by a submerged pump at a flow rate of 0.3 L min^{-1}. A tipping bucket distributed the water in a wave-like interval of 6- 7 s^{-1}, to increase the contacting surface of biofilm with air and reduce diffusional resistance (Wilkie and Mulbry 2002).

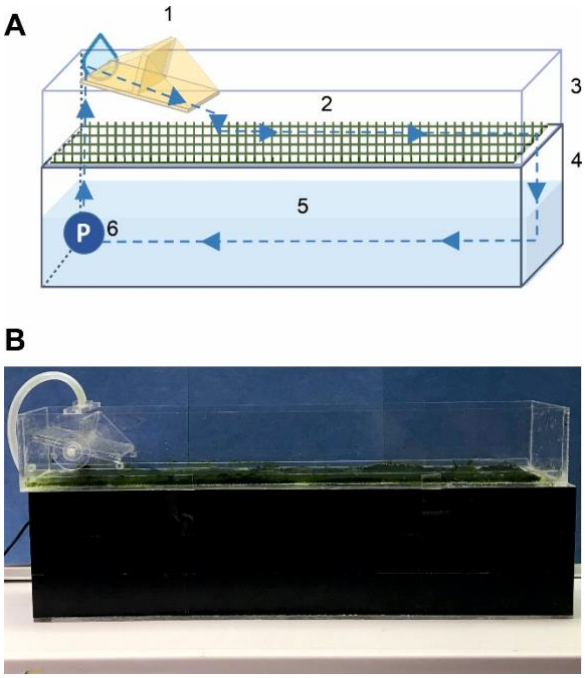

Figure 3-1 Schematic drawing (A) and photograph (B) of the lab-scale Algal Turf Scrubber (ATS). Components are: (1) tipping bucket; (2) mesh for biofilm attach; (3) flow-way; (4) container; (5) medium; (6) pump. Note, the container was covered with opaque material to limit the light influx.

3.3.2 Culture conditions

The standard medium was based on BG11 medium (1 L holds $CaCl_2 \cdot 2\ H_2O$, 36 mg; $MgSO_4 \cdot 7\ H_2O$, 75 mg; $Fe(NH_4)_3(C_6H_5O_7)_2$, 6 mg; EDTA-2 Na, 1 mg; $C_6H_8O_7 \cdot H_2O$, 6 mg; H_3BO_3, 2.86 mg; $MnCl_2 \cdot 4\ H_2O$, 1.81 mg; $ZnSO_4 \cdot 7\ H_2O$, 0.22 mg; $NaMoO_4 \cdot 2\ H_2O$, 0.39 mg; $CuSO_4 \cdot 5\ H_2O$, 0.08 mg; $Co(NO_3)_2 \cdot 6\ H_2O$, 0.05 mg) (Stanier et al. 1971). The standard

medium was supplemented with $NaNO_3$, K_2HPO_4, and $NaHCO_3$ according to the experimental design. 5 L medium was added to the container of each ATS at the start of the experiment. Deionized water was regularly added to the system to compensate for evaporation. Each ATS was inoculated with 1 g fresh ATS-biomass of a continuous ATS system (wild-type mesocosm, green-house, 3 years) and no pre-selection was performed. The ATS was kept at ambient room temperature and a 16:8 h light:dark cycle**.** Experiments were conducted in batches, for 7 days, after which the biomass was harvested and the dry weight (DW), ash-, C-, N-, and P-contents were recorded. The dissolved oxygen (DO), pH-value, total phosphorus (TP), and nitrogen (TN) in the medium were measured daily.

3.3.3 Box-Behnken design (BBD) of experiment

To evaluate the impacts of the three key independent variables: TIC concentration, N:P ratio, and light intensity on the P and N removal efficiencies and biomass productivity, a 3^k factorial BBD was applied by the Design-Expert software version 13.0 (STAT-EASE Inc. ®, USA) and R 4.0.5. The three independent variables (symbols: A, B, C) were coded at three levels namely, low (-1), central (0), and high (+1), Table 3-2. TIC concentration was calculated based on the CO_2 concentration in the atmosphere, Table S 3-1. Accordingly, 15 treatments were conducted with 3 replications of the central point for an accurate estimate of pure experimental error (Table S 3-2). All treatments were conducted in triplicate (data shown as mean ± standard error). After conducting the experiments, the full quadratic second-order equation with interaction terms was used to model the relationship between dependent and independent variables, Eq. (1):

$$y = \beta_0 + \sum_{i=1}^{k} \beta_i x_i + \sum_{i=1}^{k} \beta_{ii} {x_i}^2 + \sum_{i=1}^{k-1} \sum_{j=i+1}^{k} \beta_{ij} x_i x_j + \varepsilon \quad (1)$$

In this equation, β_0, β_i, β_{ii} and β_{ij} are regression coefficients for intercept, linear, quadratic, and interaction coefficients, respectively, x_i and x_j are coded independent variables, and ε is the residual. The 3D response surface and contour plots were generated to visualize the interactive effects of the independent variables of the responses. The perturbation plots were generated to illustrate the sensitive independent variables. They show one variable over its full range while fixing all other variables at the midpoint (coded 0). Responsiveness to a variable was indicated by a steep slope or curvature. We applied the numerical optimization

function of the Design-Expert software, which uses the desired function of the algorithm, to adjust the growth conditions for maximum nutrient removal efficiency and biomass productivity. Finally, the optimized growth conditions were experimentally tested (n = 3) to verify the validity of our model.

Table 3-2 Actual and coded levels of the independent variables of the Box-Behnken design (BBD). TIC, Total inorganic carbon; N:P, Nitrogen: Phosphorous ratio; TP, Total phosphorous.

Independent variables	Symbol	Experimental values		
		Low (-1)	Central (0)	High (+1)
TIC (mM)	A	1.8	5.4	9
N:P ratio (TP: 10 mg L^{-1})	B	5	10	15
Light Intensity (µE)	C	100	300	500

3.3.4 Wastewater analysis

A water sample (2 mL) was collected daily from each ATS and filtered (0.45 µm, LCW 916, Hach-Lange®, USA) before analysis. TP was determined spectrophotometrically (880 nm, SPECORD 200 PLUS, Jena Analytik®, Germany) according to the ammonium molybdate spectrometric method (ISO 2004). TN was determined spectrophotometrically (220 and 275 nm) following the UV-screening method (Association 1998). The DO concentration and pH-value were measured daily *in situ* using specific sensors and a data-logger (LabQuest 3, Vernier®, USA).

3.3.5 Biomass analysis

The attached algal biofilm was harvested from the nylon netting at the end of each batch experiment, on day 7. The biofilm was centrifuged at 4200 *g* at 4 ˚C for 10 min. The supernatant medium was discarded, and the biofilm pellet was stored at -20 ˚C before freeze-drying for dry weight (DW) determination. The suspended biomass was harvested by

sampling and filtrating 100 mL of culture medium (1822-047, Whatman®, USA). The loaded filter was dried to a consistent weight at 70 ˚C for 24 h. The total DW was calculated as the sum of attached and suspended biomass. The total ATS biomass productivity was calculated as follows, Eq. (2)

$$\begin{aligned}&\text{ATS biomass productivity (g m}^{-2}\text{ d}^{-1}\text{)}\\ &= \text{Total DW (g) / ATS area (m}^2\text{) / cultivation days (d)}\end{aligned} \quad (2)$$

Ash content was determined by combustion of 100 mg lyophilized biomass in a muffle furnace at 550 ˚C for 2 h (Chen et al. 2015). The C and N contents were determined by elemental analysis (Vario® Elementar, Germany) using 8-10 mg lyophilized biomass. The P content was determined by Inductively Coupled Plasma- Optical Emission Spectrometry (ICP-OES Ultima 2, HORIBA®, France) in 200 mg lyophilized biomass pretreated with 5 mL HNO_3 and microwave digestion (MARS6, CEM®, USA).

3.4 Results and Discussion

3.4.1 Water quality and nutrient removal in ATS

3.4.1.1 Dissolved oxygen and pH-value

The effect of selected TIC concentrations, N:P ratios, and light intensities on the ATS biofilm and water quality, were monitored via DO and pH measurements, Fig. 3-2. Within the first 2 days, the DO concentrations increased from ~ 6.5 to 11.6 ± 0.8 mg L^{-1} depending on the light intensity, Fig. 3-2 A-C. Between day 3 and 7, the DO concentration leveled off under all light intensities, Fig. 3-2 A-C. Under low light intensity (100 µmol photons m^{-2} s^{-1}) the DO concentration remained similar for all TIC concentrations and N:P ratios over 7 days, Fig. 3-2 A. Comparably, the pH-values initially increased in all treatments from ~ 7.6 to 9.0 ± 0.1 or 10.9 ± 0.4, over the first day, Fig. 3-2 D-F. Between day 2 and 7, all treatments reached stable pH-values between 10.5 ± 0.3 to 11.2 ± 0.7, Fig. 3-2 D-F. Similar trends in pH-value were reported for outdoor ATS systems, which increased from pH 7.0 to > 8.5, within 48 h (Liu et al. 2016).

The lower DO concentrations observed under high N:P ratios (15:1) and medium light (300 µmol) may be due to an increased oxygen consumption during NO_3^- assimilation, Fig. 3-2 B squares (Perez-Garcia et al. 2011). The high DO concentrations under high light intensity

(500 µmol) suggest that the ATS biofilm has robust photosynthesis under higher light intensity over a wide range of TIC and N:P ratios, Fig. 3-2 C. A simultaneous increase in DO concentration and light intensity during peak times was previously confirmed by Sandefur et al. (2011). The high pH-values in our ATS system might be caused by the high CO_2 uptake, the OH^- released from the hydrolysis of HCO_3^- and the strong NO_3^--N consumption by algae biofilm during the growth and photosynthesis (Chi et al. 2011, Perez-Garcia et al. 2011, Xie et al. 2017). We identified a positive correlation between DO concentration and pH value (R^2 = 0.64), which was identified with previous research on ATS systems (Khan et al. 2019, Zang et al. 2011).

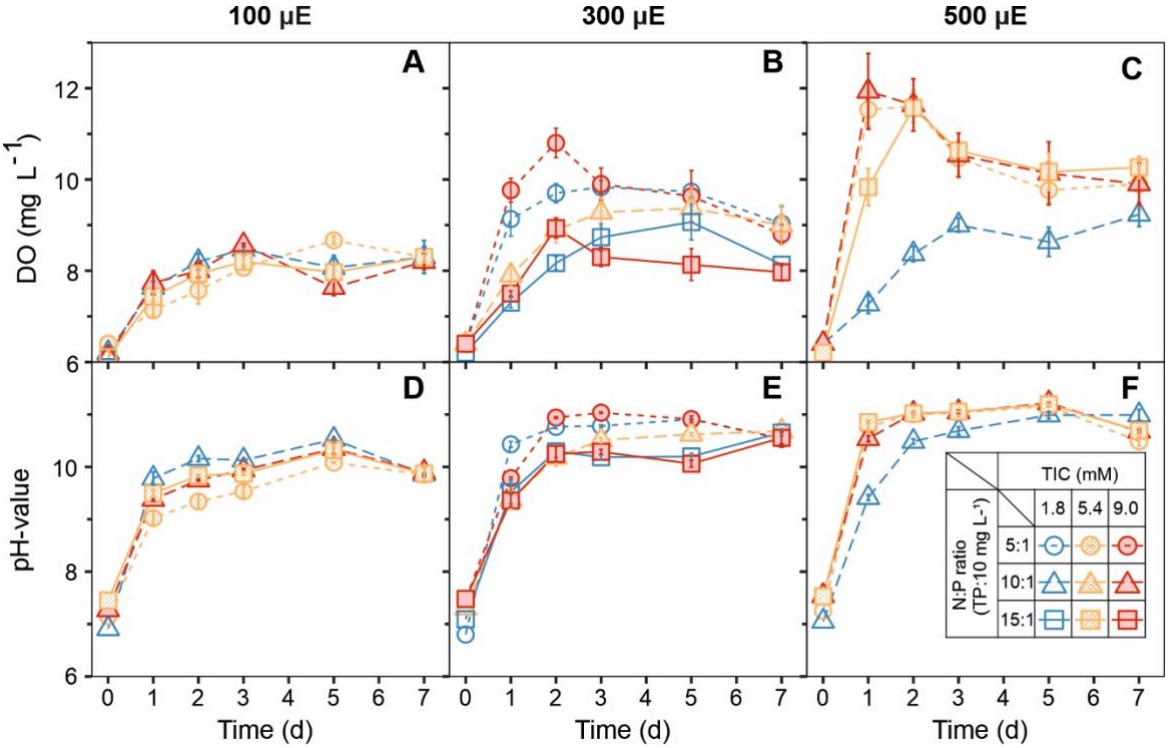

Figure 3-2 ATS- biofilms established a stable medium chemistry under all treatments, within 3 days. Increasing light intensities of (A, D) 100, (B, E) 300, and (C, F) 500 µmol photons m^{-2} s^{-1} increased the dissolved oxygen and pH-value, respectively. Data are presented as mean ± standard error (SE, n = 3, except the treatment of central point: TIC = 5.4 mM, N:P ratio = 10:1 and Light intensity = 300 µmol, n = 9). TIC, Total inorganic carbon; N:P, Nitrogen: Phosphorous ratio; TP, Total phosphorous.

3.4.1.2 Phosphorus and nitrogen removal

The nutrient removal capacity of the ATS system, depending on TIC concentrations, N:P ratios, and light intensities, was monitored daily by measuring the residual TP and TN concentrations in the medium, Fig. 3-3. Within 7 days, the ATS biofilm removed between 7.5 ± 0.2 to 10.4 ± 0.1 mg L^{-1} of TP. The maximum TP removal (99.6 ± 0.4 %) was found under TIC 5.4 mM, N:P ratio 5:1, and high light intensity of 500 µE, Fig. 3-3 C circles. Approximately 80% of TP was removed within 24 h, Fig. 3-3 C. Accordingly, the lowest TP removal (73.4 ± 2.3 %) was found under low light, Fig. 3-3 A. Similarly, within 7 days the ATS biofilm removed between 35.2 ± 4.5 and 64.7 ± 3.8 mg L^{-1} TN, Fig. 3-3 D-F. The maximum TN removal (100%) occurred under TIC 9.0 mM, N:P ratio 5:1, and light intensity of 300 µmol photons m^{-2} s^{-1}, Fig. 3-3 E circles.

In this study, the maximum TP removal rate (8.25 mg L^{-1} d^{-1}) was two-fold higher than previously reported in an outdoor ATS system (3.9 mg L^{-1} d^{-1}) (Liu et al. 2016) and six-fold higher than an indoor algal biofilm system (1.3 mg L^{-1} d^{-1}) (Shi et al. 2007). It is known that algae have various mechanisms to assimilate, absorb and precipitate P out of the medium (Su et al. 2011, Xu et al. 2014). At optimal pH values between 9 and 11, the P-adsorption to the algal cell wall can occur within minutes (Nurdogan and Oswald 1995, Sañudo-Wilhelmy et al. 2004). The high pH values (pH > 9 after 24 h) and high P removal rate in our ATS system confirmed that the P precipitation and adsorption were high in our biofilm. Likewise, our maximum TN removal rate (19.1 mg L^{-1} d^{-1}), was six-fold higher than the previously reported 3.1 mg L^{-1} d^{-1} for the algal biofilm system (Shi et al. 2007). In contrast to P, the N-uptake in algae is an energy-dependent assimilation process (Perez-Garcia et al. 2011). In a highly light-dependent, stepwise reduction process eukaryotic algae reduce NO_3^- to NO_2^- and NH_4^+ in their cytosol and chloroplasts, respectively (Sanz-Luque et al. 2015, Su 2020). Accordingly, we found the highest nitrogen removal rates in the ATS under high light conditions, Fig. 3-3 C.

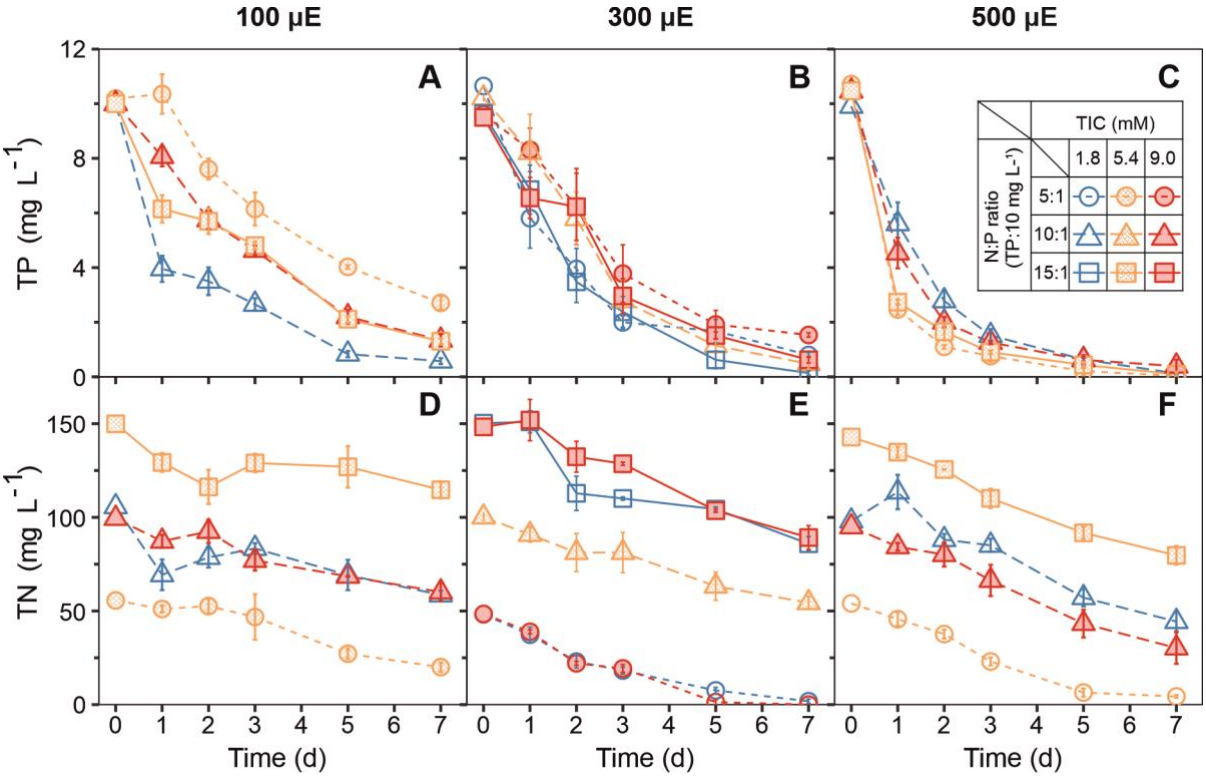

Figure 3-3 ATS- biofilms showed a continuous nutrient removal from the medium under all treatments, throughout 7 days. Increasing light intensities of (A, D) 100, (B, E) 300, and (C, F) 500 µmol photons m^{-2} s^{-1}, respectively, increased the removal of phosphorus and nitrogen. Data are presented as mean ± standard error (SE, n = 3, except the treatment of central point: TIC = 5.4 mM, N:P ratio = 10:1 and Light intensity = 300 µmol, n = 9). TIC, Total inorganic carbon; N:P, Nitrogen: Phosphorus ratio; TP, Total phosphorus; TN, Total nitrogen.

3.4.2 Culture conditions for improved nutrient removal

3.4.2.1 Statistical analysis

The relationship between the three independent variables and six dependent variables (responses) was analyzed by RSM. The two-factor interaction and the quadratic model were used for data fitting. The final model equations, cleared of insignificant variables and interactions, and the ANOVA results for the responses, are shown in Table 3-3.

For all responses, the low probability values (≤ 0.01) revealed that the generated models were significant. Experimental results were well aligned with the generated models as confirmed by analyzing predicted against measured values, Fig. S 3-1. For all six responses, most of the points were within the 95% confidence interval region. Adequate precision was

measured by the signal-to-noise ratio and a value greater than 4 was desirable for good discrimination. All generated models met this requirement. Meanwhile, low variation coefficients (3.7 - 8.1%) indicated a high precision and experimental reliability for all models. The *F*-test of sum of squares to lack of fit confirmed the adequacy of our quadratic model. A *p*-value of lack of fit greater than 0.05 (> 0.32) implied that the *F*-statistic was insignificant for all the models. A detailed analysis of the response models is presented in the following sections.

Table 3-3 ANOVA analysis for the applied response surface model. TP, Total phosphorus; TN, Total nitrogen; A, Total inorganic carbon (TIC); B, Nitrogen: Phosphorus ratio (N:P ratio); C, Light intensity; R^2, Determination coefficient; a.R^2, Adjusted R^2; a.P., Adequate precision; SD, Standard deviation; CV, Coefficient of variation.

Responses	Modified equations with significant terms	Probability	R^2	a.R^2	a.P.	SD	CV (%)	Sum of squares		Probability for lack of fit
								Pure error	Lack of fit	
TP removal (%)	94.54 - 2.96A + 3.56B + 6.56C - 3.52BC - 3.67B^2	< 0.01	0.83	0.74	11.5	3.67	3.96	23.00	98.28	0.52
TN removal (%)	45.78 – 1.15A -25.22B + 10.93C – 4.61AC + 9.89 A^2 + 14.05B^2 -3.92C^2	< 0.01	0.98	0.96	22.9	4.55	8.06	21.03	123.89	0.32
Productivity (g m^{-2} d^{-1})	6.77 + 0.65A + 0.3B + 2.62C - 0.49B^2 + 0.7C^2	< 0.01	0.98	0.97	30.0	0.35	5.12	0.14	0.98	0.37
P content (%)	1.78 + 0.05A + 0.02B - 0.11C - 0.26AB + 0.07BC - 0.13A^2 - 0.14B^2 - 0.14C^2	0.01	0.93	0.84	9.3	0.08	5.49	0.01	0.03	0.61
N content (%)	7.14 - 0.08A + 0.58B - 0.51C + 0.61BC - 0.68B^2 + 0.38C^2	< 0.01	0.94	0.90	16.7	0.26	3.73	0.16	0.38	0.65
Ash content (%)	8.18 - 0.62A + 0.05B - 1.14C - 0.31AB - 0.44AC	< 0.01	0.93	0.89	15.9	0.35	4.28	0.14	0.96	0.38

3.4.2.2 Phosphorus removal

The independence and interdependency of the different variables were analyzed to determine the relationships between TP removal and cultivation conditions. 3D response surfaces and contour plots obtained by the quadratic model were generated, Fig. 3-4. One variable was kept at an optimal level and two variables were allowed to vary within the experimental range, Fig. 3-4. The curvatures reveal that there is a strong interactive effect between the N:P ratio and light intensity, Fig. 3-4 A. The N:P ratio shows an optimum of TP removal efficiency, while the efficiency decreased at larger and smaller ratios, Fig. 3-4 A and C. The individual effects of three independent variables on the TP removal are visualized via perturbation plot, Fig. 3-5 A. The TP removal was sensitive to all three independent variables, Fig. 3-5 A. Strikingly, the light intensity (term C) had the highest coefficient in the modified model equation, Table 3-2. It was the most significant variable for TP removal under all tested light intensities. This is contrary to single cell cultures, where similar light intensities can be harmful and decrease TP removal (Al Ketife et al. 2017).

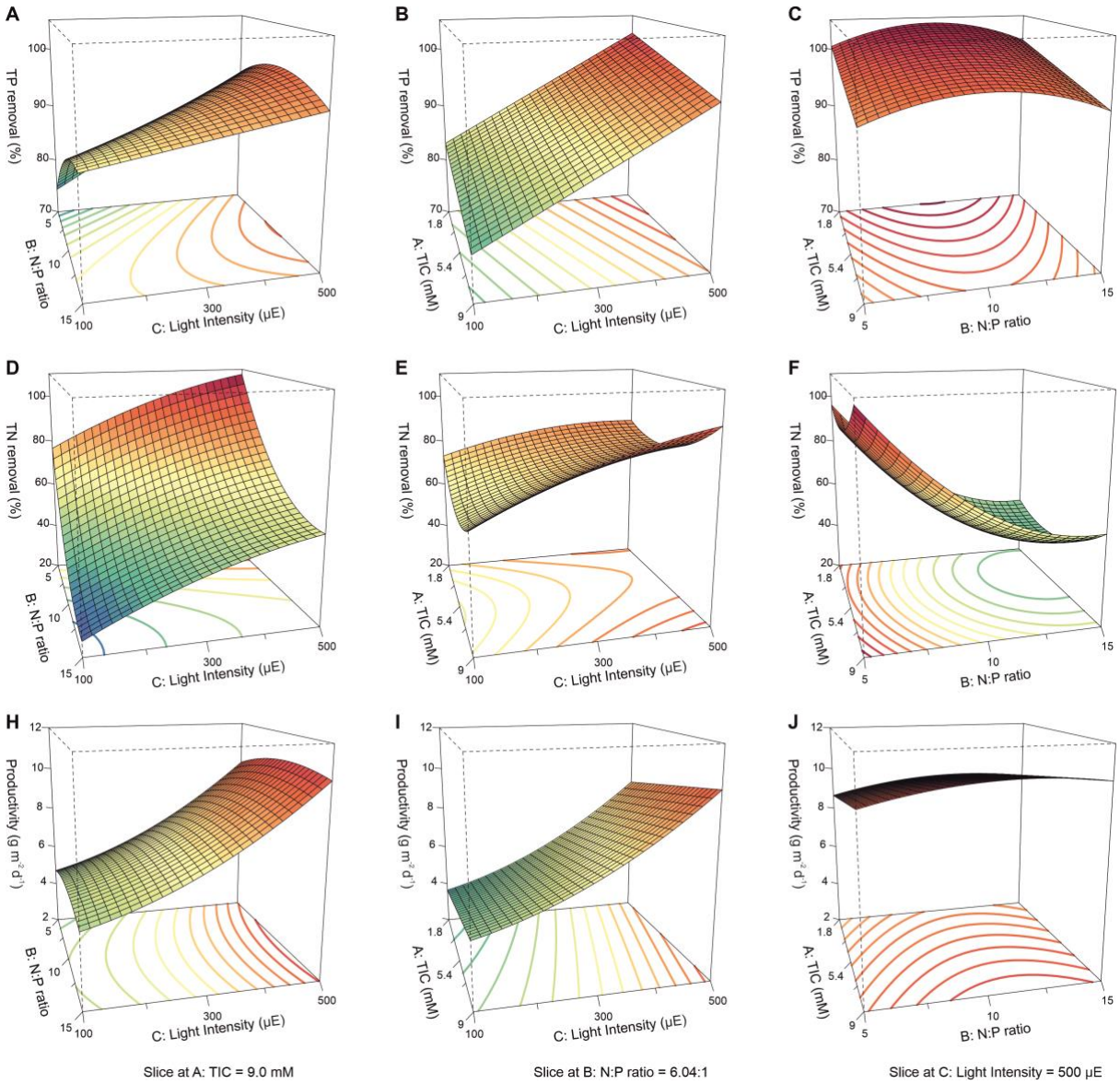

Figure 3-4 3D response surface and contour plots visualizing the interactive effects between TIC concentration, N:P ratio and light intensity for ATS performance. TP removal, TN removal and biomass productivity are shown as a function of N:P ratio vs. light intensity at fixed TIC concentration of 9.0 mM (A, D, H); TIC concentration vs. light intensity at fixed N:P ratio of 6.04:1 (B, E, I); TIC concentration vs. N:P ratio at fixed light intensity of 500 µmol photons m^{-2} s^{-1} (C, F, J), respectively. TIC, Total inorganic carbon; N:P, Nitrogen: Phosphorus ratio; TP, Total phosphorus; TN, Total nitrogen.

3.4.2.3 Nitrogen removal

Similarly, the relationships between TN removal efficiency and cultivation conditions were analyzed. 3D response surface and contour plots and perturbation plots obtained by the

quadratic model of Table 3-3 are shown in Fig. 3-4 D- F and Fig. 3-5, respectively. The interactive effect of TIC concentration and light intensity is displayed in Fig. 3-4 E. The TN removal efficiency was more sensitive to N:P ratio and light intensity than TIC concentration, Fig. 3-5 B, as confirmed by the linear model coefficients. High initial TN concentration may contribute to lower removal efficiency. This is consistent with previous studies showing that TN removal efficiency in algae dropped under high N:P ratios (Liu and Vyverman 2015, Xin et al. 2010). Moreover, the significant positive effect of light intensity on TN removal efficiency confirmed that NO_3^- -N assimilation in algae is an energetically expensive process (Perez-Garcia et al. 2011).

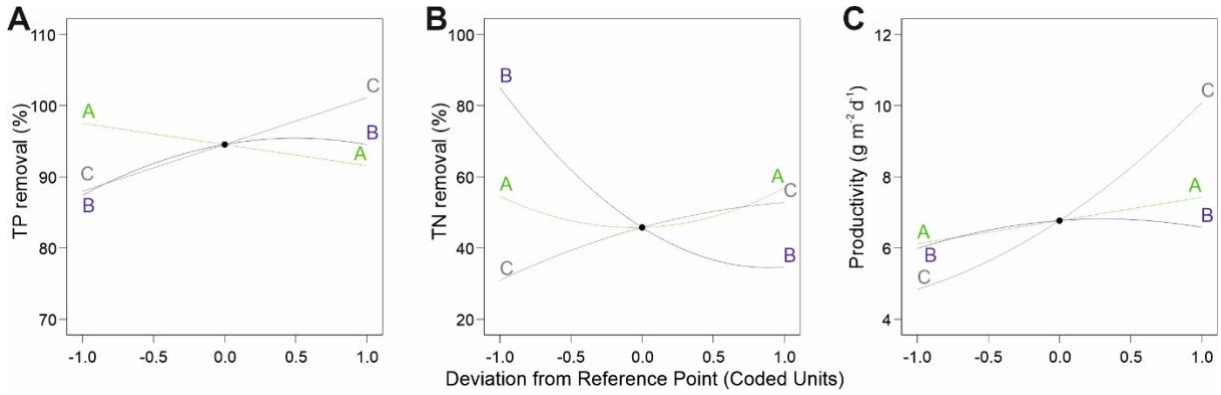

Figure 3-5 Perturbation plot of the dependent variables (A) Total phosphorus and (B) Total nitrogen as well as (C) Biomass productivity. Legend: A, Total inorganic carbon; B, Nitrogen: Phosphorus ratio; C, Light intensity.

3.4.2.4 Biomass productivity

The third performance indicator for the ATS effectivity was biomass productivity. Overall, the productivity of ATS was 4.14 to 11.23 g m^{-2} d^{-1} under all the treatments, Table S 3-2. Our results are in line with other studies, despite the wide range of ATS productivities (2 - 49 g m^{-2} d^{-1}) due to the different cultivation and nutrient conditions (Liu et al. 2016, Marella et al. 2019, Walter et al. 2008).

Parameters of the quadratic model to biomass productivity are presented in Table 3-3. The 3D response surface and contour plots are shown in Fig. 3-4 H-J and Fig. 3-5 C, respectively. The biomass productivity was sensitive to all three independent variables, Fig. 3-5 C. Again, light intensity had a strong positive effect and showed the highest coefficient in the model equation, Table 3-3. This aligns with previous studies demonstrating the increased

light resilience of algal biofilm compared to single-cell cultures (Al Ketife et al. 2017). Naturally, photosynthetic bacteria and algae stratify within a biofilm matrix according to the light availability and their preference (Thapa et al. 2017). Additionally, the TIC concentration had a significant positive effect on ATS biomass productivity. Although we found no publication reporting on the effect of TIC concentration on ATS biomass productivity, it has been shown that bicarbonate can promote higher biomass productivity (Su 2020, Zhu et al. 2021).

3.4.2.5 Biomass P, N, and ash content

For a subsequent valorization of the nutrient-rich biomass, the P-, N-, and ash-contents were quantified under the different growth conditions, Fig. S 3-2 A-J. The P-content ranged from 1.1 ± 0.1 to 1.9 ± 0.2% DW, Fig. S 3- 2 A-C. Similar P-values of 0.9-3.2% DW were reported for ATS biomass using municipal WW (P: 3.7- 4.4 mg L^{-1}). Additionally, we identified a significant interactive effect for the P-content between TIC concentration and N:P ratio, Fig. S 3- 2 C.

The N-content reached 7.8 ± 0.2% DW, Fig. S 3- 2 D-F. At this level, we identified a significant interactive effect on the N-content by light intensity and N:P ratio in the medium, Fig. S 3- 2 D. Strikingly, the N-content reached its maximum at a medium N:P ratio of 10:1, while a higher N:P ratio (15:1) caused a reduced N-content of the biomass, Fig. S 3- 2 D.

The ash-content of ATS biomasses ranged from 6.4 ± 0.2 to 9.5 ± 0.4% DW, Fig. S 3- 2 H, I, J. These values are 6- to 10-fold lower than those previously reported for ATS biomass grown in agricultural drainage or reservoir water (Chen et al. 2015, Kangas and Mulbry 2014). Based on microscopic observations, we suggest that the low ash content was due to the low number of diatomaceous sediments and suspended solids, the major contributors to the ash. Moreover, we found an inverse correlation (R^2 = -0.73) between biomass productivity and ash content. Increased growth at high TIC concentration and light intensity decreased the final ash content of the biomass, Fig. S 3- 2 I.

3.4.3 Process optimization

We identified via BBD-RSM the optimal cultivation conditions (TIC 5 mM, N:P ratio 6.04, light intensity 500 µE) to simultaneously maximize TP and TN removal, as well as the biomass productivity. Accuracy of the optimal conditions was confirmed by experimental

data within the prediction interval (PI) and in proximity to the predicted values, Table 3-4. It should be noted that the optima of TIC concentration and light intensity were both located at the very limit of the chosen range. However, under these optimal conditions, the predicted nutrient removal was very close to 100%, Table 3-4. Considering that light was the most important variable in ATS performance, we experimented with the higher light intensity of 1000 µmol photons m^{-2} s^{-1}. We then set the other variables at their predicted optimal values. We found no significant differences ($p < 0.5$) between in TP and TN removal or biomass productivity at the 500 and 1000 µmol photons m^{-2} s^{-1}, respectively, Table S 3-3. This indicates that 500 µmol photons m^{-2} s^{-1} light intensity is close to the saturation level for nutrient removal in our ATS system.

Table 3-4 Validation results under optimized growth conditions of TIC (9 mM), N:P ratio (6.04, TP 10 mg L^{-1}), and light intensity (500 µmol photons m^{-2} s^{-1}). Data are presented as mean ± standard error (SE, n = 3). TP, Total phosphorus; TN, Total nitrogen; PI, Prediction interval.

Responses	Experimental (mean ± SE)	95% PI (low)	Predicted	95% PI (high)	Error (%)
TP removal (%)	97.25 ± 0.81	82.27	95.85	109.43	1.44
TN removal (%)	91.25 ± 0.44	84.93	100.0	115.07	8.75
Productivity (g m^{-2} d^{-1})	10.58 ± 0.28	9.06	10.22	11.38	3.40

3.5 Conclusion

The ATS is a promising algal-based WW treatment technology. It can achieve high nutrient removal in a short time. This study successfully demonstrated the RSM-based optimization of both nutrient uptake and biomass productivity in a lab-scale ATS. Up to 80% of phosphorus was removed within 24 h. We were able to show the correlation of independent variables such as TIC, N:P, and light with nutrient removal and biomass production. Ongoing studies utilize these findings to optimize nutrient removal at a production scale in ATS systems at WW treatment facilities and using other WW types.

4 Stable year-round nutrients removal and recovery from wastewater by technical-scale Algal Turf Scrubber (ATS)

Based on a journal article published as Gan, X., Klose, H. and Reinecke, D., 2023. Stable year-round nutrients removal and recovery from wastewater by technical-scale algal Turf Scrubber (ATS). *Separation and Purification Technology, 307, p.122693*. https://doi.org/10.1016/j.seppur.2022.122693

Contribution: Design 70%, Experimentation 100%, Analysis 90%, Publication work 80%

4.1 Introduction

Ever increasing amounts of nutrient-rich and problematic wastewaters are discharged into natural water bodies, causing a chronic nutrient loss and environmental damages (Daud et al. 2015, Pittman et al. 2011). Thus, wastewaters need to be treated and nutrients removed for reuse. Here, algal-based bioremediation technologies are an attractive approach, they can offer high nutrient removal and broad recovery capacity (Gan et al. 2016, Kube et al. 2020, Li et al. 2019c, Li et al. 2022, Su 2020, Wang et al. 2018b, Wei et al. 2020). The two major algal cultivation technologies are the suspended microalgal and the attached biofilm cultures. Suspended cultures have been hindered from widespread implementation, due to low biomass density and resulting high harvest costs (Kesaano and Sims 2014, Su 2020, Zhu et al. 2021, Zhu et al. 2019). Harvest processing can account for up to one-third of the total costs Acién et al. (2012). Algal biofilm systems were proposed in wastewater treatment for their higher biomass density and easier harvesting process (Kesaano and Sims 2014, Wang et al. 2018a). A mesocosmic biofilm of bacteria, pro- and eukaryotic algae, fungi, and protozoa is cultivated with polluted waters or wastewaters (Kangas et al. 2017, Kebede-westhead et al. 2003, Kesaano and Sims 2014, Liu et al. 2016, Mulbry and Wilkie 2001). One of these algal biofilm systems is the Algal Turf Scrubber (ATS). The ATS biofilm is attached to a substrate, submerged in water, and can easily and cost-effectively be harvested by draining and scraping-off (Kesaano and Sims 2014, Pizarro et al. 2006). The nutrient-rich ATS biofilm can be valorized as fresh or dried fertilizer, soil conditioner or biogas substrate (Cheenakula et al. 2022, Gray 2021, Marella et al. 2019, Pizarro et al. 2006, Ray et al. 2015, Schreiber et al. 2018). ATS systems have successfully tested with agricultural, industrial and urban wastewaters (D'Aiuto et al. 2015, Higgins and Kendall 2011, Mulbry et al. 2008, Ray et al. 2015, Reinecke et al. 2022, Walter et al. 2008). Thus, ATS systems could be a promising technology for nutrient cycling in a circular bioeconomy.

Yet, biological wastewater treatment technologies, such as the ATS, are effected by various culture and environmental variables, e.g. system design, shear force, retention time, nutrient load, light quantity and quality, osmolarity, temperature, and biotic factors (D'Aiuto et al. 2015, Gan et al. 2022, Liu et al. 2016). Multiple variables and their interactive effects have to be taken into account and simultaneously optimized in industrial-scale systems under field conditions. Here, water temperature and light intensity were identified as critical

independent variables in modulating the ATS performance (Kesaano and Sims 2014, Mulbry et al. 2008). Therefore, it remains essential to understand and control the interactive effects of daily and seasonal water temperature and light intensity in outdoor ATS systems. However, previous studies often focused on just one variable and its effect on ATS biofilm performance (Kesaano and Sims 2014, Zhu et al. 2022).

In this study, three technical-scale ATS systems were continuously operated to evaluate the nutrient removal and recovery under greenhouse conditions, over one year. The independent and interdependent effects of water temperature and light intensity on the biomass composition, and nutrient removal and recovery were identified via mathematical modeling. The obtained data were used for an ad-hoc economic evaluation.

4.2 Materials and methods

4.2.1 Algal Turf Scrubber (ATS) system

Three identical technical-scale ATS systems were designed and constructed based on our previous research (Fig.3-1) (Gan et al. 2022). They were positioned in North-South- direction in a greenhouse without climate control in western Germany (N 50°54´20; E 6°25´4). The flow-way surface area was 0.5 x 1.6 m (0.8 m^2). The flow-ways were lined with polystyrene plates (100 x 50 x 1 cm) for thermal insulation, transparent pond liner for wastewater containment, and glass-fiber reinforcement fabric (mesh: 0.35 x 0.35 cm) for biofilm attachment (growth substratum). The substrate material was selected for its hydrophobic and rugged material properties (Zhou et al. 2021). Moreover, its mesh promoted a stable biofilm formation and provided niches for residual biofilm (10%) during harvest, allowing the continuous cultivation. The slope of the flow-way was adjusted at 1% (3.6°) inclination. A submersible pump in the wastewater container delivered medium at 2 L min^{-1} onto the flow-way. A tipping bucket made by acrylic distributed the water in a wave-like fashion at the interval of 10 min^{-1}. The medium drained from the flow-way back into the container.

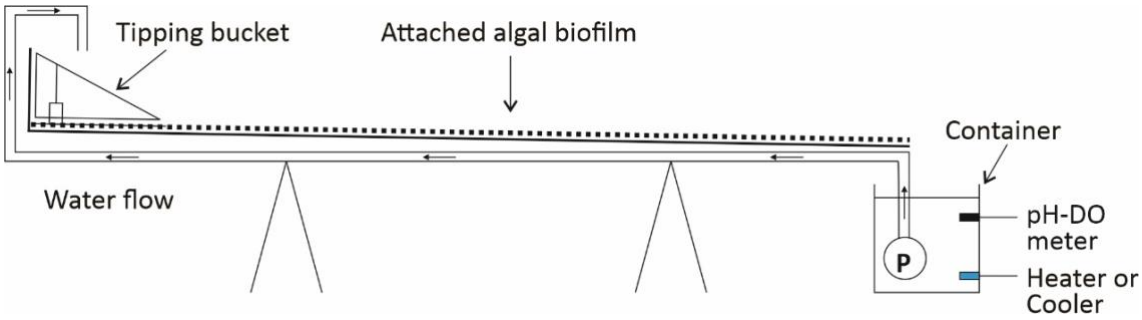

Figure 4-1 Schematic drawing (side view) of technical-scale Algal Turf Scrubber (ATS).

4.2.2 Experimental design and culture conditions

To evaluate the nutrient removal and recovery performance of ATS systems under seasonal changes, three ATSs were continuously operated in a greenhouse for one year. All ATS were inoculated with one pre-existing ATS biofilm. Two months pre-cultivation was given to establish a mature biofilm. Ten months (July, 2021 to May, 2022) were used for experiments under various water temperatures and light intensities (n = 37). The ATSs were operated in four phases, I: natural environmental conditions; II: controlled and increased water temperature (heater); III: controlled and increased light intensity (lamps); IV: controlled and decreased water temperature (cooler) (Fig. S 4-1). Sensors were used to measure the water temperature in the container (HOBO, UA-002-64, HOBO Pendant®, USA) and the light intensity on the flow-way (BayEOS, BayCEER, Germany). Weekly measurements of water temperature and light intensity were used for data modeling (Section 3.2.5).

Each experiment was conducted for 7 days. At the start (d_0) of each experiment, 70 L of artificial wastewater was added to the container of each ATS. The artificial wastewater was based on optimized BG11 medium with TN (60.4 mg L^{-1}), TP (10 mg L^{-1}), and TIC (9 mM) according to our previous research (Gan et al. 2022). Evaporation losses were compensated with tap water throughout. The dissolved oxygen (DO), pH-value, total phosphorus (TP), and nitrogen (TN) in the medium were measured daily. At the end (d_7) of each individual experiment, biofilms were harvested. The harvest was done by stopping the water flow, draining, and scraping off the algal biofilm. Biofilms were portioned and oven or freeze-dried for analysis. Residual ATS biofilm which contained bacteria, pro- and eukaryotic algae, fungi and ciliates at the substrate served as inoculum for the next experiment (Fig. S 4-2). New experiments were started immediately after harvest.

4.2.3 Wastewater analysis

2 mL of wastewater were collected from each ATS container. The wastewater samples were filtered through a 0.45 µm filter (LCW 916, Hach-Lange®, USA). The filtrate was used for further analysis. TN (220 and 275 nm) and TP (at 880 nm) were determined spectrophotometrically according to the UV-screening method (Association 1998) and the ammonium molybdate spectrometric method (ISO 2004), respectively. A data-logger (LabQuest 3, Vernier®, USA) equipped with specific sensors was used to measure the DO concentration and pH-value *in situ*.

4.2.4 Biomass analysis

The attached algal biomass was harvested by scraping off the ATS biofilm from the substrate mesh-net with a metal scraper (d_7). The total wet biomass was weighed by scale. Approximately 100 g of well-mixed biofilm was weighed and centrifuged at 4200 *g* and 4˚C for 10 min. The biofilm pellet was freeze-dried to determine its dry weight (DW). Suspended algal biomass was determined in 100 mL culture medium sampled from the container and filtered through a 0.45 µm filter (1822-047, Whatman®, USA). The loaded filter was oven dried to a consistent weight at 70 ˚C to determine the dry weight. The sum of attached and suspended biomass was calculated as the total DW. The total biomass productivity was calculated as follows, Eq. (1):

$$\begin{aligned}&\text{ATS biomass productivity (g m}^{-2}\text{ d}^{-1}\text{)}\\ &= \text{Total DW (g) / ATS area (m}^2\text{) / cultivation days (d)}\end{aligned} \quad (1)$$

8-10 mg lyophilized biomass was used to determine the C and N content via an elemental analyzer (Vario® Elementar, Germany). About 200 mg of lyophilized biomass was digested with 5 mL of HNO_3 in a microwave digestion apparatus (MARS6, CEM®, USA), and the digested liquid was used for the determination of P and K content by Inductively Coupled Plasma- Optical Emission Spectrometry (ICP-OES Ultima 2, HORIBA®, France). Approximately 100 mg of lyophilized biomass was combusted in a muffle furnace at 550 ˚C for 2 h to determine the ash content (Chen et al. 2015).

4.2.5 Mathematical model analysis of ATS performance

4.2.5.1 Regression model building

To evaluate the effect and relationship of the environmental conditions, water temperate and light intensity on the nutrient recovery efficiency and biomass productivity of ATS, four different models were applied by R 4.2.0®: linear, 2-factors interaction, quadratic, and cubic models, Eq. (2-5):

$$y = \beta_0 + \beta_1 T + \beta_2 I + \varepsilon \quad (2)$$

$$y = \beta_0 + \beta_1 T + \beta_2 I + \beta_{12} TI + \varepsilon \quad (3)$$

$$y = \beta_0 + \beta_1 T + \beta_2 I + \beta_{12} TI + \beta_{11} T^2 + \beta_{22} I^2 + \varepsilon \quad (4)$$

$$y = \beta_0 + \beta_1 T + \beta_2 I + \beta_{12} TI + \beta_{11} T^2 + \beta_{22} I^2 + \beta_{112} T^2 I + \beta_{122} TI^2 + \beta_{111} T^3 + \beta_{222} I^3 + \varepsilon \quad (5)$$

Where y is the response variable to be modeled. β_0; β_1, β_2; β_{11}, β_{22}; β_{111}, β_{222}; β_{12}, β_{112}, β_{122} are regression coefficients for intercept; linear; quadratic; cubic; interaction coefficients, respectively. T (weekly water temperature) and I (weekly light intensity) are independent variables and ε is the residual.

4.2.5.2 Model selection

Different statistical regression metrics were used for measuring regression model quality and for comparing models. They are Akaike's Information Criteria (AIC), Bayesian Information Criterion (BIC), Root Mean Squared Error (RMSE), percentage prediction error (PER), and Adjusted R-squared (Adjusted R^2). The most suitable model was selected specifically for each response based on a comprehensive analysis of regression metrics.

4.2.5.3 Model visualization

The independent and interactive effects of the independent variables on the ATS performance in the selected model were visualized in 3D response surface and contour plots, generated with R 4.2.0®. Scatter plots of measured experimental data were added to illustrate the accuracy of the models. The average of three ATSs (3 biological replicates) was used for

the modeling of TP and TN removal efficiency, and of biomass productivity, whereas just one ATS was used for the other responses.

4.3 Results and discussion

4.3.1 Effect of water temperature and light intensity on nutrient removal

To quantify the potential of ATS biofilms in nutrient removal under variable temperature and light conditions, the TN and TP concentrations in the medium were measured daily in 37 experiments. A detailed overview to the tested water temperatures and light intensities is presented in Fig. S 4-1. The operation of the three ATS systems started in July 2021. Within two months of pre-cultivation, the mesocosmic biofilm fully covered the substrate. All three ATS biofilms showed a comparable broad range of genera including eukaryotic filamentous und single-cell green algae (Chlorophyceae), diatoms (Diatomeae), gold algae (Chrysophyceae), fungi and ciliates (Chromista) as well as prokaryotic cyanobacteria (Cyanophyceae) and bacteria (Fig. S 4-2). Comparable to previous studies, our ATS biofilm showed a variable assembly of mixed environmental populations under the tested light and temperature conditions (Kangas et al. 2017, Kebede-westhead et al. 2003, Park et al. 2022, Wicker et al. 2023, Zhou et al. 2021).

Throughout 10 months of operation (n = 37), the water temperature and light intensity ranged from 7.6 to 26.6 °C and from 6.3 to 324.9 µmol photons m^{-2} s^{-1} (Fig. S 4-1), respectively. Within 7 days of each experiment, the ATS biofilm removed 11 to 84% (6.79 ± 0.54 to 50.88 ± 1.78 mg L^{-1}) of TN and 72 to 99% (7.17 ± 0.02 to 9.87 ± 0.02 mg L^{-1}) of TP (Fig. 4-2, Table S 4-1). Within 24 h, the pH value increased to > 9, (data not shown) and 86% of the TP was removed from the medium (Fig. 4-2B). These patterns were consistent with our previous works (Gan et al. 2022). The high pH-value may cause the unspecific P-precipitation and -adsorption processes, as previously described for suspended microalgal and biofilm cultures (Nurdogan and Oswald 1995, Sañudo-Wilhelmy et al. 2004). Contrasting, the TN concentrations showed a stable decrease, over 7 days (Fig. 4-2A). This suggests that energy-dependent assimilation processes were the main mechanism of N-removal (NO_3^-) in our ATS biofilms (Sanz-Luque et al. 2015, Su 2020). The average TN and TP removal rates were 4.42 and 1.28 mg L^{-1} d^{-1}, respectively (Fig. 4-2). ATS biofilms showed a stable TN and TP removal under the tested water temperatures and light intensities.

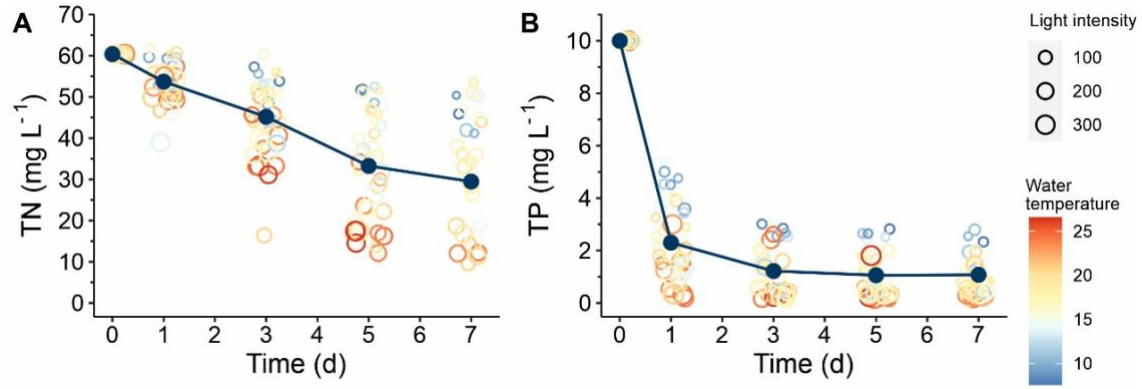

Figure 4-2 Effect of water temperature and light intensity on residual total nitrogen (TN) (A) and total phosphate (TP) (B) concentration in artificial wastewater in ATS systems. Empty circles (○): average of single experiments (n = 3), error bars of single experiments were omitted to improve clarity; solid circles (●): average of all 37 experiments (n = 111).

4.3.2 Mathematical models of nutrient removal

4.3.2.1 Statistical analysis

The statistical regression metrics of different regression models to the nutrient removal are shown in Table S 4-1. To achieve an unbiased estimate with low prediction error, the model of the lowest AIC, BIC and RMSE, RET score was prioritized. Herein, the quadratic model exhibited the highest accuracy in describing the TN and TP removal.

4.3.2.2 Statistical evaluation of nutrient removal

3D response surface and contour plots, obtained by the quadratic models (Table 4-1) were used to visualize the independent and interdependent effects of water temperature and light intensity on nutrients removal (Fig. 4-3). The high degree of prediction accuracy for our selected models is shown in scatter proximity surface plots (Fig. 4-3 A and C) and confirmed by high adjusted R^2 values (Table S 4-1).

The light intensity had a significant positive effect on the TN removal efficiency (Fig. 4-3 A and B). These findings are in line with our previous works (Gan et al. 2022). Generally, photosynthetic activity increases with the light intensity up to the point of light saturation and subsequent photoinhibition. The range of light quantity is specie-dependent and varies according to the physiological state of the individual algal cells (Arhonditsis et al. 2004, Banaś et al. 2012, Bender et al. 2012, Bhandari and Sharma , Campenni et al. 2013, Singh and

Singh 2015). Our data show that the tested growth conditions caused no light inhibition in the ATS biofilm but proved growth sustaining (Fig. 4-3). The algae gained enough energy to reduce the NO_3^- to NO_2^- in their cytosol, to recycle the NH_4^+, and to complete metabolization (Foyer et al. 2012, Sanz-Luque et al. 2015, Su 2020). The tested water temperatures had no significant effect on the TN removal efficiency (Fig. 4-3 A and B). Even winter-like temperatures (> 7.6 °C) did not inhibit the photosynthetic and metabolic performance of the ATS biofilm.

Contrasting, the TP removal efficiency was significantly affected by both, water temperature and light intensity, (Fig. 4-3 C and D). Phosphate was rapidly precipitated from the medium with the raising pH-value, and subsequently adsorbed and assimilated by the algae (Zhou et al. 2017). In a comparable study with algal biofilms under greenhouse conditions, P removal increased with increasing light intensity Sukačová et al. (2015). Our results confirm that light intensity is one of the dominant variables for nutrient removal in ATS systems.

Table 4-1 Equations of selected mathematical models for nutrient removal in ATS.

Response	Equation of selected model
TN removal (%)	$9.00 - 0.43T + 0.42I + 5.86e-03TI + 2.40e-02T^2 - 1.09e-03I^2$
TP removal (%)	$49.81 + 2.18T + 0.25I - 4.09e-03TI - 3.10e-02T^2 - 4.13e-04I^2$

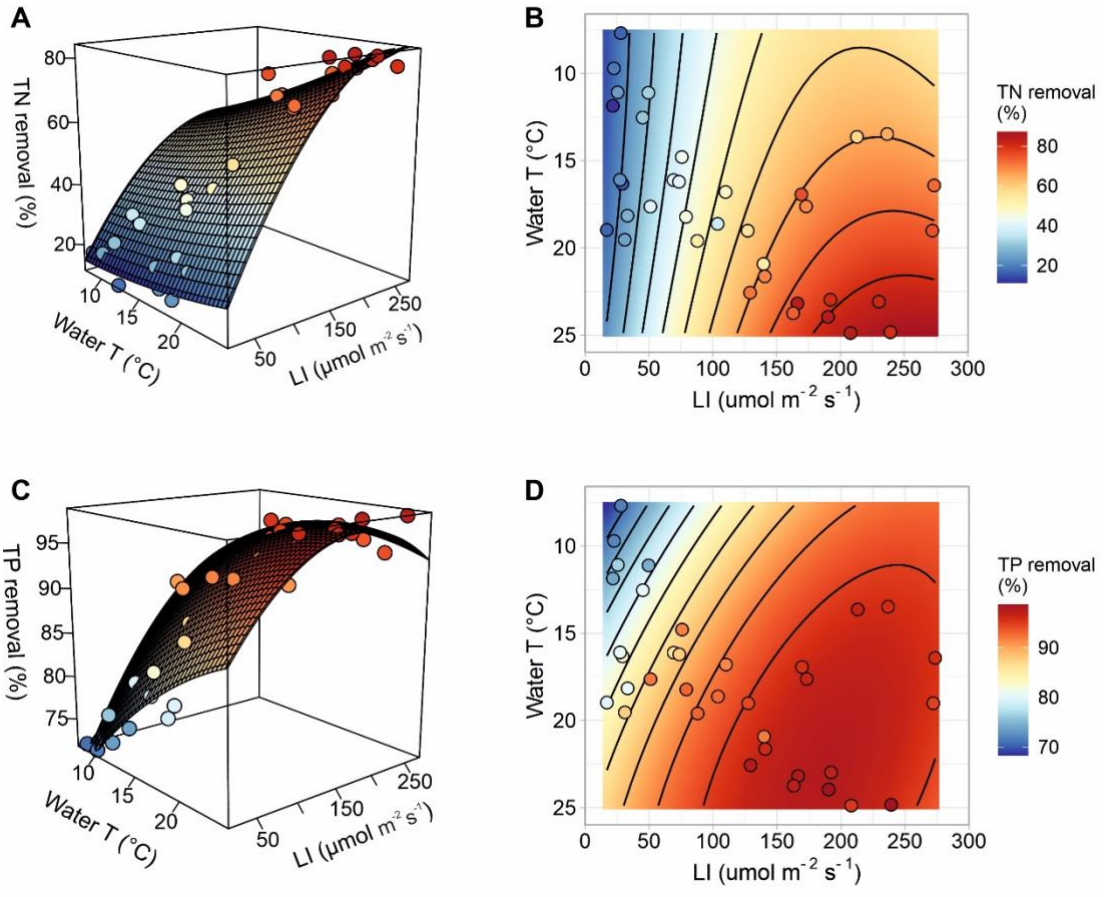

Figure 4-3 3D response surface and contour plots for total nitrogen (TN) (A, B) and total phosphate (TP) (C, D) removal efficiency. Circles (●): experimental data; Water T: water temperature; LI: light intensity. High values are displayed in red and the low values in blue.

4.3.3 Mathematical models of biomass productivity and nutrient content

4.3.3.1 Statistical analysis

The choice of a suitable mathematical model for the biofilm productivity and nutrient content was based again on the lowest AIC, BIC, RMSE, and PER values. Table S 4-2 shows the quadratic models chosen. Based on the statistical regression metric, no model was suitable to describe the K content of ATS biofilms. Therefore, no model was selected for the K content.

4.3.3.2 Statistical evaluation of biomass productivity and nutrient content

Table 4-2 Equations of selected mathematic models for biomass productivity and nutrient contents.

Responses	Equations of selected models
Biomass productivity (g m^{-2} d^{-1})	$-1.00 + 0.55T - 6.56e-03I + 2.21e-03TI - 1.74e-02T^2 + 5.55e-05I^2$
C content (%)	$27.71 + 8.54e-02T + 0.12I + 5.43e-04TI - 5.05e-03T^2 - 3.19e-04I^2$
N content (%)	$3.99 + 8.55e-03T + 1.91e-02I + 2.25e-04TI - 7.35e-04T^2 - 4.87e-05I^2$
P content (%)	$1.86 + 2.97e-02T - 8.40e-03I - 1.67e-04TI - 2.13e-04T^2 + 2.54e-05I^2$
K content (%)	N/A

The 37 independent experiments, with 3 biological replicates each (n = 111), were analyzed for nutrient recovery, biomass productivity and composition (C, N, P, K). 3D response surface and contour plots, obtained by the quadratic models (Table 4-2), visualize the independent and interdependent effects of water temperature and light intensity on nutrient content in the ATS biofilm (Fig. 4-4).

The biomass productivity of our ATS systems ranged from 2.88 ± 0.08 to 10.55 ± 0.01 g m^{-2} d^{-1} (Fig. 4-4 A and B). These results are consistent with our previous findings (4.14 to 11.23 g m^{-2} d^{-1}) in lab-scale ATS under similar culture conditions (Gan et al. 2022). Additionally, a strong positive interactive effect between water temperature, light intensity and the biomass productivity was found (Fig. 4-4 A and B). Similarly, other studies showed that both water temperature and light intensity have significant positive effects on algal biomass productivity (Aston et al. 2018, Chaiwong et al. 2021). Yet, often studies are limited to a single independent variable, few repetitions, or very artificial growth conditions. This can limit their comparability and applicability to field-studies. Our results indicate that the simultaneous increase in water temperature and light intensity increased biomass productivity, a typical response in outdoor ATS systems.

The biomass C, N, P and K content were used to evaluate the nutrient transfer from wastewater to biofilm, and its suitability as fertilizer. The biomass C content reached up to 40.6% DW under high light intensity and light intensity was the dominant variable for C content (Fig. 4-4 C and D). Higher light intensities may facilitate the energy-demanding carbon concentration mechanism in the algal biofilm (Raven et al. 2008, Su 2020). The N content reached up to 7.45% DW (Fig. 4-4 E and F). The light intensity had a significant positive effect on N content, too. Nitrogen uptake requires a variety of complementary energy-dependent pathways which can be accelerated under higher light intensities (Perez-Garcia et al. 2011, Su 2020). The P content reached up to 2.19 % DW (Fig. 4-4 H and I). While light intensity had a significant negative effect on P content, since P uptake is not strictly light driven (Moseley and Grossman 2009). Even an increased acidic polyphosphate accumulation was described under lower light intensity (60 μmol m^{-2} s^{-1}) in algae Powell et al. (2009). The K content reached up to 1.28% of DW, but none of our models could describe its dependency of light or temperature conditions. This might be related to the multiple complimentary and energy-dependent pathways of potassium assimilation in algae (Talling 2010).

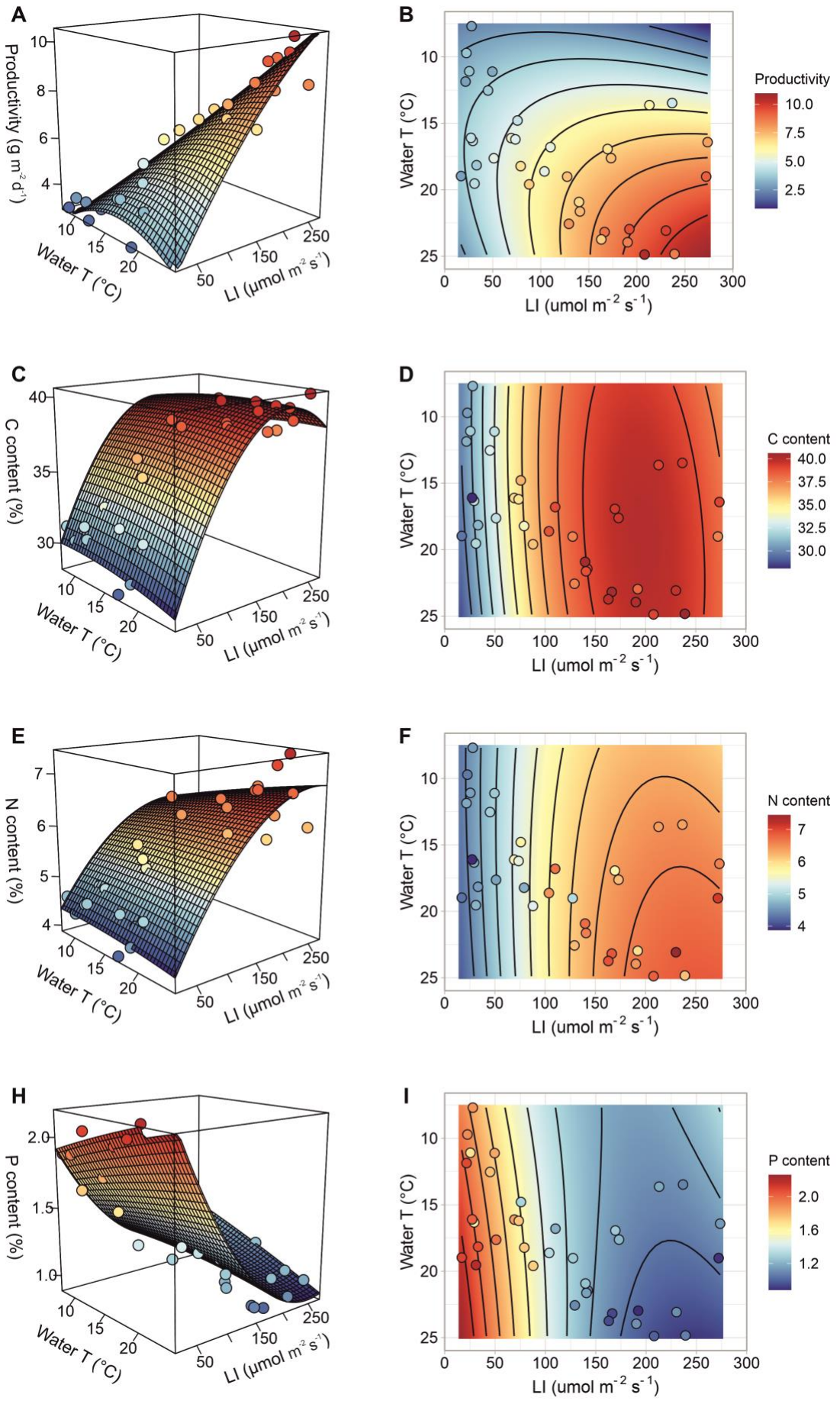
A
Productivity (g m-2 d-1)
Water T (°C)
LI (µmol m-2 s-1)
B
Water T (°C)
LI (umol m-2 s-1)
Productivity
10.0
7.5
5.0
2.5
C
C content (%)
D
C content
40.0
37.5
35.0
32.5
30.0
E
N content (%)
F
N content
7
6
5
4
H
P content (%)
I
P content
2.0
1.6
1.2

Figure 4-4 3D response surface and contour plots of biomass productivity (A, B), C content (C, D), N content (E, F), and P content (H, I). Circles (●): experimental data; Water T: water temperature; LI: light intensity. High values are displayed in red and the low values in blue, respectively.

4.3.4 Correlation analysis

Pearson correlation analysis was used to evaluate the interrelationships between the dependent variables of ATS biofilm response (Fig. 4-5). The TN and TP removal efficiencies showed a significant correlation (r = 0.83). The biofilm productivity was positively correlated with TN (r_{TN} = 0.87) and TP (r_{TP} = 0.78) removal efficiencies, respectively (Fig. 4-5). Further, biofilm productivity was significantly positive correlated with its C (r = 0.74) and N (r = 0.71) content (Fig. 4-5). Yet, biofilm productivity was negatively correlated with its P (r = -0.77) and ash (r = -0.86) content (Fig. 4-5). No correlations were found between the K content and any other variable. Further research is need to the potassium removal and metabolization in ATS biofilm, prior its valorization as fertilizer.

Our ATS biofilms showed significant correlations between the nutrient recovery and biomass composition (Fig. 4-5). These findings are in line with previous studies, directly linking nutrient removal and biofilm growth (Craggs et al. 1996, Gross and Wen 2014), Kesaano and Sims (2014), (Schnurr and Allen 2015). Therefore, it is possible to deduce, to a certain extent, the growth and nutrient removal of ATS biofilms by one variable. This would enable daily monitoring of the ATS performance by selecting an “easy to measure” variable, such as TN in the effluent.

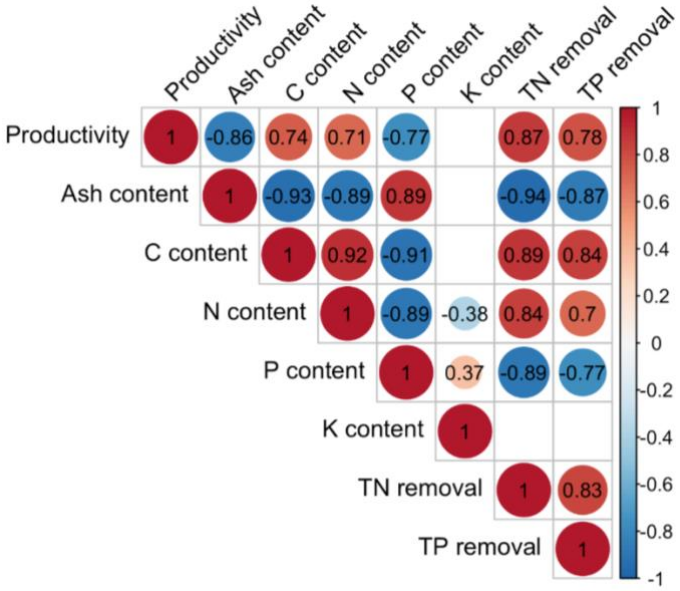

Figure 4-5 Pearson correlation matrix for nutrient recovery and removal capacity of ATS biofilm (n = 37). The correlation coefficients are shown in a heatmap ($p < 0.05$) as positives (red) and negatives (blue).

4.3.5 Cost estimates of annual nutrient recovery in ATS

To evaluate the economic potential of ATS systems in nutrient recovery from wastewater, we estimated the capital (CapEx) and annual operating costs (OpEx) for an industrial-scale (1ha) ATS system located in Germany based on the average biomass productivity and nutrient contents from the technical scale ATS in current study (Tables 3-3 and 3-4). It was assumed that the ATS system was at ground level, to reduce construction, material and maintenance costs. The ATS biofilms required no centrifugation or filtration prior solar drying. The ATS system was assumed to operate at 300 days per year for 20 years. The costs for land, materials, labor, and electricity were based on average German market prices in 2021. Such an ATS system would require an approximate capital investment of 221,790 € and an annual operational budget of 40,610 € (Tables 3-3 and 3-4). Our estimate identified the costs for site preparation (54.5%) and electricity (56%) as the major drivers of CapEx and OpEx, respectively (Tables 3-3 and 3-4). The estimated production costs of algal biofilm, N and P were 2.27, 39.77, and 156.31 € kg^{-1}, respectively (Table 4-4). In other ATS systems the costs of N and P fixation can range between $US 5 to 90 and 25 to 830 kg^{-1}, respectively (Craggs et al. 1996, Kangas and Mulbry 2014, Pizarro et al. 2006). Our cost estimates fall in the lower range, despite higher costs for land (100,000 €, $US 4,000) and

electricity (0.32 €, $US 0.06 kWh^{-1}) (Tables 3 and 4) (Kangas and Mulbry 2014, Pizarro et al. 2006). Biomass production costs in our ATS system were just 18% of those in tubular photobioreactors (12.60 € kg^{-1}) (Acién et al. 2012). A comparable price (2.22 €) was found for ATS biofilms grown in municipal wastewater in a system of 0.18 ha (Reinecke et al. 2022). This cost reduction in ATS systems could be achieved by lowering the CapEx (simple design, easy-to-install, marginal land), OpEx (easy maintenance, harvest and drying, less energy consumption) and a high biomass density of the algal biofilm. Therefore, ATS systems can be a low-cost algal-based technology for nutrient recovery from various wastewaters.

Table 4-3 Estimated capital costs (CapEx) of an industrial-scale (1 ha) ATS system in wastewater treatment.

	Cost (€)	Percentage of Total (%)
Site preparation	**120,000**	**54.5**
Land for ATS system (1 ha)	100,000	
Land for solar drying	3,000	
Construction & Earthworks	20,000	
Raw materials	**60,000**	**26.6**
Pond liner [1]	48,000	
Substrate mesh-net [2]	8,000	
Tipping bucket [3]	1,500	
Pipes & hoses	2,000	
Electricity cables	500	
Pump [4]	5,000	
Labor	**4,992**	**2.2**
Supervisor [5]	3,120	
Workers [6]	1,872	
Subtotal	184,992	
Engineering and contingencies (20% of subtotal costs)	**36,798**	**16.7**
Total capital investment	**221,790**	

[1] Value based on 4.80 € m^{-2} for pond liner.

[2] Value calculated using 0.80 € m^{-2} for nylon netting.

[3] Value based on 10 tipping buckets.

[4] Value based on 10 pumps (1 kW).

[5] Estimated cost of one supervisor based on 40,- € h^{-1} for 2 weeks (39 h per week).

[6] Estimated costs of two workers based on 12,- € h^{-1} for 2 weeks (39 h per week).

Table 4-4 Estimated annual operational costs (OpEx) of an industrial-scale (1 ha) system in wastewater treatment. Based on 300 days of operation per year, and 20-year depreciation on capital costs.

	Cost (€)	Percentage of Total (%)
Capital expenses	11,090	**27.3**
Labor [1]	6480	**15.9**
Electricity pump [2]	23,040	**56.7**
Total annual operational costs	**40,610**	
Cost per kg sun-dried biofilm [3]	2.27	
Cost per kg N [4]	39.77	
Cost per kg P [5]	156.31	

[1] Estimated cost of one operator based on 540,- € per 40 h and month.

[2] 0.32 € kWh^{-1} national average price, retrieved on 18.07.2022.

[3] Based on total costs and average annual biomass productivity (6 g m^{-2} d^{-1}, 18 t a^{-1}).

[4] Based on total costs and nitrogen recovery rate (0.342 g N m^{-2} d^{-1}, 1.026 t a^{-1}).

[5] Based on total costs and phosphate recovery rate (0.087 g P m^{-2} d^{-1}, 0.261 t a^{-1}).

4.4 Conclusion

Our results illustrate the highly efficient and year-round nutrient recovery and biomass production in ATS systems. Under winter conditions, an increase in light intensity was the most effective way to increase ATS performance. Under balanced growth conditions, an easily measured growth variable can be employed to deduce the overall ATS performance. Our cost estimate for ATS biomass was just 18% (2.27 €) of the production costs in conventional tubular photobioreactors. Our results demonstrate that ATS systems can be a cost-effective technology for nutrient removal from wastewaters under a wide range of temperature and light condition

5 Synergistic effects of arbuscular mycorrhizal fungi and *Sebacina vermifera* on wheat growth and phosphorus uptake from algal biofilms produced on municipal wastewater effluent

Based on a to be submitted manuscript by Gan, X., Janus, J., Willbold, S., Dombinov V.,, Amelung W., Klose, H., and Schrey S.

Contribution: Design 60%, Experimentation 60%, Analysis 70%, Publication work 60%

5.1 Introduction

One of the most urgent problems in agriculture is the supply of nutrients necessary for plant productivity. Phosphorus (P) is one of the most important nutrients for plant growth. At present, most of the P used to produce agricultural fertilizer is mined and extracted from rock phosphate. Since P has an extremely long geological cycle - estimates range from hundreds of millions to billions of years (Smil 2000) - and is thus considered a non-renewable resource, strategies to reduce P losses and recover P from waste streams are crucial to prevent possible shortages in the future.

Phosphorus from mineral fertilizers such as ammonium phosphate or superphosphate is highly available to plants, but it can be rapidly immobilized by microbes and fixed by oxides, ultimately limiting its availability to plants (Roy et al. 2016). However, phosphorus can also be lost through runoff, with eutrophication of water bodies being a particularly serious consequence. A common outcome is the occurrence of algal blooms in lakes, rivers and oceans. This phenomenon can be explained by the evolutionary adaptation of algae to environments with rapidly changing nutrient levels, in which they have developed a high efficiency of nutrient uptake. In this context, algae-based bioremediation technologies have emerged as a nature-based solution with considerable nutrient recovery potential. Various technologies including high-rate algal ponds, closed algal photobioreactors, immobilized algal systems and attached algal systems exploit the ability of algae to recover nutrients from a wide range of wastewaters (Mohsenpour et al. 2021, Wang et al. 2018a). The attached algal biofilm reactors are low-cost devices that contain a net-like matrix for the attachment and growth of algal biofilms. Once the algal biofilm (ABF) is sufficiently developed, it can be easily collected by scraping the accumulated biomass from the matrix. One of the algal biofilm systems is the Algal Turf Scrubber (ATS), which has successfully been used for the treatment of manure, agricultural drainage, and urban wastewater (Adey and Bannon 2011, Mulbry et al. 2008, Ray et al. 2015). An industrial scale ATS system (1 ha) can produce 18 tons of dry biomass per year, recovering up to 0.26 and 1 ton P and N, respectively (Gan et al. 2022, 2023). As P recovery from wastewater becomes mandatory in Europe, algae-based systems could become a valuable option to achieve this goal (Hukari et al. 2016).

The algal biofilm, which harbors pro- and eukaryotic algae, bacteria, fungi, and protozoa (Kangas et al. 2017, Liu et al. 2016), can now serve as an intermediate nutrient carrier between wastewater and plant production. Several studies have shown the positive effects of algal fertilizer on plant growth due to its P availability and, to a lesser extent, its nitrogen availability (Coppens et al. 2016b, Mau et al. 2022, Mau et al. 2021, Schreiber et al. 2018). Yet, the P in algal biofilms must be released from the cells and mineralized in order to become available to plants. In the soil, decomposers, among them arthropods, protozoa, fungi, and bacteria break down recalcitrant organic matter and thus initiate the mineralization process (Ekschmitt et al. 2005). Coupled with plant or microbial enzymatic activity, organic P (P_o) is finally converted to inorganic P (P_i) that can be taken up from the plant rhizosphere (Richardson et al. 2011). Some of the above-mentioned studies have investigated nutrient mobilization from algal biomass (Coppens et al. 2016b, Mau et al. 2021), or the mutual effects of microbial communities and algal biomass in soils (Alobwede et al. 2022, Suleiman et al. 2020).

The interaction of algal biomass with soil fungi has received less attention. This is surprising, as it is well known that the arbuscular mycorrhiza fungi (AMF) in particular can contribute to P uptake in mycorrhizal plants (Etesami et al. 2021, Martin and van Der Heijden 2024). AMF are predominantly beneficial for P_i uptake, since these fungi lack the enzymes required to break down organic biomass, and they exert their effects by exploring soil volumes that go way beyond what the roots can reach (Hayman and Mosse 1972, Smith and Read 2010). In the presence of P_o, AMF have been shown to cooperate with phosphate-solubilizing bacteria (Etesami et al. 2021, Zhang et al. 2014). While the benefits of organic fertilization over mineral fertilization in terms of soil biological and biochemical properties are well established (Xie et al. 2014), the effects of organic fertilizers on AMF are less clear, and there is evidence of both beneficial and detrimental effects (Gosling et al. 2006).

The Sebacinales are a group of plant-beneficial root endophytic fungi that has gained increasing attention in the last decade due to their potential for use in agriculture (Ray and Craven 2016, Varma et al. 2012). Root colonization by members of this order can result in increased biomass formation, as well as increased resistance to biotic and abiotic stresses (Ghimire and Craven 2011, Gill et al. 2016). What makes them interesting for agricultural

applications is the fact that they seem to have no host specificity and have been described in numerous plant species, including experimental hosts *Arabidopsis thaliana*, switchgrass (*Panicum virgatum*), barley, maize and wheat (Oberwinkler et al. 2013, Ray and Craven 2016). Switching from conventional agriculture to organic management of agricultural fields resulted in a significant increase in the abundance of members of the Sebacinales in wheat roots (Verbruggen et al. 2014). It has been hypothesized that Sebacinales may be sensitive to mineral fertilizers and pesticides or particularly responsive to organic fertilizers. Clearly, Sebacinales that form mycorrhiza with plants in the Ericaceae family (Selosse et al. 2007) seem to thrive in soils that are rich in organic matter (Verbruggen et al. 2014). Interestingly, the sequenced genome of the isolate *Sebacina vermifera* (*S. vermifera*) contains a range of carbohydrate-active enzymes (CAZymes), indicating that it has saprotrophic abilities (Ray et al. 2019). Even though it is currently still unclear whether CAZymes are expressed during plant-fungus interaction and, if so, whether mobilized nutrients from organic sources are transferred to the host plant, the potential of Sebacinales to contribute to the recovery of organically bound nutrients is intriguing.

The first objective of this work was therefore to analyze the P species in ABF produced by an ATS system and P release into the plant grow substrate. To do so, we conducted an integrated approach that included ^{31}P NMR analyses of ABF, assessment of P release via leachate analyses and a greenhouse experiment to monitor spring wheat (cv. Scirocco) growth and its P uptake from ABF. Secondly, we tested the impact of single and dual inoculation of wheat with AMF and *S. vermifera* on plant growth and P uptake from ABF. We conducted a greenhouse experiment with spring wheat (cv. Scirocco), fertilized with ABF and mineral fertilizer, inoculated with AMF either alone or in combination with *S. vermifera*, and observed plant growth, P uptake, and root colonization by fungi.

5.2 Materials and Methods

5.2.1 Fertilizer

The ABF used as fertilizer in the greenhouse experiments was produced in an ATS system located within a wastewater treatment plant (WWTP; N 51º36’15’’, E 8º46’01’’). The ATS was fed with secondary clarified effluent under field conditions, as described in Reinecke et al. (2023). The biomass from the ATS was harvested on Aug. 26th and Sep. 9th

2021 and pooled. The elemental composition of the ABF was as follows: C: 26.54%, N: 3.94%, P: 1.35%, and K: 0.85%. Additional fertilizers for the greenhouse trials were Triple-superphosphate (TSP, Trifetro Fertilizers (Netherlands)), Hakaphos® Gelb, N:P:K 20:0:16, (COMPO EXPERT GmbH (Germany)) and potassium sulfate (K_2SO_4, Sigma-Aldrich (USA)). Exclusively for the leaching experiment (see below), a second algal biomass (nutrient composition C: 17.2%, N: 1.94%, P: 8.70%, and K: 0.28%) was used which was harvested from an ATS situated within a WWTP at Forschungszentrum Jülich (coordinates N 50º54'36'', E 6 º24'49''). This ATS received effluent directly from the WWTP and operated under field conditions (unpublished).

5.2.2 ^{31}P NMR analysis of algal biofilm

The P from the ABF was extracted by agitating approximately 1 g of dried and milled ABF in a 30 mL extraction solution consisting of 0.25 M NaOH and 50 mM Na_2EDTA. The extraction was carried out for 16 hours. The resulting mixture was centrifuged at 14,000 *g* for 30 minutes prior to collecting the supernatant. The supernatant was frozen and lyophilized at -80 °C. 100 mg of freeze-dried solids was dissolved in 500 µL of a mixture of NaOD and D_2O at pH 13, and 100 µL of methylenediphosphonic acid (MDPA, 0.84 mg mL^{-1} in D_2O) was added as internal reference. After centrifuging the extracts for 30 min at 14,000g, solution 1D ^{31}P NMR data were acquired on a Varian 400 MHz spectrometer equipped with a 5mm broadband probe tuned to ^{31}P nucleus. Spectra were acquired with the following parameters: 45° pulse calibrated at 9.57 µs, 1.0 s acquisition time, 5 s relaxation delay, 32678 scans, proton inverse-gated decoupling at room temperature. Identification of the P species was based on previous measurements of model compounds and natural soils spiked in NaOH-EDTA soil extracts (Missong et al. 2016). The area of each peak was identified to calculate the ratio of P species.

5.2.3 Growth substrate

To represent nutrient-poor substrate with a negligible content of plant-available N, P and K, a mixture of sand (RBS GmbH, Germany; particle size < 1mm) and a nutrient-deficient artificial substrate called "Null Erde" (Einheitserdewerke Werkverband e.V., Germany) was used. The physical properties and nutritional composition of sand (Dombinov et al. 2022) and Null Erde are shown in Table S 5-1.

5.2.4 Phosphorus release dynamics from ATS biofilms

The P release dynamics in water and 50 mM citric acid from two different algal biofilms, the ABF used in the greenhouse experiment containing 1.35% P and a high-P biomass containing 8.7% P, as well as from mineral fertilizers was assessed in a plant-free system. Nutrient addition was identical to pot experiment 2 (see Section 2.3) and fertilizers were mixed with wheat growth substrate, sand: Null Erde, 1:1 *v:v*. Fifty mL reaction tubes (Falcon, USA) were perforated with several 2 mm diameter holes and filled with 50 g of the substrate and the respective fertilizer blend. To adjust water holding capacity (WHC) to 70%, 30 mL of distilled water or 50 mM citric acid were added, respectively. Subsequently, 6-10 mL of distilled water or 50 mM citric acid, respectively, were added every other day to trigger nutrient leaching. The leachates were collected approximately 2h later and the volumes (in mL) were recorded. The leachates were analyzed spectrophotometrically (880 nm, SPECORD 200 PLUS, Jena Analytics, Germany) for bioavailable phosphorus (PO_4^{3-}) according to the protocol for ammonium molybdate spectroscopy (ISO, 2004). Leaching with water was carried out for 42 days, leaching with citric acid for 14 days. Each sampling was carried out with five replicates.

5.2.5 Greenhouse pot experiments

Two pot experiments were conducted in the greenhouse at Forschungszentrum Jülich, Germany (N 50º54’36’’, E 6 º24’49’’) to investigate the effect of ABF and/or fungal inoculation on wheat (*Triticum aestivum*, var. Scirocco, KWS SAAT SE, Germany) growth. The nutrient poor substrate, i.e. sand/ Null Erde mixture, was homogeneously fertilized with ABF or TSP, equivalent to 37 mg kg^{-1} P. As the N and K in ABF were insufficient for wheat growth, Hakaphos® Gelb (containing only N and K) and K_2SO_4 were added at 377.6 N mg kg^{-1} and 303.8 K mg kg^{-1}. Negative control in experiment 1 was the pure nutrient-poor substrate, while in experiment 2 the nutrient-poor substrate was supplemented with identical N and K concentrations as the mineral treatment.

The BayEOS sensor (BayCEER, Germany) was used to measure the light intensity on the plant surface between 6 a.m. to 10 p.m., as well as the air temperature inside the greenhouse. An automatic drip irrigation system was used to water approximately 60% of the respective

water-holding capacity of the substrate with salt-free water. All the pots were regularly randomly arranged to ensure a randomized placement of experimental units.

5.2.5.1 Response of wheat growth to fertilization with algal biofilms (Experiment 1)

Experiment 1 was conducted from April to June 2022 and aimed to investigate the impact of ABF on wheat growth and P uptake. To do so, 18 pots (17 cm Ø, 2 L) were filled with 1.8 kg of nutrient-poor substrate (sand: Null Erde, 1:2 *v:v*) containing the fertilization treatments described above. Five wheat seeds germinated in the fertilized substrates and were then thinned to 3 seedlings per pot after 3 days (d). The plants were grown over a course of 9 weeks and harvested 3, 6, and 9 weeks after seed germination. The developmental stages of the plants were recorded weekly according to the phenological developmental stages of wheat (Witzenberger and Hack 1989). All three harvests included dry weight analyses (shoot, root, root mass fractions), and P contents in the biomass were analyzed following the 9-week harvest. The average daily air temperature and light integral were 22.9 °C and 10 mol photons m^{-2} d^{-1}, respectively.

5.2.5.2 Response of wheat to algal biofilm fertilization and fungal inoculation (Experiment 2)

Experiment 2 was conducted from September to December 2022 and aimed to investigate synergistic or antagonistic effects of ABF and fungal inoculation with S. vermifera on wheat growth and P uptake. Three pots (Ø 12 cm, 1 L) per treatment were filled with 0.8 kg of substrate (sand/Null Erde, 1:1 *v:v*) fertilized as described above. Wheat seedlings were pre-germinated for 3 d and either inoculated with AMF and *S. vermifera*, individually or in combination, or remained without inoculation as the negative control. Five pre-germinated seedlings were planted per pot, which were thinned to three plantlets per pot after 3 days growing. Each treatment comprised 3 replications.

The inoculation of wheat seedlings was performed as follows: a vermiculite-bound arbuscular mycorrhizal (AMF) inoculum, namely INOQ AGRI, including *Rhizoglomus irregulare*, *Funneliformis mosseae,* and *Funneliformis geosporum* was obtained from INOQ GmbH (Schnega, Germany) and used according to the manufacturer's instructions. Briefly, 20 mL of the inoculum was mixed with the nutrient poor substrate and used as a 5 cm thick top

layer into which the seedlings were transplanted. Control treatments received the same amount of vermiculite mixed into the substrate. *Sebacina vermifera* (MAFF 305830) was kindly provided by Prof. Alga Zuccaro from the Institute for Plant Sciences, University of Cologne, Germany. *S. vermifera* was maintained on mannitol egg yolk polymyxin medium (MYP, Merck, Germany) containing 1.5% agar at 28°C for 3 weeks as described in (Sarkar et al. 2019). To produce the inoculum for roots, the surface mycelia were scraped off the agar surface with a scalpel and transferred into 100 mL liquid MYP medium and incubated at 23 °C and 120 rpm for 12 d. The mycelium was then carefully crushed with a blender (Homogenizer Ultra-Turrax, ULTRA-TURRAX®) and allowed to regenerate for a further 3 d. Prior to root inoculation, the hyphal aggregates were poured into a square Petri dish and washed 3 times with sterile tap water. Subsequently, the emerging roots of 3 d old wheat seedlings were immersed in the solution and carefully planted into the fertilized substrate. All the procedures up to the root dipping were conducted under sterile conditions. The flow chart is shown in Fig. S 5-1. The wheat plants were harvested after 6 weeks of growth. Dry weight of roots and shoots as well as P content of the biomass was determined and fungal colonization of wheat roots was evaluated (see below). Over the course of the experiment, the average daily air temperature and light integral were 20.4 °C and 5 mol photons m^{-2} d^{-1}, respectively.

5.2.5.3 Plant harvest and chemical analysis of plant material

The harvested biomass was separated into shoots and roots and dried to constant weight at 60 °C (TR 1050, Nabertherm GmbH, Lilienthal, Germany) before measuring dry weights. For experiment 2, about 0.5 g of the fresh root were randomly sampled from each pot, carefully washed to remove the adhering substrate, and stored in 50% ethanol prior to microscopic assessment of fungal colonization.

While in Experiment 1 dry shoots and roots were ground (MM 400, Retsch GmbH, Haan, Germany) collectively to analyze the biomass for P, in Experiment 2 dry root and shoots were ground separately to determine if P distribution was influenced by fungal inoculation. Ground biomass was digested with 5 mL HNO_3 in a microwave (MARS6, CEM®, USA) and measured for P by Inductively Coupled Plasma- Optical Emission Spectrometry (ICP-OES Ultima 2, HORIBA®, France).

5.2.5.4 Quantification of fungal colonization of wheat roots

A non-vital staining procedure was used for evaluation of mycorrhizal colonization based on Vierheilig et al. (1998). Briefly, roots samples collected at harvest and preserved in 50% ethanol were washed in tap water to remove the ethanol, then cleared by boiling in a 10% potassium hydroxide (KOH) solution for 5 min and rinsed several times with tap water. The samples were boiled for another 3 minutes in a 5% solution of ink vinegar containing pure white household vinegar (5% acetic acid) and blue Pelikan 4001 ink (Pelikan, Hannover, Germany). The roots were again rinsed with tap water and stored at 4 °C in water with a pH of 4.5 prior to microscopic observation. Root colonization was quantified by counting arbuscules, vesicles, hyphae, or fungus-free structures under a light microscope (Zeiss, Germany) as described in (McGonigle et al. 1990). In case of *S. vermifera* inoculation, we identified hyphae and hyphal branches between root cells, and root cortical cells completely packed with fungal hyphae, as described for wheat by (Ray and Craven 2016). In roots inoculated with both, AMF and *S. vermifera*, no effort was made to discriminate the fungal structures, as the hyphae did not show any easily recognizable distinguishable characteristics.

5.2.6 Statistical analysis

R studio, version 2023.06.1 (2023), was used for statistical analyses and generation of figures. Prior to statistical analyzes, the Levene test (R package “heplots”) was used to prove the normality of data. One-way and two-way analyses of variance (ANOVA), were conducted to test the differences among treatments and the statistical significance in the interaction of fertilizers and mycorrhizal applications, followed by Tukey's multiple comparisons (R package “agricolae”). Differences were considered significant at $p < 0.05$ level of significance. All data obtained in the current research were generated using the R packages “ggplot2” and “ggpattern” and are presented as mean ± standard error (SE). All graphics were compiled with “BioRender.com”.

5.3 Results

5.3.1 Phosphorus species in ABF

To identify the P species that are available from the ABF, ^{31}P NMR analyses were conducted. The results show that more than 80% of the P extracted by NaOH-EDTA was in

the form of orthophosphate and around 15% were present as orthophosphate monoesters. Further species like orthophosphate diesters and pyro-phosphate were found in negligible amounts (Table 5-1). Neither phosphonates or polyphosphates could be detected.

Table 5-1 Percentages of the signal areas of the P compound classes measured with ^{31}P NMR spectroscopy after EDTA+NaOH extraction.

Phosphorus compounds	Proportion (%)
Orthophosphate	82.9
Orthophosphate-Monoesters	14.7
Orthophosphate-Diesters	0.7
Pyro-phosphate	1.8

5.3.2 Phosphorus release dynamics

Analyses of leachates collected over the course of 42 days for water as an extractant and 14 days for 50mM citric acid as an extractant revealed differences in P release dynamics between the extractants and the fertilizers (Fig. 5-1).

Over the course of 42 days with sampling every other day, ABF linearly released only 1.1% of the total supplied P. Hence, mere leaching of P out of the ABF cells is insufficient to feed the plant. In contrast, TSP released around 20% of supplied P over the same time course, with the highest release (15%) occurring before day 14, after which P release gradually decreased. We tested also an ABF containing 8.7% P in addition to the ABF with 1.35% P used for the pot experiments to identify P release dynamics between two contrary ABFs. P release of the 8.7% P was also linear over 42 days adding up to a total P of 3.4% of the supplied P (Fig. 5-1A). The experiment was repeated for a time course of 14d and using 50mM citric acid as a root exudate proxy. P release dynamics changed compared to water as an extractant. In citric acid the largest amounts of P (2.5%, 5.6% for low and high P ABF, respectively and 8.0% for TSP) were released within the first five days, after which its release decreased, irrespective of the fertilizer (Fig. 5-1B).

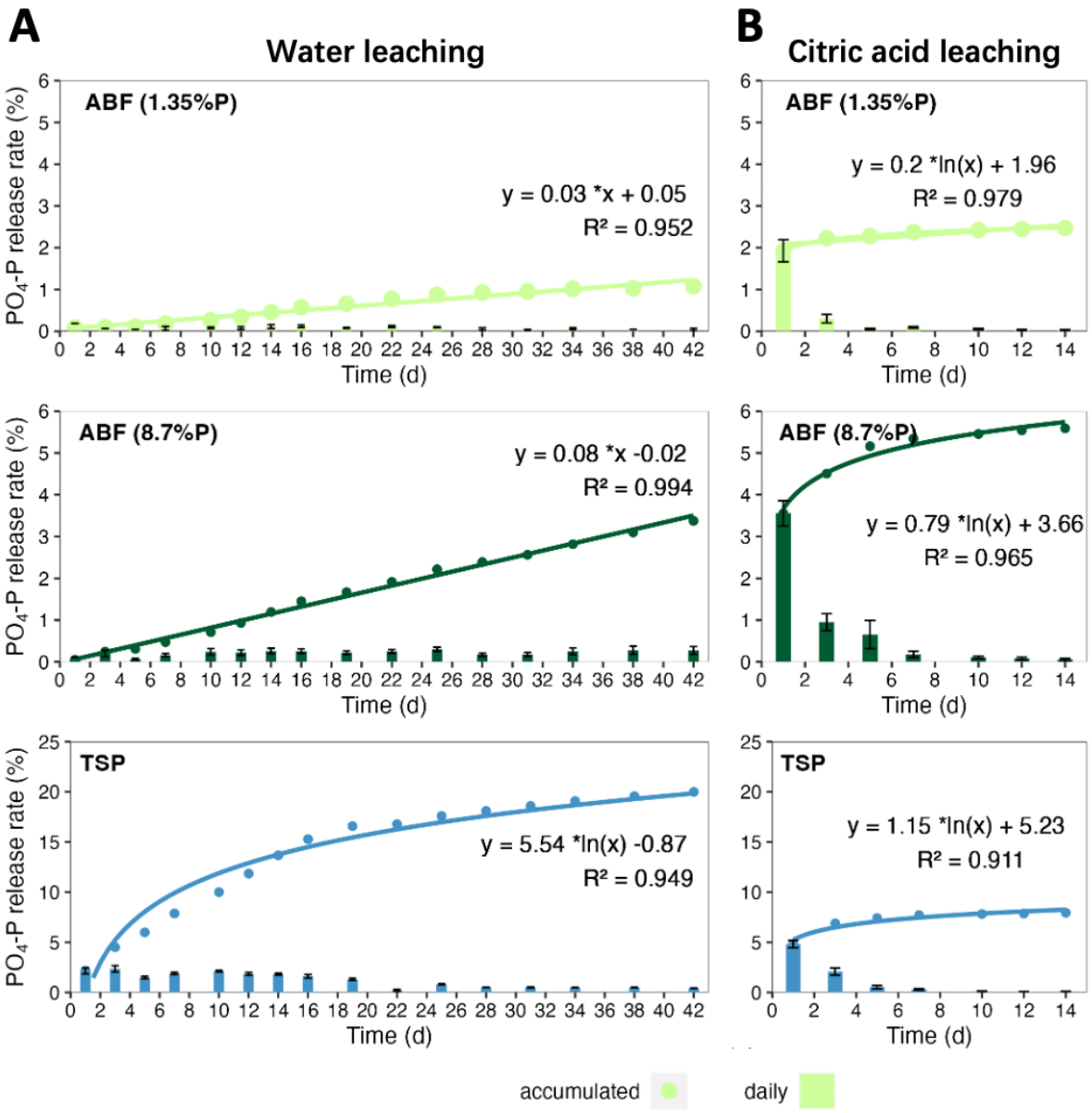

Figure 5-1 P mobilization dynamics shown as proportion of total P supplied from a plant free mixture of growth substrate with ABF (containing 1.35% P and 8.7% P, equivalent to 37 mg kg^{-1} as 100%, denoted as light green and dark green, respectively), or TSP (37mg P kg^{-1} as 100%), leached by water (A, 42 days, 6-10 mL d^{-1}) or 50 mM citric acid (B, 14 days, 6-10 mL d^{-1}). Each graph shows P release (bars) and the cumulative P release (circles). (n= 5, error bars indicate 5 biological replicates)

5.3.3 Similar growth performance of ABF- and TSP-fertilized wheat plants despite lower P uptake from ABF (Experiment 1)

The first experiment aimed to determine the effect of ABF as a fertilizer for wheat. Wheat phenological development (based on BBCH scale), dry biomass and P content (mg P g^{-1} DW) shows that fertilized plants performed notably different from unfertilized plants. While ABF and TSP fertilized plants were in the same developmental stage at all harvest times, i.e. 3, 6 and 9 weeks, negative control plants had a slower start and then developed faster than ABF and TSP fertilized plants (Fig. 5-2A). As expected, unfertilized wheat accumulated significantly less biomass than either ABF or TSP fertilized plants at all harvest times (Fig. 5-2B). Wheat that received P from TSP produced only slightly but significantly more biomass in the harvests at 3, 6 and 9 weeks than ABF fertilized plants (Fig. 5-2B). At the final harvest, the total P content (mg pot^{-1}) of ABF fertilized plants was significantly less than of TSP fertilized plants (Fig. 5-2C). Relative P (mg g^{-1} DW) of ABF fertilized plants notably but not significantly differed from either negative control or TSP fertilization (Fig. 5-2D).

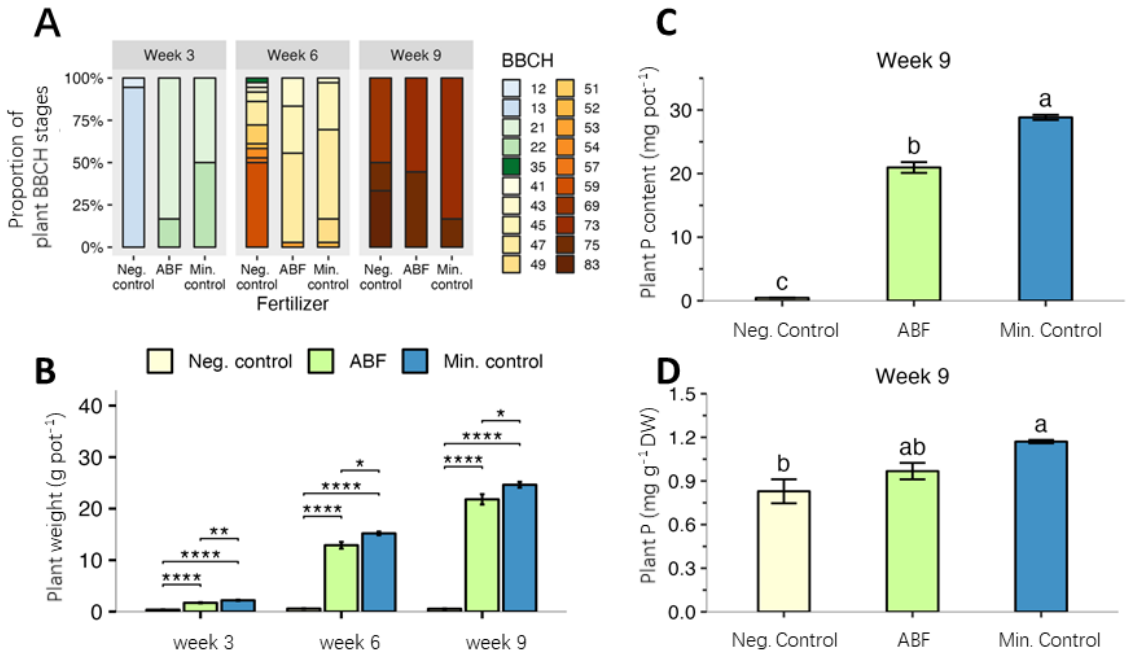

Figure 5-2 Development of wheat plants according to BBCH phenological monitoring (A), total dry weight of unfertilized (yellow) and algal biofilm (ABF) fertilized (green) or TSP fertilized (blue) wheat plants, harvested after 3, 6 and 9 weeks (B), total P recovered by control,

ABF- and TSP-fertilized wheat after 9 weeks (C), and relative P content of wheat plants after harvest at week 9 (D). (Tukey's HSD test, different letters denote significant differences between treatments at $p < 0.05$, $n = 3$)

5.3.4 Fungal colonization rates differ between fertilizers and fungal inoculum (Experiment 2)

The roots of wheat plants without fungal inoculation showed no fungal structures after 6 weeks of growth (Fig. 5-3A), whereas all plants inoculated either with AMF, *S. vermifera*, or both, showed the typical structures of fungal colonization in the root cortex cells (Fig. 5-3B-D). Inoculation with AMF resulted in the development of hyphae, arbuscules and vesicles (Fig. 5-3B). In roots inoculated with *S. vermifera*, chlamydospores were observed but not counted, while hyphae, hyphae-filled root cortical cells and vesicle-like structures were considered and counted (Fig. 5-3C). In co-inoculated roots, all structures indicating fungal colonization were counted without differentiating between AMF and *S. vermifera* inoculants (Fig. 5-3D). In all AMF inoculated plants, colonization rates were higher than in *S. vermifera* inoculation alone. In mineral fertilized plants, overall colonization rate was lowest while it was highest in ABF fertilized plants. Interestingly, colonization rate with *S. vermifera* was significantly higher in ABF fertilized plants compared to either TSP- or non-fertilized control (Fig. 5-3E).

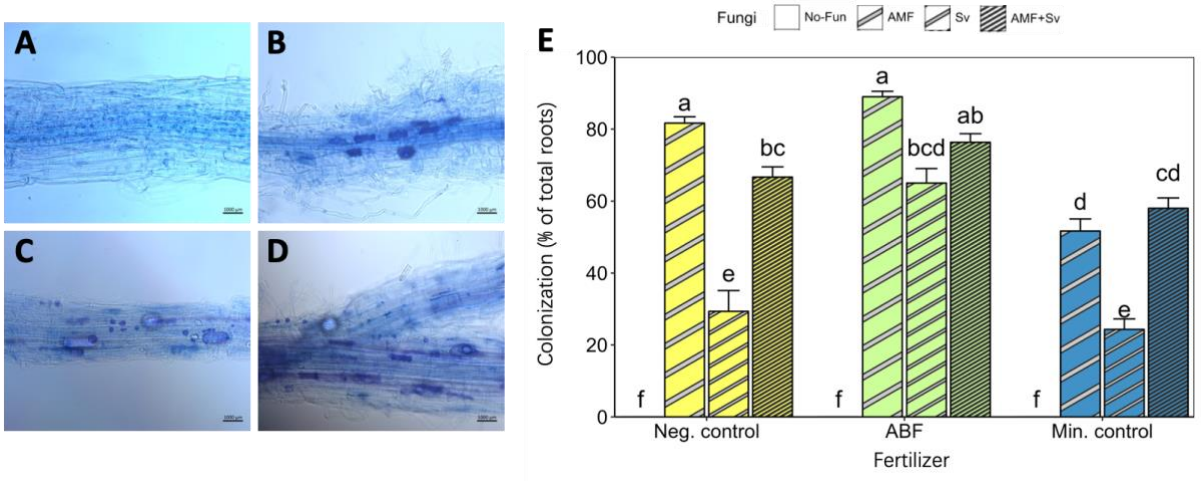

Figure 5-3 Exemplary pictures of a typical wheat root segment after staining. (A), no inoculation; (B) arbuscular mycorrhizal fungi (AMF) inoculation (C) *S. vermifera* colonization and (D) dual AMF- *S. vermifera* inoculation. Fungal colonization rate of wheat roots as

determined by microscopic observation (E) based on McGonigle et al. (1990). (Tukey's HSD test, different letters denote significant differences between treatments at $p < 0.05$, $n = 3$)

5.3.5 Fungal inoculation differentially affects wheat growth and P uptake from algal biofilm (Experiment 2)

In the second experiment, we focused on the effects of fungal inoculations with arbuscular mycorrhizal fungi (AMF), *S. vermifera* (Sv) or both in combination (AMF+Sv), on wheat growth and P uptake from ABF. A No-P treatment and TSP fertilization with identical fungal treatments served as negative and positive controls, respectively. After 6 weeks of growth, plants were harvested and separated into shoots and roots, followed by measuring growth parameters and P allocation (Table 5-2, Fig. 5-4).

Overall, total dry weight (DW, g pot^{-1}) and relative P content (mg g^{-1} DW) increased depending on the fertilizer treatment (no-P < ABF < TSP), with only minor effects of fungal inoculation (Fig. S5-2). If the shoot and root tissue are considered separately, a differentiated pattern emerges (Table 5-2, Fig. 5-4). First, both tissue types responded differently to fertilizer and fungal treatments: shoot and root parameters (DW, P content, total P) significantly depended on fertilization ($p < 0.01$ for all parameters), whereas root parameters also showed a fungal inoculation-specific pattern. Second, No-P and ABF fertilization generated a similar pattern in all observed parameters. Third, in TSP fertilization only minor contributions of fungal inoculation to biomass and P content were detected.

More specifically, AMF inoculation alone reduced shoot and root DW in No-P control and in ABF fertilized wheat (not significant, Fig. 5-4 A,B). Wheat root DW was significantly promoted by *S. vermifera* in ABF treatment as well as by double inoculation of AMF and *S. vermifera* in No-P and ABF treatment (Fig. 5-4B). AMF inoculation tended to result in higher relative P content in shoots and roots compared to no AMF inoculation across all fertilizer treatments, this was significant for root P content following ABF fertilization (Fig. 5-4 C,D). In shoots, total P content was highest in TSP fertilized wheat, but not significantly so (Fig. 5-4E) while there was a significant increase in total P in the roots of wheat following double inoculation with *S. vermifera* and AMF (Fig. 5-4F).

Regarding the effects of fungal inoculation on wheat performance following ABF fertilization this shows that AMF moderately enhanced P uptake but also negatively affected plant growth. In contrast, *S. vermifera* alone had no effect on P uptake but instead promoted root growth. Double inoculation with both fungi resulted in higher total P uptake from algal biofilms, resulting in significantly more total P content in wheat roots than following TSP fertilization, used here as a positive control. Thus, P transfer from ABF biofilms to plants can be enhanced by co-inoculation with mycorrhizal fungi and the beneficial root endophyte fungi *S. vermifera*.

Table 5-2 Results of two-way ANOVA test. P-values (*p*) of significant effects (*p* <0.05) of fungal and/or fertilizer and interaction between them are highlighted in bold.

Dependent variables	Fungi		Fertilizer		Fungi × Fertilizer	
	F value	*p*	F value	*p*	F value	*p*
Shoot DW (g pot^{-1})	4.409	**0.013**	72.561	**<0.001**	0.953	0.477
Root DW (g pot^{-1})	49.402	**<0.001**	60.287	**<0.001**	9.412	**<0.001**
P in shoots (mg g^{-1} SDW)	2.754	0.065	23.595	**<0.001**	0.641	0.696
P in roots (mg g^{-1} RDW)	7.051	**0.001**	6.392	**0.006**	2.232	0.075
Total P in shoots (mg pot^{-1})	1.052	0.388	65.452	**<0.001**	0.757	0.610
Total P in roots (mg pot^{-1})	20.007	**<0.001**	31.877	**<0.001**	6.931	**<0.001**
DW total plant (g)	7.958	**<0.001**	77.414	**<0.001**	1.890	0.124
P in total plant (mg g^{-1} DW)	3.237	**0.040**	24.178	**<0.001**	0.512	0.793

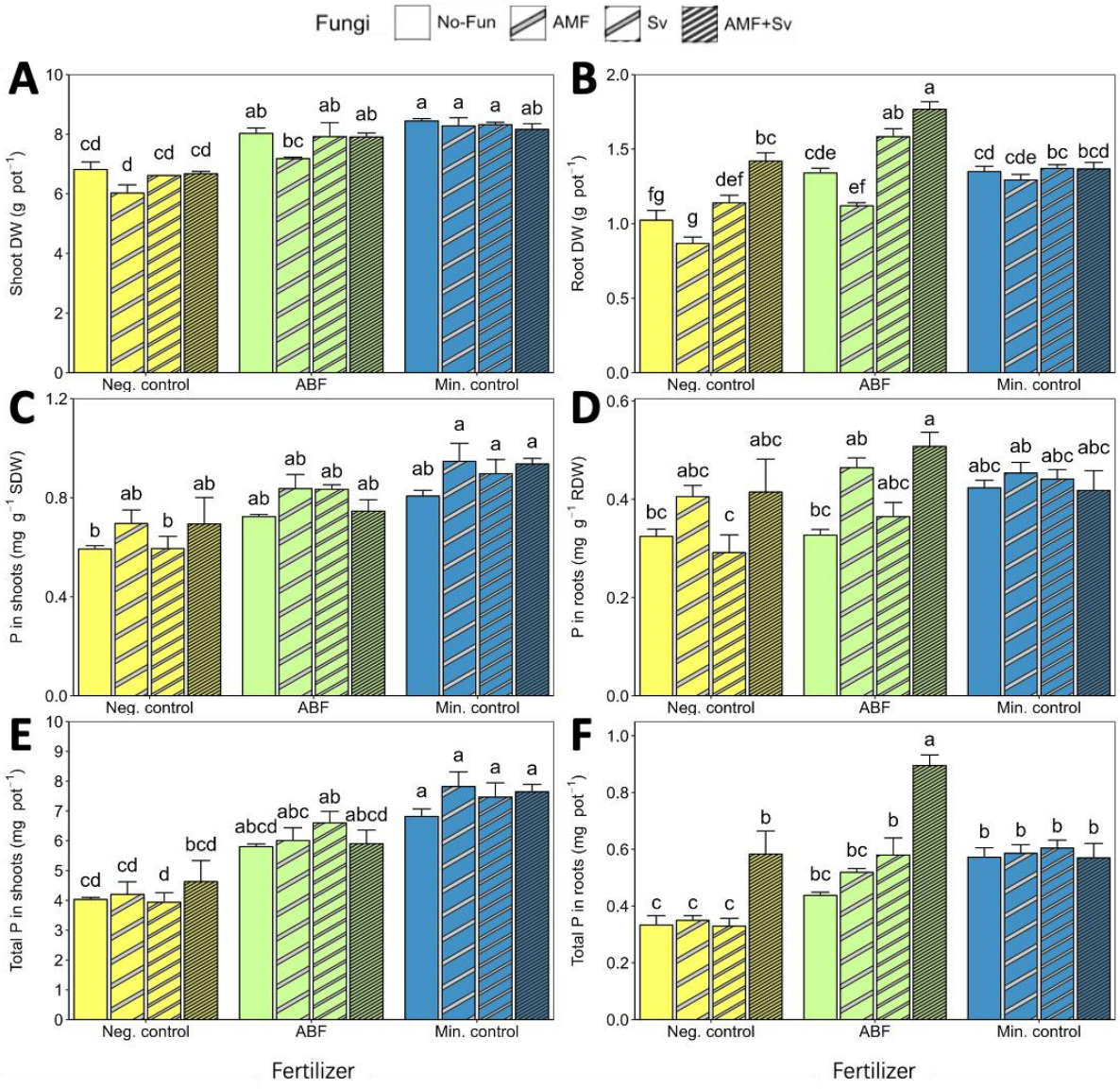

Figure 5-4 Wheat dry biomass of shoots (A) and roots (B), relative P content of shoots (C) and roots (D), and total P content of shoots (E) and roots (F) of no-P fertilized wheat plants (Neg. control), algal biofilm (ABF) fertilized, and triple-superphosphate (TSP) fertilized plants; non-inoculated (No-Fun), arbuscular mycorrhizal fungi inoculated (AMF), *Sebacina vermifera* inoculated (Sv) and AMF + *S. vermifera* double (AMF+Sv). Wheat was harvested after 6 weeks of growth. (Tukey's HSD test, different letters denote significant differences between treatments at $p < 0.05$, $n = 3$)

5.4 Discussion

In this study we show the potential and limitations of algal biofilm (ABF) produced on the effluent of treated municipal wastewater using the ATS system as a phosphorus (P) fertilizer for wheat. Although orthophosphate is the main P species in NaOH labile P fraction of ABF, it was less prone to leaching and less available to wheat plants during 42 d growth compared to TSP. We further show that the co-inoculation of wheat with arbuscular mycorrhizal fungi (AMF) and the root beneficial fungus *Sebacina vermifera* resulted in a comparable fertilizer efficiency of ABF and TSP, which was due to a synergistic effect of root growth promotion by *S. vermifera* and enhanced P uptake by AMF.

5.4.1 ^{31}P NMR analysis reveals orthophosphate as the dominant P species in ABF

The NaOH-extractable fraction of P from ABF consisted mainly of orthophosphate (83 %), followed by orthophosphate-monoesters (15%), pyrophosphate (2%) and orthophosphate-diesters (<1%; Table 5-1). The same P species but also phosphonates and polyphosphates were previously detected in algae (Wang et al. 2019b). In our study, we did not detect phosphonates and polyphosphates, which could have been due to different cultivation conditions, differences in the algae community and / or their amounts being below the limit of quantification. In addition, polyphosphate may have been hydrolyzed during alkaline extraction, resulting in its conversion to pyrophosphate (He et al. 2011). To test such underlying processes, Wang et al. (2021) had extracted the algae also with deuterated solution, which allowed to quantify hydrolytic decay based on changes in chemical shifts at the slightly modified electron density of the nuclei. The authors reported that algal P also constituted significant portions of RNA-P (1.260 g kg^{-1}; in similar amounts as monoester-P) in addition to some phospholipid P (340 mg kg^{-1}), which both escape common analytical windows at alkaline extraction.

NaOH-EDTA has been widely used to extract P from environmental samples. In soils and sediments, extraction of P with 0.25 M NaOH and 50 mM EDTA resulted in recovery rates between 57 and 90 % of total P (Makarov et al. 2002, Missong et al. 2016). Although the extraction method was optimized for soil samples, it has also been used successfully for algal biomass (Feng et al. 2019, Feng et al. 2016). Feng et al. (2019) applied the extraction solution

to aquatic macrophytes and algae and achieved a P recovery of around 90 %. Mackay et al. (2017) observed that the high amounts of orthophosphate in different organic soil amendments did not always correspond to higher plant availability. Instead the composition and changes within the P pools over time had a governing effect on plant available P. Similarly, Peirce et al. (2013) compared P species in chicken manure over a 12 months period and identified increasing concentrations of orthophosphate with increasing age which corresponded to reduced P availability to plants. The authors suggested increased binding of the orthophosphate to calcium in the substrate. Algal biofilms produced on municipal wastewater may contain around 2% calcium (Reinecke et al. 2023), which may, upon decomposition of algal biomass immobilize orthophosphate. Furthermore, Schreiber et al. (2018) analyzed P availability from algal biomass composed of *Chlorella vulgaris* and observed differences between dry and wet algae as well as sandy and organic-rich substrates, indicating effects of biomass processing and growing medium on the P availability to plants.

Other than orthophosphate, ABF contains negligible amounts (<1%) of the easily mineralizable orthophosphate diester-P (Condron et al. 1990) and around 2% of less plant available pyrophosphate (Sutton and Larsen 1964), while around 15% was in the form of orthophosphate monoester. Monoesters may readily sorb to soil surfaces, making them stable and they are assumed to be less susceptible to mineralization (Giles et al. 2011, Turner et al. 2005).

Plants are able to utilize P in the form of inorganic orthophosphate (Pi), and the high orthophosphate concentration of ABF would be expected to correspond to high plant availability (Penn and Camberato 2019). However, as discussed below (5.4.2), plant P availability was consistently lower than from TSP, which likely reflects that large parts also comprised organic P that is not readily taken up.

5.4.2 P release dynamics from ABF with water and citric acid as extractants predict low leaching and high plant availability of ABF-P

The leaching experiment conducted after mixing ABF or TSP with the growing medium (plant-free) showed that the P release dynamics were different between the two fertilizers. ABF-P was much less water soluble than P from TSP, reflecting that other P forms existed in ABF. Leaching dynamics were not different between an ABF containing 1.35% and one

containing 8.7% P, only absolute amounts differed but not leaching rates, indicating that P forms may be similar in both algal biofilms. The high P content in ABF may be due to the high pH environment (pH 9-11) caused by algal growth, which precipitates P in the water onto the algal biofilm (Gan et al. 2023). It would make sense to harvest ABF under such conditions for fertilizer use because it would also deliver much higher amounts of P and less biomass would need to be applied.

The slow P release from ABF contrasts with the comparatively high P uptake by the plants (see 5.4.3), suggesting that other, probably plant-related processes contributed to P acquisition. ON the one hand, P may be rapidly released from organic forms upon mineralization, as other studies showed even showed similar P availability to plants from algae as from TSP (Schreiber et al. 2018, Siebers et al. 2019). On the other hand, to become available to plants, P that is adsorbed to soil or precipitated must be desorbed or solubilized from the pool of total P (Richardson et al. 2011). To improve the access to such P, plants utilize a number of mechanisms including the exudation of low molecular mass organic acids that cannot only release phosphate from its binding sites, but also dissolve hydroxyapatite P, thus increasing the availability of P to plants (Wang and Lambers 2020). The short-term leaching experiment conducted here with 50 mM citric acid, a commonly exuded and frequently used organic acid to study P dynamics in soils (Santos et al. 2017), shows that the release dynamics changed compared to water as an extractant and now resemble the dynamics observed in P leaching from TSP. In water, ABF-P was released gradually, while in citric acid the largest amounts of P were released within the first few days, after which its release decreased, irrespective of the fertilizer (Fig. 5-1 B). Citric acid can be considered as proxy for acidic root exudates, and its effect indicate that ABF-P can become plant available in the presence of a root.

5.4.3 P from ABF is readily available for wheat, but to a notably lesser extent than P from TSP

Our first plant growth experiment using 1.35% P ABF as a fertilizer showed that phenological development based on BBCH and root mass fraction of wheat plants fertilized with ABF and TSP were similar after 3, 6 and 9 weeks, while biomass and P contents differed slightly but significantly (Fig. 5-2). In the unfertilized control, on the other hand, higher root

growth was observed early on, concomitant with a later onset of above-ground plant growth. Overall, biomass remained significantly below the fertilized plants. Nevertheless, wheat fertilized with ABF produced a significant though smaller amount of biomass and, therefore, also acquired significantly less total P. These results are in accordance with previous reports on plant growth fertilized with algal biomass (Schreiber et al. 2018). Mau et al. (2021) used phenological data and data from the literature to interpret the growth of wheat on an algal fertilizer consisting of *Chlorella* sp. and concluded that the P was directly available from the algal biomass and gradually released over time, resulting in growth comparable to mineral fertilizer, albeit also with a lower total P uptake.

5.4.4 Double inoculation of wheat with arbuscular mycorrhizal fungi and the beneficial root endophyte *Sebacina vermifera* improved P transfer from ABF to the roots, which retained more P than from easily available TSP

Our next aim was to analyse whether and to what degree wheat P uptake can benefit from a synergistic collaboration of arbuscular mycorrhizal fungi (AMF) and *S. vermifera* when ABF is used as fertiliser. The contribution of AMF to plant P uptake is well understood (Jansa et al. 2011, Smith and Read 2010), while it is much less clear for *S. vermifera* and other members of the Sebacinales. It has been shown that P acquisition by host plants can be enhanced under some experimental conditions, but the mechanisms differ significantly from those identified in AMF (Weiß et al. 2016). To get an insight into the interaction of wheat with both types of beneficial fungi, we inoculated wheat seedlings with AMF and *S. vermifera*, alone and in combination, and harvested the roots and shoots after 6 weeks of growth.

Independently of the fertilizer treatment, all typical mycorrhizal structures could be detected in AMF-inoculated, as well as in *S. vermifera*-inoculated roots, indicating the establishment of functional root-fungus interactions (Fig. 5-3). Using ABF as a fertilizer, root colonization with *S. vermifera* was significantly higher than with TSP fertilization and in No-P treatment. Sebacinales have been found to proliferate in soils that are high in organic matter and were also found to increase following transition from conventional to organic agriculture (Verbruggen et al. 2014). In double inoculation, the presence of *S. vermifera* had no effect on AMF colonization in ABF and TSP treatments, while significantly lower colonization was

observed in the No-P treatment compared to AMF inoculation alone. This suggests that *S. vermifera* may inhibit AMF in its ability to colonize wheat roots at extremely low P availability. Sarkar et al. (2019) studied *S. vermifera* in the interaction with the plant pathogenic fungus *Bipolaris sorokiniana*. The authors found that genes encoding cell wall-degrading enzymes, particularly chitinases and glucanases, were upregulated in *S. vermifera* during direct confrontation with *B. sorokiniana*. Since the identified gene products are important for mycoparasitism (Sarkar et al. 2019), it is feasible to assume that such antagonism also may play a role in the interaction between AMF and *S. vermifera,* which may in turn affect the ability of AMF to colonize plant roots.

AMF inoculation had a negative effect on plant biomass formation, while the relative P content increased (albeit not significantly) compared to non-inoculated plants (Fig. 5-4). In wheat, which is often regarded as non-responsive to AMF, such an outcome has been described before. However, previous researchers have demonstrated that considerable amounts of P were delivered by AMF to wheat, even when the growth response was negative (Li et al. 2006, Li et al. 2005). This indicates that the growth response may not be suited to judge the fungal contribution to P-use efficiency of plants.

In our study, *S. vermifera* alone did not affect P uptake but significantly promoted wheat root growth following ABF fertilization. *S. vermifera* promotes the growth of many different plant hosts, including the model plant *Arabidopsis* and *Nicotiana* but also the biomass plant switchgrass (*Panicum virgatum*), fennel (*Foeniculum vulgare*) and rice (Dolatabadi et al. 2011, Pirdashti et al. 2012, Ray and Craven 2016). Achatz et al. (2010) reported that growth promotion in barley (*Hordeum vulgare*) by *Serendipita indica* (syn. *Pirformospora indica*), a close relative of *S. vermifera*, was not accompanied by increased P content. Other member of the order Sebacinales in contrast have been shown to provide N and P to host plants, especially when these nutrients were limited (Nurfadilah et al. 2013). Ray et al. (2019) reported a significant increase in the number of lateral roots in young wheat seedlings in winter wheat inoculated with *S. vermifera ssp. bescii* under N- or P-limiting conditions. However, under these conditions no impact on shoot N or P content conditions was observed, and, in tun, no growth promotion under optimum N and P conditions was evident. The authors suggested that shoot nutrient acquisition and plant growth promotion may not necessarily be

positively correlated phenotypic traits. In the wheat-*S. vermifera* interaction introduced in our study, similar dynamics could be at play (Fig. 5-4).

Co-inoculation of AMF and *S. vermifera* led to a significant increase in root P content but only a slightly positive, non-significant, trend concerning the aboveground biomass. Positive synergistic effects of co-inoculation of plants with AMF and *S. indica* have been described to alleviate saline stress (Heidarianpour et al. 2020), drought stress (Tyagi et al. 2023), and to reduce heavy metal uptake (Wang et al. 2023). He et al. (2022) co-inoculated the legume *Vicia villosa* with AMF and *S. indica*, resulting in increased plant biomass, a significantly improved P uptake and increased nitrogen (N) availability in the soil. Similarly, Hallasgo et al. (2020) studied the synergistic effects of AMF and two different endophytes, *S. indica* and *S. williamsii*, on tomato plants. Double inoculation enhanced the N concentration in tomato shoots without reducing the P transfer by AMF. Moreover, the authors observed that *S. williamsii* performed differently from *P. indica* when co-inoculated with AMF, indicating that interaction patters, even between close relatives, are highly individual. Here, we used an AMF inoculum consisting of three arbuscular mycorrhizal fungi, *Rhizoglomus irregulare, Funneliformis mosseae,* and *Funneliformis geosporum,* and we can´t exclude that the individual AMF species perform differently in *S. vermifera* interaction and that individual effects may be lost in the combination. Thus, it would be interesting to further investigate the specific interactions with *S. vermifera* as, to our knowledge, no other studies on potential synergism or antagonism between *S. vermifera* and AMF isolated have been conducted.

In summary we show that P recovery from ABF by wheat plants can be enhanced by co-inoculation with arbuscular mycorrhizal fungi and the beneficial root endophytic fungi *S. vermifera*. Even though under the chosen experimental conditions there was no positive effect on overall plant biomass, more total P was retained in belowground organic plant matter, preventing it from being leached or immobilized in the soil. Li et al. (2005) reported that the wheat growth depression induced by AMF observed at early growth stages (up to 6 weeks) disappeared at maturity. It would thus be essential to conduct next experiments until wheat maturity to evaluate the potential of dual inoculation on the wheat seed production, quality and P recovery from ABF.

5.5 Conclusion

Our study shows that ABF is an effective, less leaching-prone organic P source for wheat. ABFs primarily consist of orthophosphate, while its lower leaching potential compared to TSP-P highlights its potential as a sustainable fertilizer. In terms of total dry matter and total phosphorus in wheat, ABF supplied less P to wheat than TSP, and remains even after 42 days of plant growth. However, co-inoculation of wheat with AMF and *S. vermifera* promoted P transfer from ABF to the roots, showing the potential and relevance of microbial involvement in the use of algae-based fertilizers and suggesting a potential strategy to improve P recovery and utilization by wheat plants. Our findings thus contribute to the growing understanding of algae-based fertilizers in plant nutrition and shed light on the potential benefits of microbial partnerships in enhancing plant nutrient uptake.

6 Final discussion

6.1 Conclusion

The treatment of vast volumes of wastewater before its discharge into natural water bodies is imperative. Algal-based wastewater treatment systems, particularly the attached system ATS, have emerged as a promising biological approach. However, there remains a lack of systematic approaches to optimize ATS performance, and the recycling of nutrients within ATS biomass has not been fully exploited. The objective of this thesis was to establish a viable pathway for the recovery of nutrients from wastewater, traversing through the algae treatment system (ATS), and culminating in the enhancement of plant growth.

In the first segment of this research, expounded upon in Chapter 3 (Gan et al. 2022), lab-built ATS systems were used to investigate and optimize the nutrient remediation efficiency. Combined effects of three cultivation variables—total inorganic carbon, nitrogen-to-phosphorous (N:P) ratio, and light intensity—were examined. The ATS nutrient removal efficiency and biomass productivity were analyzed via the response surface methodology (RSM). The maximum removal rates of total P and N were 8.3 and 19.1 mg L^{-1} d^{-1}, respectively. As much as 99% of total P and 100% of total N were removed within 7 days. Over the same period, the dissolved oxygen concentration and pH value of the medium increased. The optimal growth conditions for simultaneous maximum P and N removal and biomass productivity were identified. Our RSM-based optimization results provide new insights into the combined effect of nutrient and light availability on the ATS remediation efficiency and biomass productivity. Overall, ATS is a promising algal-based wastewater treatment technology that can achieve high nutrient removal within a short time.

Building upon the promising outcomes of the initial research, Chapter 4 delves into the subsequent phase, where ATS systems were scaled up to a technical level and deployed in a greenhouse environment for a year, as detailed in the second paper (Gan et al. 2023). Mathematical modeling was used to identify the independent and interdependent effects of water temperature and light intensity on dependent variables, including nutrient removal and recovery. Over 7 days, the average total nitrogen and phosphorous removal rates and efficiencies were 30.93 and 8.95 mg L^{-1} and 51.2 and 89.5 %, respectively. Based on a statistical regression matrix, the quadratic models were chosen to analyze data on nutrient

removal and recovery. In this study, light intensity was the dominant variable for ATS performance. Under winter conditions, an increase in light intensity was the most effective way to increase ATS performance. Significant positive correlations were found between nutrient removal and recovery, and biomass productivity. The annual production costs for dried algal biomass, N and P were 2.27, 40 and 156 € kg^{-1}, respectively, which was just 18% (2.27 €) of the algal biomass production costs in conventional tubular photobioreactors. Our results indicated that the ATS technology can be efficient and cost-effective in nutrients removal and recovery from wastewaters under a wide range of temperature and light conditions.

Chapter 5 provides insight into the potential of ATS system for nutrient recovery from municipal wastewaters. Specifically, two greenhouse-based pot experiments were used to explore the potential of ATS algal biofilms (ABF) which produced from municipal wastewater as a phosphorus (P) fertilizer for wheat and examine the effects of arbuscular mycorrhizal fungi (AMF) and the beneficial root endophyte *Sebacina vermifera* (*S. vermifera*) on plant performance and P uptake. The results showed that ABF, while rich in orthophosphate, had lower water solubility compared to mineral P sources, resulting in reduced P availability to wheat. Despite this, ABF proved effective as an organic P source for wheat. Interestingly, the presence of AMF reduced wheat growth in ABF-fertilized plants but did not affect P uptake. However, co-inoculation with *S. vermifera* mitigated the negative effects on wheat growth and significantly increased root growth and P content in roots.These findings highlight the potential of ABF as an organic P fertilizer for wheat and underscore the importance of microbial interactions, particularly with AMF and *S. vermifera*, in optimizing nutrient uptake efficiency in plants. This research contributes to the development of sustainable agricultural practices and the efficient utilization of algae-based fertilizers for nutrient management in wastewater treatment systems.

In summary, this research provides a comprehensive understanding of the potential of ATS technology for sustainable wastewater treatment, nutrient removal, and recovery, highlighting its significance in addressing the challenges of wastewater management and resource sustainability. The findings presented in this thesis offer valuable insights for the future development and application of algae-based systems in wastewater treatment and nutrient recycling.

6.2 Synthesis

6.2.1 Utilization ATS systems in wastewater treatment and water purification

The results presented previously demonstrate that ATS systems are highly efficient in removing and recovering nutrients from municipal wastewater. In this section, we evaluate the broader potential applications of ATS systems in a variety of environmental contexts. While the scope of this thesis has focused on specific cultivation and climatic conditions, we will now explore the applicability of ATS systems in more diverse wastewater environments.

Agricultural runoff is one of the most urgent environmental problems to be solved, mainly caused by irrigation and rainfall, which leads to increasing environmental problems due to its high nutrient and heavy metal content (Xia et al. 2020). In addition, the high volume of agricultural runoff, the relatively low concentration of pollutants compared to other types of wastewater, and the absence of obvious point sources pose a great challenge for collection and management (Li et al. 2019a, Wang et al. 2019a). Building on the findings of this thesis, it becomes evident that the ATS system has the potential to be an important tool for the final treatment of agricultural runoff. Their capacity for high nutrient removal (as demonstrated by the removal of up to 99% of total P and 100% of total N within 7 days, detailed in Chapter 3), cost-effectiveness in installation and operation, simplicity in management (as evidenced by annual production costs for dried algal biomass, N, and P amounting to 2.3, 40, and 156 € kg^{-1}, respectively—just 18% of the production costs in conventional tubular photobioreactors, as discussed in Chapter 4), and capability to process organic matter make them an attractive option. Furthermore, the harvested biomass can be repurposed as organic fertilizer (explored in Chapter 5), thus closing the nutrient loop. However, it's worth noting that the extensive land may be required for ATS systems when dealing with large volumes of runoff.

In addition to nutrients, ATS systems are capable of treating a broader spectrum of pollutants, including heavy metals and organic matter. Algae not only take up heavy metals through photosynthesis, but also remove them through non-metabolic mechanisms such as ion exchange, complexation, chelation, and precipitation (Su et al. 2011, Xu et al. 2014). The increase in dissolved oxygen from photosynthesis further facilitates the breakdown of organic matter into smaller, more treatable molecules. However, it is important to thoroughly assess the further utilization of the biomass treated by ATS systems for these diverse pollutants.

Adherence to criteria and risk assessment in accordance with local guidelines is essential in this regard.

There are also concerns about the limitations of biological wastewater treatment systems under unfavorable conditions, especially with respect to microbial growth requirements (Bitton 2005). However, this thesis demonstrates that the ATS system can remain functional even under lower temperature conditions as long as there is sufficient light intensity to support the ATS biofilm.

In conclusion, the versatility and effectiveness of the ATS system in nutrient removal, pollutant remediation, and its adaptability to different environmental conditions make it a promising solution for a variety of wastewater treatment challenges, including agricultural runoff treatment and broader water purification. Further research and practical application of ATS systems in different environments will have great potential for sustainable water management and environmental protection.

6.2.2 Utilization of ATS systems for phosphorus recycling from wastewater for P-rich organic fertilizer production

Phosphorus, an indispensable nutrient for agriculture, is a finite, non-renewable resource derived primarily from phosphate rock, which is rapidly being depleted (Cordell et al. 2009). Recovery of phosphorus from wastewater provides a sustainable industrial feedstock for phosphate fertilizer production (De-Bashan and Bashan 2004).

Traditional methods of phosphate removal from wastewater, such as metal slate precipitation, result in phosphate precipitates that cannot be recovered for industrial processing into fertilizers (De-Bashan and Bashan 2004, Donnert and Salecker 1999). In contrast, bioremediation processes offer a viable method of phosphorus recovery, with the potential to recover 10% to 80% of the phosphorus content (De-Bashan and Bashan 2004, Gaterell et al. 2000). Our studies have shown that the ATS system is remarkably efficient at removing phosphate from wastewater, with removal rates as high as 99% (Chapter 3). In addition, the biomass of the ATS system showed an amazing ability to accumulate phosphorus at about 2% of its composition, which is comparable to that found in other plants (Chapter 3 and 4). In addition, our pot experiments verified the suitability of ATS biomass as a fertilizer. Wheat grown with ATS-derived biomass confirmed that the phosphorus accumulated in the biomass could be effectively taken up by the crop, highlighting its

potential as a valuable source of fertilizer. However, there is room for improvement to reduce the production cost of phosphorus. The current cost of 116 € kg^{-1} (Chapter 4) is considerably higher than the conventional chemical phosphorus precipitation (6-10 € kg^{-1}) in sewage treatment (Ye et al. 2020).

In summary, the recovery of phosphorus from wastewater using the ATS system not only addresses the urgent need to conserve this finite resource, but also provides a sustainable solution for the production of phosphorus-rich organic fertilizers. This approach is consistent with the principles of resource efficiency and environmental sustainability and marks an important step towards more responsible phosphorus management in agriculture and wastewater treatment.

6.3 Outlook

To unlock the full potential of ATS systems, several crucial steps must be taken. These systems hold significant promise for addressing various pollutants and achieving widespread practical adoption. The following key considerations should shape the future of ATS systems:

- **Industrial-Scale Evaluation**: Currently, ATS systems are mainly tested at laboratory and technical scales (Gan et al. 2022, 2023, Kangas and Mulbry 2014, Liu et al. 2016, Valeta and Verdegem 2015). While some research has explored industrial-scale applications, these studies often lack organized systems and experimental designs (Kangas et al. 2017, Mulbry et al. 2008). To establish the economic and operational feasibility of large-scale ATS deployment, it is essential to not only record nutrient removal efficiency but also consider energy consumption and manpower requirements. Furthermore, when applying ATS systems outdoors, careful experimental design becomes critical due to the multitude of variables involved. Identifying the critical parameters can be challenging but is necessary for successful implementation.
- **Integration with Complementary Technologies**: While ATS systems are efficient at nutrient removal, certain challenges must be addressed before widespread application. These challenges include high suspended matter, primarily consisting of suspended microalgae, and elevated pH levels resulting from photosynthesis (Gan et al. 2022). Integrating ATS systems with complementary remediation technologies could offer solutions. Constructed

wetlands, known for their biological nutrient remediation capabilities and sediment removal, present a viable option (Vymazal 2011). Exploring various constructed wetland combinations with ATS systems in laboratory settings can guide their further application.

- **Ecological Dynamics**: ATS biofilm comprises a variety of organisms, including bacteria, pro- and eukaryotic algae, fungi, and protozoa (Kangas et al. 2017, Kebede-westhead et al. 2003, Kesaano and Sims 2014, Liu et al. 2016, Mulbry and Wilkie 2001). Understanding the precise function of each organism in pollutant remediation remains a challenge. Therefore, investigating the composition of ATS biofilm to identify efficient organisms is essential. Furthermore, studies have reported temporal and spatial changes in organism species within ATS biofilm (Adey et al. 2013, Liu et al. 2016). Researching the ecological dynamics of ATS biofilm, tracking constituent organism species over time and across different flow-oriented dimensions, will contribute to a comprehensive understanding of the system's long-term viability and adaptability.
- **Toxic Cyanobacterial Production**: The use of ATS biomass as fertilizer raises concerns about the presence of cyanobacteria, some of which can produce toxic substances, such as microcystins (Gärtner et al. 2021). The mechanisms of toxic cyanobacterial production and the production of microcystins within ATS biofilm remain unclear. It is imperative to conduct experiments to identify toxic cyanobacteria and microcystin production. This is crucial for ensuring the safety and efficacy of nutrient recovery processes, especially in sensitive ecosystems.

In summary, ATS systems offer a promising solution for nutrient cycling, but realizing their full potential necessitates ongoing research and practical applications that address these critical considerations.

Appendix

Appendix A: supplemental material for Chapter 3

Supplementary data associated with this article can be found, in the online version, at https://www.frontiersin.org/articles/10.3389/fbioe.2022.962719/full

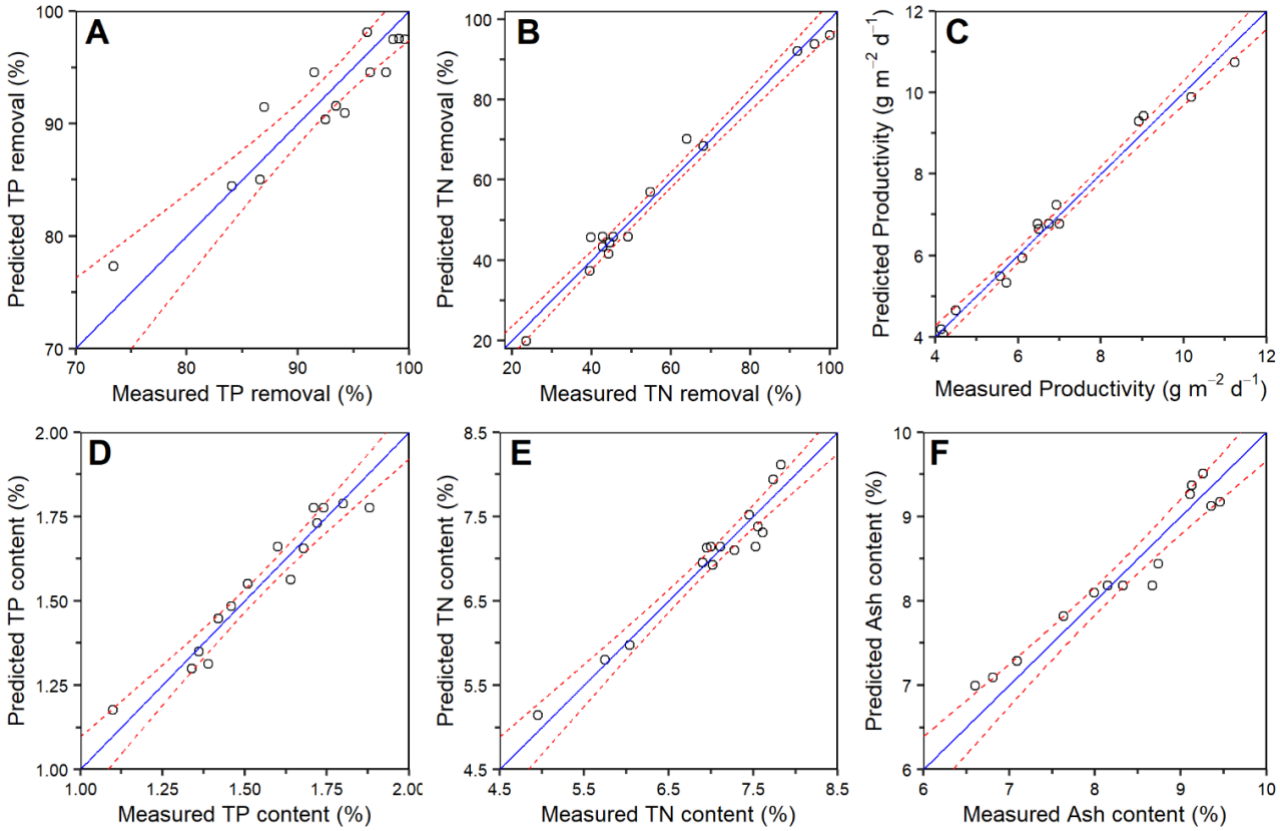

Figure S 3 - 1 Recovery rates of predicted and measured dependent variables. Tested were (A) Phosphorus and (B) Nitrogen removal from the medium. And the biomass (C) productivity, and its (D) phosphorus, (E) nitrogen, and (F) ash content, respectively. (—) full recovery of 100%, (- - -) Regression line with 95% confidence interval.

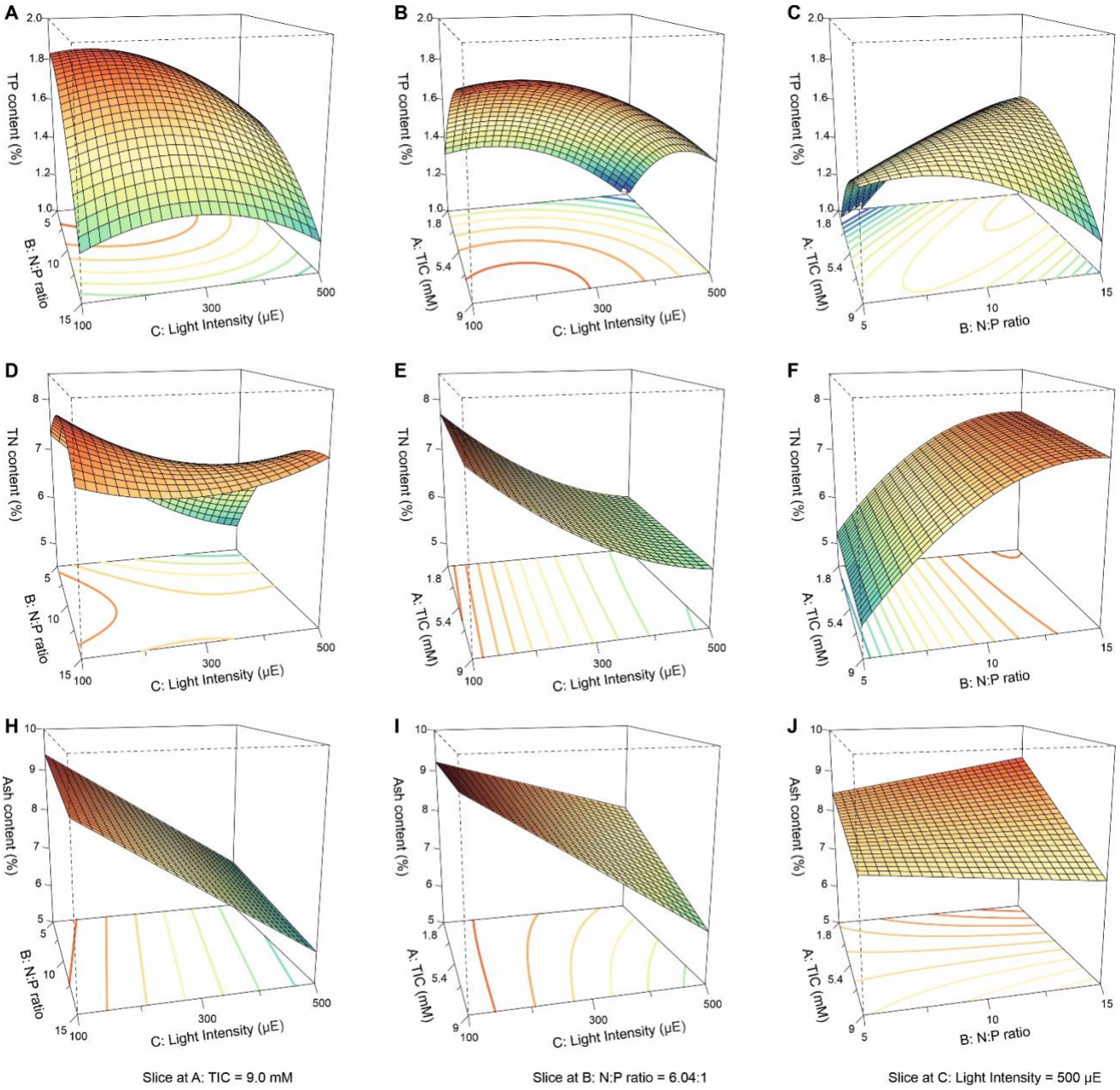

Figure S 3 - 2 3D response surface and contour plots visualizing the interactive effects between TIC concentration, N:P ratio and light intensity for ATS biofilm composition. TP, TN and ash content are shown as a function of N:P ratio vs. light intensity at fixed TIC concentration of 9.0 mM (A, D, H); TIC concentration vs. light intensity at fixed N:P ratio of 6.04:1 (B, E, I); TIC concentration vs. N:P ratio at fixed light intensity of 500 µmol photons m^{-2} s^{-1} (C, F, J), respectively. TIC, Total inorganic carbon; N:P, Nitrogen: Phosphorus ratio; TP, Total phosphorus; TN, Total nitrogen.

Table S 3 - 1Transfer of atmospheric CO_2 into the culture medium by bubbling.

CO_2 concentration	CO_2 volume by bubbling	CO_2 amount	CO_2 molarity
C_{CO2} (ppm)	V_{CO2} (mL) = C ÷ 10^6 × 50 mL min^{-1} × 10080 min	N_C (mmol) = V_{CO2} ÷ 22.4 L mol^{-1}	c_{CO2} (mM) = N_C ÷ 5 L
407.0	205.13	9.16	1.8
1203.5	606.56	27.08	5.4
2000.0	1008.00	45.00	9.0

Table S 3 - 2 BBD experimental data of the independent variables (coded factors) and of the dependent variables (responses). Data are presented in mean ± SE (n = 3). TP, Total phosphorus; TN, Total nitrogen.

Run	Coded factors			Responses					
	A	B	C	TP removal (%)	TN removal (%)	Productivity (g m^{-2} d^{-1})	TP content (%)	TN content (%)	Ash content (%)
1	-1	-1	0	92.5 ± 0.88	96.2 ± 2.38	5.72 ± 0.39	1.09 ± 0.04	6.04 ± 0.21	8.74 ± 0.11
2	1	-1	0	84.0 ± 0.84	100 ± 0	6.49 ± 0.51	1.79 ± 0.01	5.74 ± 0.08	7.63 ± 0.11
3	-1	1	0	98.5 ± 0.81	42.8 ± 2.52	6.09 ± 0.39	1.71 ± 0.13	6.94 ± 0.09	9.45 ± 0.35
4	1	1	0	93.4 ± 1.22	39.8 ± 4.29	6.93 ± 0.48	1.38 ± 0.16	6.90 ± 0.29	7.09 ± 0.85
5	-1	0	-1	94.2 ± 1.08	44.5 ± 2.15	4.14 ± 0.36	1.63 ± 0.05	7.82 ± 0.18	9.25 ± 0.17
6	1	0	-1	86.6 ± 2.24	39.5 ± 4.90	5.56 ± 0.61	1.60 ± 0.03	7.74 ± 0.19	9.36 ± 0.10
7	-1	0	1	98.7 ± 0.28	54.7 ± 5.36	9.02 ± 0.72	1.35 ± 0.08	7.27 ± 0.00	7.98 ± 0.20
8	1	0	1	96.2 ± 2.27	68.1 ± 8.88	11.2 ± 0.46	1.42 ± 0.13	7.01 ± 0.07	6.35 ± 0.19
9	0	-1	-1	73.4 ± 2.34	64.0 ± 4.38	4.18 ± 0.34	1.68 ± 0.25	7.56 ± 0.32	9.11 ± 0.30
10	0	1	-1	86.9 ± 1.16	23.5 ± 3.01	4.49 ± 0.24	1.50 ± 0.10	7.61 ± 0.07	9.13 ± 0.47
11	0	-1	1	99.6 ± 0.37	91.9 ± 1.41	8.92 ± 0.28	1.34 ± 0.08	4.94 ± 0.05	6.59 ± 0.26
12	0	1	1	99.1 ± 0.88	44.2 ± 3.47	10.1 ± 0.48	1.45 ± 0.21	7.44 ± 0.05	6.81 ± 0.30
13	0	0	0	97.9 ± 0.85	49.2 ± 6.46	6.46 ± 0.56	1.71 ± 0.22	6.99 ± 0.18	8.33 ± 1.13
14	0	0	0	96.4 ± 0.73	45.3 ± 2.30	6.73 ± 0.13	1.73 ± 0.12	7.52 ± 0.02	8.15 ± 0.21
15	0	0	0	91.4 ± 2.40	42.7 ± 4.17	6.99 ± 0.82	1.87 ± 0.15	7.10 ± 0.06	8.67 ± 0.09

Table S 3 - 3 Results under high light (1000 µmol photons m^{-2} s^{-1}) and optimized growth conditions of TIC (9 mM) and N:P ratio (6.04, TP 10 mg L^{-1}). Data are presented as mean ± standard error (SE, n = 3). TP, Total phosphorus; TN, Total nitrogen.

Responses	Experimental (mean ± SE)	Independent t-test p^*
TP removal (%)	96.05 ± 1.09	0.496
TN removal (%)	92.75 ± 0.41	0.067
Productivity ($g\ m^{-2}\ d^{-1}$)	10.96 ± 0.35	0.445

Appendix B: supplemental material for Chapter 4

Supplementary data associated with this article can be found, in the online version, at https://www.sciencedirect.com/science/article/abs/pii/S138358662202250X

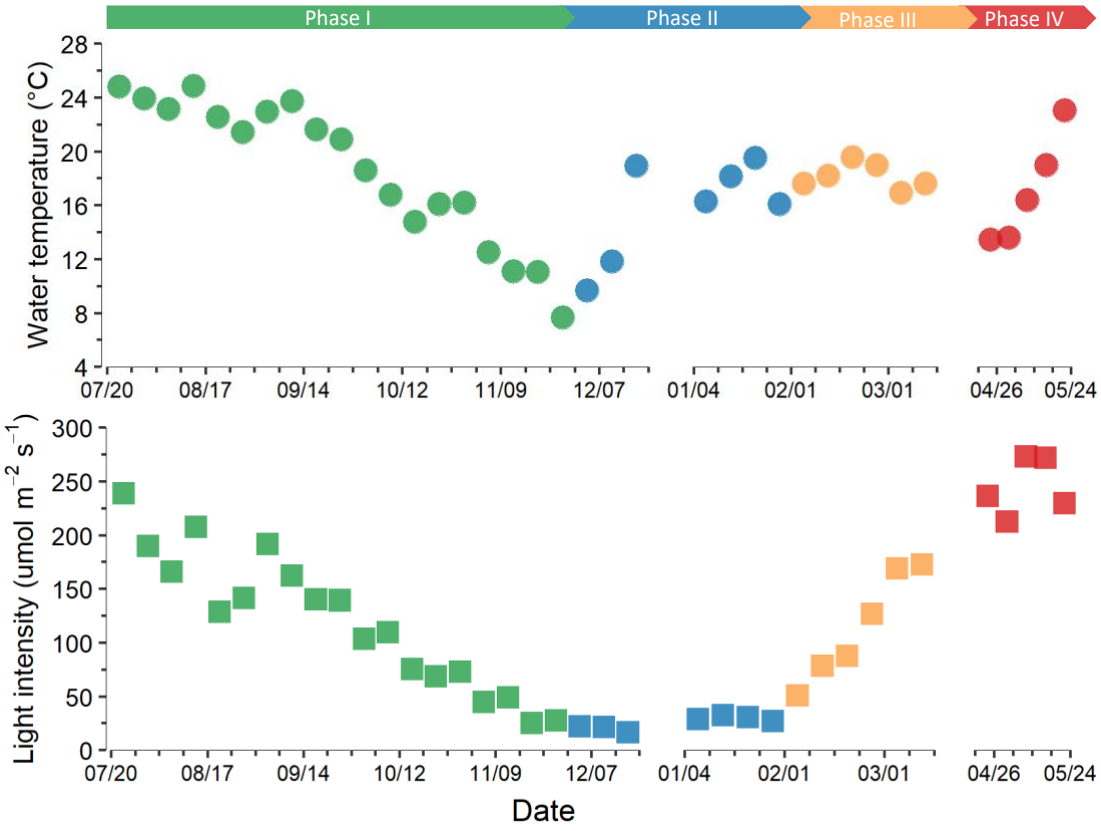

Figure S 4 - 1 The weekly water temperature (top) and light intensity (bottom) in ATS systems over 10 months. Data-gaps indicate times of ATS operation without experiments. Phases: I, natural conditions; II, increased water temperature; III, increased light intensity; IV, decreased water temperature.

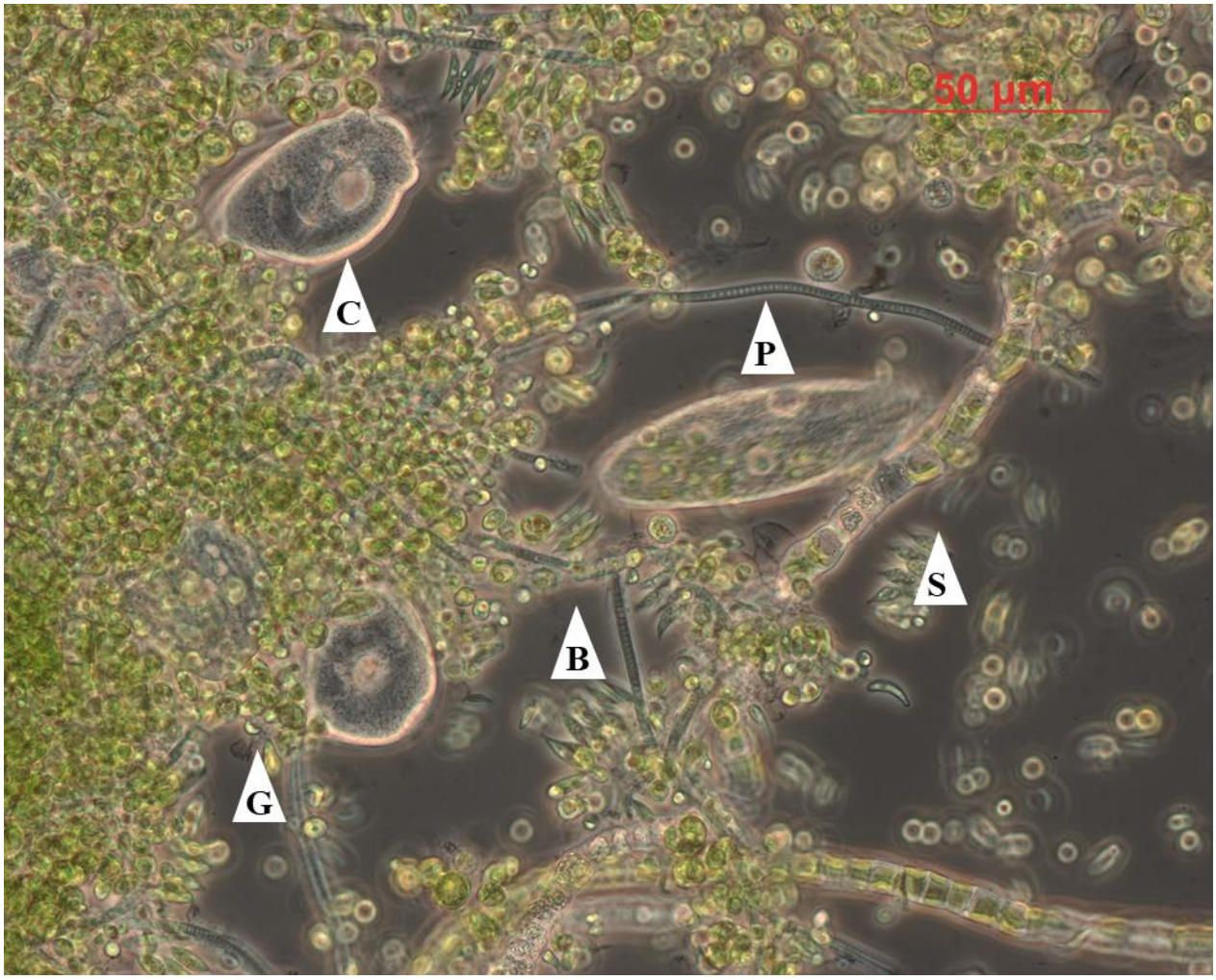

Figure S 4 - 2 Light microscopic image of an ATS biofilm. Sample showes a typical mesocosmic assembly with Scenedesmaceae (arrow S**), filamentous und single-cell green algae (Chlorophyceae) (arrow** G**), Pseudoanabaena sp. (Cyanophyceae) (arrow** P**), Ciliates (Chromista) (arrow** C**), and bacteria (arrow** B**). Scale bar = 50 µm.**

Table S 4 - 1 Statistical regression metrics for the different regression models of TN (A) and TP (B) removal. The selected models are marked in bold. Akaike's Information Criteria (AIC), Bayesian Information Criterion (BIC), Root Mean Squared Error (RMSE), Percentage prediction error (PER), and Adjusted R-squared (Adjusted R^2).

(**A**)

Models for TN removal (%)	AIC	BIC	RMSE	PER	Adjusted R^2	*p*
Linear	256.676	263.010	7.651	15.8%	0.887	< 0.001
2 Factor Interaction	257.592	265.510	7.537	15.8%	0.887	< 0.001
Quadratic	**237.334**	**248.419**	**5.381**	**11.7%**	**0.938**	**< 0.001**
Cubic	239.627	257.046	4.971	11.6%	0.939	< 0.001

(**B**)

Models for TP removal (%)	AIC	BIC	RMSE	PER	Adjusted R^2	*p*
Linear	197.905	204.126	3.647	4.3%	0.798	< 0.001
2 Factor Interaction	183.644	191.421	2.891	3.4%	0.869	< 0.001
Quadratic	**165.954**	**176.841**	**2.121**	**2.6%**	**0.925**	**< 0.001**
Cubic	171.182	188.291	2.039	2.7%	0.919	< 0.001

Table S 4 - 2 Statistical regression metrics of the regression models for biomass productivity and nutrient content. (A) Biomass productivity; (B) Biomass C content; (C) Biomass N content; (D) Biomass P content; (E) Biomass K content. Selected models are marked in bold. Akaike's Information Criteria (AIC), Bayesian Information Criterion (BIC), Root Mean Squared Error (RMSE), Percentage prediction error (PER), and Adjusted R-squared (Adjusted R^2).

(**A**)

Models for biomass productivity (g m^{-2} d^{-1})	AIC	BIC	RMSE	PER	Adjusted R^2	*p*
Linear	96.871	103.205	0.831	14.4%	0.847	< 0.001
2 Factor Interaction	92.197	100.115	0.758	13.3%	0.869	< 0.001
Quadratic	**89.677**	**100.761**	**0.692**	**12.5%**	**0.883**	**< 0.001**
Cubic	89.939	107.357	0.622	12.1%	0.891	< 0.001

(**B**)

Models for biomass C content (%)	AIC	BIC	RMSE	PER	Adjusted R^2	*p*
Linear	155.935	162.379	1.786	5.2%	0.751	< 0.001
2 Factor Interaction	157.334	165.389	1.772	5.2%	0.747	< 0.001
Quadratic	**113.662**	**124.938**	**0.930**	**2.8%**	**0.926**	**< 0.001**
Cubic	120.346	138.066	0.914	3.0%	0.918	< 0.001

(**C**)

Models for biomass N content (%)	AIC	BIC	RMSE	PER	Adjusted R^2	*p*
Linear	58.978	65.312	0.491	9.0%	0.727	< 0.001
2 Factor Interaction	60.951	68.869	0.491	9.2%	0.719	< 0.001
Quadratic	**55.937**	**67.022**	**0.433**	**8.4%**	**0.766**	**< 0.001**
Cubic	60.192	77.611	0.411	8.5%	0.757	< 0.001

(**D**)

Models for biomass P content (%)	AIC	BIC	RMSE	PER	Adjusted R^2	*p*
Linear	-8.893	-2.449	0.193	13.8%	0.760	< 0.001
2 Factor Interaction	-8.000	0.055	0.190	13.8%	0.760	< 0.001
Quadratic	**-23.374**	**-12.098**	**0.146**	**11.0%**	**0.849**	**< 0.001**
Cubic	-21.256	-3.536	0.135	10.9%	0.852	< 0.001

(**E**)

Models for biomass K content (%)	AIC	BIC	RMSE	PER	Adjusted R^2	*p*
Linear	-29.367	0.104	0.146	18.810	0.104	0.058
2 Factor Interaction	-29.745	0.135	0.141	18.489	0.135	0.051
Quadratic	-26.371	0.094	0.140	18.916	0.094	0.153
Cubic	-20.352	0.014	0.137	19.733	0.014	0.423

Appendix C: supplemental material for Chapter 5

Figure S 5 - 1 Preparation of *S. vermifera* solution for seed dipping.

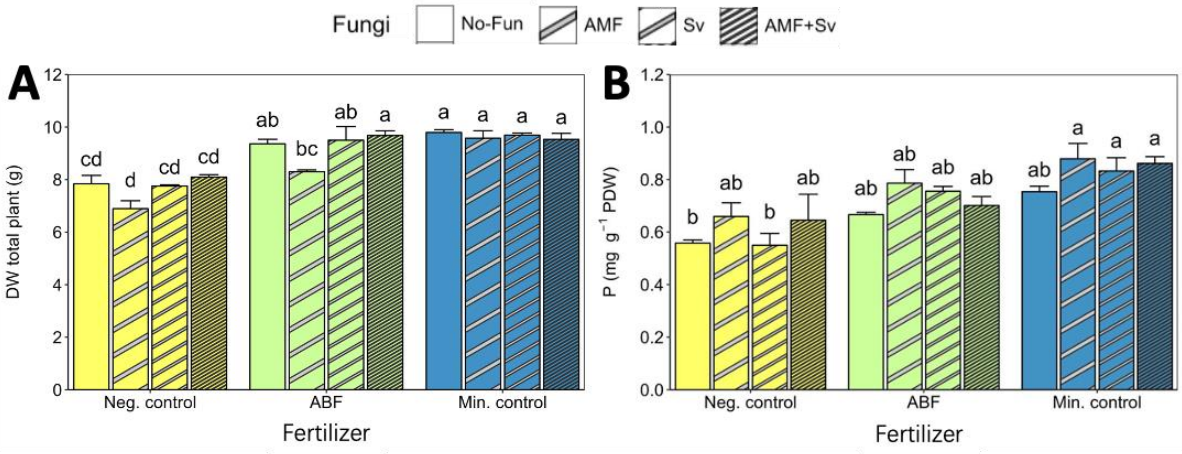

Figure S 5 - 2 Wheat total dry biomass (A), and relative P content (B) of no-P fertilized wheat plants (Neg. control), algal biofilm (ABF) fertilized, and triple-superphosphate (TSP) fertilized plants; non-inoculated (No-Fun), arbuscular mycorrhizal fungi inoculated (AMF), *Sebacina vermifera* inoculated (Sv) and AMF + *S. vermifera* double (AMF+Sv). Wheat was harvested after 6 weeks of growth. (Tukey's HSD test, different letters denote significant differences between treatments at $p < 0.05$, $n = 3$)

Table S 5 - 1 Physical properties and nutritional composition of Null Erde substrate.

	Unit	Sand	Null Erde
Bulk Density (Dry)	$g\ L^{-1}$	1510	266
pH (in $CaCl_2$)		6.94	6
Nitrogen	$mg\ g^{-1}$	<0.10	< 0.01
Phosphorus (P_2O_5)	$mg\ g^{-1}$	<0.05	< 0.01
Potassium (K_2O)	$mg\ g^{-1}$	13.4	< 0.02
Magnesium	$mg\ g^{-1}$	1.02	0.22

Acknowledgements

I extend my heartfelt gratitude to my Doctorvater, Prof. Dr. Wulf Amelung, whose guidance, support, and invaluable advice were instrumental in the completion of this thesis. I am deeply grateful to my main supervisors, Dr. Diana Reinecke-Levi and Dr. Silvia Schrey, for their unwavering support and professional guidance throughout my doctoral studies. Many thanks to them for always taking the time to reflect on my questions and especially for their constant encouragement throughout my research work. I would also like to extend a special thanks to Dr. Holger Klose for his insightful comments during the planning and development of the project, as well as for his invaluable assistance in the preparation and submission of the article. I would also like to thank Dr. Ladislav Nedbal and China Scholarship Council grant for providing me with the opportunity to pursue my PhD in the research program.

I would like to sincerely thank my colleagues at IBG2, including Isabel Muser, Marina Heinen, Marion Roeb, Dagmar Drobietz, Beate Uhlig, Benedict Ohrem, and Andrea Neuwohner, for their generous support in the field, greenhouse, and laboratory and their technical guidance. Special thanks go to Dr. Sara Bauke and Angelika Veits from the University of Bonn for their help with nutrient analyses. In addition, I would like to thank Dr. Gregor Huber for supporting and modifying the statistical analyses.

My heartfelt appreciation to my colleagues at IBG-2 for their invaluable help and friendship during my work: Khadija Boughazi, Dr. Fang He, Jimena Martinez Diaz, Dr. Yuxi Niu, Congcong Zheng, Daniel Klasen, Haiyue Peng and Felix Frimpong. Whether it was in the office, cafeteria or badminton club, I was inspired and uplifted by their conversations and support.

I would also like to extend a special thank you to my lovely husband, Kunpeng Cao, whose unwavering support and encouragement has been a guiding light along the way. I am also deeply grateful to my parents for their upbringing and values that have shaped me. Additionally, I extend my thanks to my sister and other friends for their support and encouragement.

References

Achatz, B., von Rüden, S., Andrade, D., Neumann, E., Pons-Kühnemann, J., Kogel, K.-H., Franken, P., Waller, F.J.P. and soil (2010) Root colonization by Piriformospora indica enhances grain yield in barley under diverse nutrient regimes by accelerating plant development. 333, 59-70.

Acién, F., Fernández, J., Magán, J. and Molina, E. (2012) Production cost of a real microalgae production plant and strategies to reduce it. Biotechnology Advances 30(6), 1344-1353.

Adey, W. and Bannon, J. (2011) Algal Turf Scrubbers: Cleaning Water While Capturing Solar Energy. Algae Biofuel, 215-227.

Adey, W.H., Laughinghouse IV, H.D., Miller, J.B., Hayek, L.A.C., Thompson, J.G., Bertman, S., Hampel, K. and Puvanendran, S. (2013) Algal turf scrubber (ATS) floways on the Great Wicomico River, Chesapeake Bay: productivity, algal community structure, substrate and chemistry. Journal of Phycology 49(3), 489-501.

Adl, S.M. (2003) The ecology of soil decomposition, CABI.

Al Ketife, A.M., Judd, S. and Znad, H. (2017) Optimization of cultivation conditions for combined nutrient removal and CO2 fixation in a batch photobioreactor. Journal of Chemical Technology and Biotechnology 92(5), 1085-1093.

Alobwede, E., Cotton, A., Leake, J.R. and Pandhal, J. (2022) The fate and distribution of microalgal nitrogen when applied as an agricultural soil fertiliser and its effect on soil microbial communities. Phycology 2(3), 297-318.

Amaya-Carpio, L., Davies, F., Fox, T. and He, C. (2009) Arbuscular mycorrhizal fungi and organic fertilizer influence photosynthesis, root phosphatase activity, nutrition, and growth of Ipomoea carnea ssp. fistulosa. Photosynthetica 47, 1-10.

Antia, N., Harrison, P. and Oliveira, L. (1991) The role of dissolved organic nitrogen in phytoplankton nutrition, cell biology and ecology. Phycologia 30(1), 1-89.

Arhonditsis, G.B., Winder, M., Brett, M.T. and Schindler, D.E. (2004) Patterns and mechanisms of phytoplankton variability in Lake Washington (USA). Water Research 38(18), 4013-4027.

Association, A.P.H. (1998) Standard methods for the examination of water and wastewater, American Public Health Association, Washington, D.C.

Aston, J.E., Wahlen, B.D., Davis, R.W., Siccardi, A.J. and Wendt, L.M. (2018) Application of aqueous alkaline extraction to remove ash from algae harvested from an algal turf scrubber. Algal Research-Biomass Biofuels and Bioproducts 35, 370-377.

Banaś, A.K., Aggarwal, C., Łabuz, J., Sztatelman, O. and Gabryś, H. (2012) Blue light signalling in chloroplast movements. Journal of Experimental Botany 63(4), 1559-1574.

Bargaz, A., Lyamlouli, K., Chtouki, M., Zeroual, Y. and Dhiba, D. (2018) Soil microbial resources for improving fertilizers efficiency in an integrated plant nutrient management system. Frontiers in microbiology 9, 1606.

Barquet, K., Järnberg, L., Rosemarin, A. and Macura, B. (2020) Identifying barriers and opportunities for a circular phosphorus economy in the Baltic Sea region. Water Research 171, 115433.

Barsanti, L. and Gualtieri, P. (2005) Algae: anatomy, biochemistry, and biotechnology, CRC press.

Bellinger, E.G. and Sigee, D.C. (2015) Freshwater algae: identification, enumeration and use as bioindicators, John Wiley & Sons.

Bender, S.J., Parker, M.S. and Armbrust, E.V. (2012) Coupled Effects of Light and Nitrogen Source on the Urea Cycle and Nitrogen Metabolism over a Diel Cycle in the Marine Diatom Thalassiosira pseudonana. Protist 163(2), 232-251.

Bhandari, R. and Sharma, P.K. Effect of UV-B and high visual radiation on photosynthesis in freshwater (nostoc spongiaeforme) and marine (Phormidium corium) cyanobacteria. (0301-1208 (Print)).

Bidyarani, N., Prasanna, R., Babu, S., Hossain, F. and Saxena, A.K. (2016) Enhancement of plant growth and yields in Chickpea (Cicer arietinum L.) through novel cyanobacterial and biofilmed inoculants. Microbiological Research 188, 97-105.

Bitton, G. (2005) Wastewater microbiology, John Wiley & Sons.

Blersch, D.M., Kangas, P.C. and Mulbry, W.W. (2013) Turbulence and nutrient interactions that control benthic algal production in an engineered cultivation raceway. Algal Research 2(2), 107-112.

BMUV, G.F.M.f.t.E., Nature Conservation, Nuclear Safety and Consumer Protection Sewage Treatment Plant.

Boelee, N., Janssen, M., Temmink, H., Taparavičiūtė, L., Khiewwijit, R., Jánoska, Á., Buisman, C. and Wijffels, R. (2014) The effect of harvesting on biomass production and nutrient removal in phototrophic biofilm reactors for effluent polishing. Journal of Applied Phycology 26, 1439-1452.

Boelee, N., Temmink, H., Janssen, M., Buisman, C. and Wijffels, R. (2011) Nitrogen and phosphorus removal from municipal wastewater effluent using microalgal biofilms. Water Research 45(18), 5925-5933.

Buchanan, N.A., Young, P., Cromar, N.J. and Fallowfield, H. (2018) Performance of a high rate algal pond treating septic tank effluent from a community wastewater management scheme in rural South Australia. Algal Research 35, 325-332.

Cai, T., Park, S.Y. and Li, Y. (2013) Nutrient recovery from wastewater streams by microalgae: status and prospects. Renewable and Sustainable Energy Reviews 19, 360-369.

Campenni, L., Nobre, B.P., Santos, C.A., Oliveira, A.C., Aires-Barros, M.R., Palavra, A.M. and Gouveia, L. (2013) Carotenoid and lipid production by the autotrophic

microalga Chlorella protothecoides under nutritional, salinity, and luminosity stress conditions. Appl Microbiol Biotechnol 97(3), 1383-1393.

Cao, J., Yuan, W., Pei, Z., Davis, T., Cui, Y. and Beltran, M. (2009) A preliminary study of the effect of surface texture on algae cell attachment for a mechanical-biological energy manufacturing system. Journal of Manufacturing Science Engineering and Mining Journal 131(6).

Chacón‐Lee, T. and González‐Mariño, G.E. (2010) Microalgae for "healthy" foods—possibilities and challenges. Comprehensive reviews in food science and food safety 9(6), 655-675.

Chae, K.-J. and Kang, J. (2013) Estimating the energy independence of a municipal wastewater treatment plant incorporating green energy resources. Energy Conversion Management 75, 664-672.

Chaiwong, C., Koottatep, T. and Polprasert, C. (2021) Development of kinetic models for organic and nutrient removal in biofilm photobioreactor for treatment of domestic wastewater. Environmental Technology & Innovation 23, 101547.

Chamizo, S., Mugnai, G., Rossi, F., Certini, G. and De Philippis, R. (2018) Cyanobacteria inoculation improves soil stability and fertility on different textured soils: gaining insights for applicability in soil restoration. Frontiers in Environmental Science 6, 49.

Chan, N.-I., Rittmann, B.E. and Elser, J. (2021) Suitability of an algal biofuel species, Scenedesmus acutus, as a fertilizer for growth of conventional and genetically modified lettuce. HortScience 56(5), 589-594.

Cheenakula, D., Hoffstadt, K., Krafft, S., Reinecke, D., Klose, H., Kuperjans, I. and Grömping, M. (2022) Anaerobic digestion of algal–bacterial biomass of an Algal Turf Scrubber system. Biomass Conversion and Biorefinery.

Chen, C.-Y., Zhao, X.-Q., Yen, H.-W., Ho, S.-H., Cheng, C.-L., Lee, D.-J., Bai, F.-W. and Chang, J.-S. (2013) Microalgae-based carbohydrates for biofuel production. Biochemical Engineering Journal 78, 1-10.

Chen, G.-Q. and Chen, F. (2006) Growing phototrophic cells without light. Biotechnology Letters 28, 607-616.

Chen, J.-H. (2006) The combined use of chemical and organic fertilizers and/or biofertilizer for crop growth and soil fertility, pp. 1-11, Citeseer.

Chen, N., Li, J., Wu, Y., Kangas, P.C., Huang, B., Yu, C. and Chen, Z. (2015) Nutrient removal at a drinking water reservoir in China with an algal floway. Ecological Engineering 84, 506-514.

Chi, Z., O'Fallon, J.V. and Chen, S. (2011) Bicarbonate produced from carbon capture for algae culture. Trends in Biotechnology 29(11), 537-541.

Chia, S.R., Ong, H.C., Chew, K.W., Show, P.L., Phang, S.-M., Ling, T.C., Nagarajan, D., Lee, D.-J. and Chang, J.-S. (2018) Sustainable approaches for algae utilisation in bioenergy production. Renewable Energy 129, 838-852.

Christenson, L. and Sims, R. (2011) Production and harvesting of microalgae for wastewater treatment, biofuels, and bioproducts. Biotechnology Advances 29(6), 686-702.

Christenson, L.B. and Sims, R.C. (2012) Rotating algal biofilm reactor and spool harvester for wastewater treatment with biofuels by ‐ products. Biotechnology bioengineering 109(7), 1674-1684.

Colla, L.M., Reinehr, C.O., Reichert, C. and Costa, J.A.V. (2007) Production of biomass and nutraceutical compounds by Spirulina platensis under different temperature and nitrogen regimes. Bioresource Technology 98(7), 1489-1493.

Condron, L., Frossard, E., Tiessen, H., Newmans, R. and Stewart, J. (1990) Chemical nature of organic phosphorus in cultivated and uncultivated soils under different environmental conditions. Journal of Soil Science 41(1), 41-50.

Conley, D.J., Paerl, H.W., Howarth, R.W., Boesch, D.F., Seitzinger, S.P., Havens, K.E., Lancelot, C. and Likens, G.E. (2009) Controlling eutrophication: nitrogen and phosphorus, American Association for the Advancement of Science.

Coppens, J., Grunert, O., Van Den Hende, S., Vanhoutte, I., Boon, N., Haesaert, G. and De Gelder, L. (2016a) The use of microalgae as a high-value organic slow-release fertilizer results in tomatoes with increased carotenoid and sugar levels. Journal of Applied Phycology 28(4), 2367-2377.

Coppens, J., Grunert, O., Van Den Hende, S., Vanhoutte, I., Boon, N., Haesaert, G. and De Gelder, L. (2016b) The use of microalgae as a high-value organic slow-release fertilizer results in tomatoes with increased carotenoid and sugar levels. Journal of Applied Phycology 28, 2367-2377.

Cordell, D., Drangert, J.-O. and White, S. (2009) The story of phosphorus: global food security and food for thought. Global Environmental Change 19(2), 292-305.

Craggs, R. (2001) Wastewater treatment by algal turf scrubbing. Water Science Technology 44(11-12), 427-433.

Craggs, R., Park, J., Heubeck, S. and Sutherland, D. (2014) High rate algal pond systems for low-energy wastewater treatment, nutrient recovery and energy production. New Zealand Journal of Botany 52(1), 60-73.

Craggs, R., Sutherland, D. and Campbell, H. (2012) Hectare-scale demonstration of high rate algal ponds for enhanced wastewater treatment and biofuel production. Journal of Applied Phycology 24, 329-337.

Craggs, R.J., Adey, W.H., Jenson, K.R., StJohn, M.S., Green, F.B. and Oswald, W.J. (1996) Phosphorus removal from wastewater using an algal turf scrubber. Water Science and Technology 33(7), 191-198.

Czaczyk, K. and Myszka, K. (2007) Biosynthesis of extracellular polymeric substances (EPS) and its role in microbial biofilm formation. Polish Journal of Environmental Studies 16(6), 799.

D'Aiuto, P.E., Patt, J.M., Albano, J.P., Shatters, R.G. and Evens, T.J. (2015) Algal turf scrubbers: Periphyton production and nutrient recovery on a South Florida citrus farm. Ecological Engineering 75, 404-412.

Daud, N.M., Abdullah, S.R.S., Abu Hasan, H. and Yaakob, Z. (2015) Production of biodiesel and its wastewater treatment technologies: A review. Process Safety and Environmental Protection 94, 487-508.

De-Bashan, L.E. and Bashan, Y. (2004) Recent advances in removing phosphorus from wastewater and its future use as fertilizer (1997–2003). Water Research 38(19), 4222-4246.

De-Bashan, L.E. and Bashan, Y. (2010) Immobilized microalgae for removing pollutants: review of practical aspects. Bioresource Technology 101(6), 1611-1627.

De Vree, J.H., Bosma, R., Janssen, M., Barbosa, M.J. and Wijffels, R.H. (2015) Comparison of four outdoor pilot-scale photobioreactors. Biotechnology for biofuels 8, 1-12.

Demirbas, A. (2010) Use of algae as biofuel sources. Energy Conversion and Management 51(12), 2738-2749.

Dhar, D.W., Prasanna, R., Pabbi, S. and Vishwakarma, R. (2015) Significance of cyanobacteria as inoculants in agriculture.

Dodds, W.K. and Smith, V.H. (2016) Nitrogen, phosphorus, and eutrophication in streams. Inland Waters 6(2), 155-164.

Dolatabadi, H.K., Goltapeh, E.M., Jaimand, K., Rohani, N. and Varma, A. (2011) Effects of Piriformospora indica and Sebacina vermifera on growth and yield of essential oil in fennel (Foeniculum vulgare) under greenhouse conditions. Journal of Basic Microbiology 51(1), 33-39.

Dombinov, V., Herzel, H., Müller, F., Willbold, S., Zang, J.W., da Fonseca-Zang, W.A., Klose, H., Poorter, H., Jablonowski, N.D. and Schrey, S.D. (2022) Sugarcane bagasse ash as fertilizer for soybeans: Effects of added residues on ash composition, mineralogy, phosphorus extractability and plant availability. Frontiers in plant science 13, 1041924.

Donnert, D. and Salecker, M. (1999) Elimination of phosphorus from waste water by crystallization. Environmental Technology 20(7), 735-742.

Dyhrman, S.T. (2016) Nutrients and their acquisition: phosphorus physiology in microalgae. The physiology of microalgae, 155-183.

Ekschmitt, K., Liu, M., Vetter, S., Fox, O. and Wolters, V. (2005) Strategies used by soil biota to overcome soil organic matter stability—why is dead organic matter left over in the soil? Geoderma 128(1-2), 167-176.

Enzing, C., Ploeg, M., Barbosa, M. and Sijtsma, L. (2014) Microalgae-based products for the food and feed sector: an outlook for Europe. JRC Scientific policy reports, 19-37.

EPA (2004) Primer for municipal wastewater treatment systems, Office of Water, Washington DC 20460.

Etesami, H., Jeong, B.R. and Glick, B.R. (2021) Contribution of arbuscular mycorrhizal fungi, phosphate–solubilizing bacteria, and silicon to P uptake by plant. Frontiers in plant science 12, 699618.

Feng, W., Li, C., Zhang, C., Liu, S., Song, F., Guo, W., He, Z., Li, T. and Chen, H. (2019) Characterization of phosphorus in algae from a eutrophic lake by solution 31 P nuclear magnetic resonance spectroscopy. Limnology 20, 163-171.

Feng, W., Zhu, Y., Wu, F., Meng, W., Giesy, J.P., He, Z., Song, L. and Fan, M. (2016) Characterization of phosphorus forms in lake macrophytes and algae by solution 31 P nuclear magnetic resonance spectroscopy. Environmental Science and Pollution Research 23, 7288-7297.

Ferreira, S.C., Bruns, R., Ferreira, H., Matos, G., David, J., Brandão, G., da Silva, E.P., Portugal, L., Dos Reis, P. and Souza, A. (2007) Box-Behnken design: an alternative for the optimization of analytical methods. Analytica Chimica Acta 597(2), 179-186.

Foo, S.C., Yusoff, F.M., Ismail, M., Basri, M., Yau, S.K., Khong, N.M., Chan, K.W. and Ebrahimi, M. (2017) Antioxidant capacities of fucoxanthin-producing algae as influenced by their carotenoid and phenolic contents. Journal of Biotechnology 241, 175-183.

Foyer, C.H., Neukermans, J., Queval, G., Noctor, G. and Harbinson, J. (2012) Photosynthetic control of electron transport and the regulation of gene expression. Journal of Experimental Botany 63(4), 1637-1661.

Gan, X., Klose, H. and Reinecke, D. (2022) Optimizing nutrient removal and biomass production of Algal Turf Scrubber (ATS) under variable cultivation conditions by using Response Surface Methodology. Frontiers in Bioengineering and Biotechnology, 1265.

Gan, X., Klose, H. and Reinecke, D. (2023) Stable year-round nutrients removal and recovery from wastewater by technical-scale algal Turf Scrubber (ATS). Separation Purification Technology 307, 122693.

Gan, X., Shen, G., Xin, B. and Li, M. (2016) Simultaneous biological desalination and lipid production by Scenedesmus obliquus cultured with brackish water. Desalination 400, 1-6.

Gao, K., Orr, V. and Rehmann, L. (2016) Butanol fermentation from microalgae-derived carbohydrates after ionic liquid extraction. Bioresource Technology 206, 77-85.

Garcia, J., Mujeriego, R. and Hernandez-Marine, M. (2000) High rate algal pond operating strategies for urban wastewater nitrogen removal. Journal of Applied Phycology 12, 331-339.

Gaterell, M., Gay, R., Wilson, R., Gochin, R. and Lester, J. (2000) An economic and environmental evaluation of the opportunities for substituting phosphorus recovered from wastewater treatment works in existing UK fertiliser markets. Environmental Technology 21(9), 1067-1084.

Gerdemann, J. (1968) Vesicular-arbuscular mycorrhiza and plant growth. Annual review of phytopathology 6(1), 397-418.

Ghimire, S.R. and Craven, K.D. (2011) Enhancement of switchgrass (Panicum virgatum L.) biomass production under drought conditions by the ectomycorrhizal

fungus Sebacina vermifera. Applied and Environmental Microbiology 77(19), 7063-7067.

Giles, C., Cade-Menun, B. and Hill, J. (2011) The inositol phosphates in soils and manures: abundance, cycling, and measurement. Canadian Journal of Soil Science 91(3), 397-416.

Gill, S.S., Gill, R., Anjum, N.A., Sharma, K.K., Johri, A.K. and Tuteja, N. (2016) Piriformospora indica: potential and significance in plant stress tolerance. Frontiers in microbiology 7, 184779.

Gladyshev, M.I., Sushchik, N.N. and Makhutova, O.N. (2013) Production of EPA and DHA in aquatic ecosystems and their transfer to the land. Prostaglandins & Other Lipid Mediators 107, 117-126.

Gosling, P., Hodge, A., Goodlass, G. and Bending, G. (2006) Arbuscular mycorrhizal fungi and organic farming. Agriculture, Ecosystems & Environment 113(1-4), 17-35.

Goswami, R., Agrawal, K., Shah, M. and Verma, P. (2022) Bioremediation of heavy metals from wastewater: a current perspective on microalgae‐based future. Letters in Applied Microbiology 75(4), 701-717.

Grady Jr, C.L., Daigger, G.T., Love, N.G. and Filipe, C.D. (2011) Biological wastewater treatment, CRC press.

Gray, N.F. (2004) Biology of wastewater treatment, World Scientific.

Gray, N.F. (2021) Natural Wastewater Treatment Systems and Sustainability, World Scientific.

Gross, M. and Wen, Z. (2014) Yearlong evaluation of performance and durability of a pilot-scale Revolving Algal Biofilm (RAB) cultivation system. Bioresource Technology 171, 50-58.

Grzesik, M., Romanowska-Duda, Z. and Kalaji, H.J.P. (2017) Effectiveness of cyanobacteria and green algae in enhancing the photosynthetic performance and growth of willow (Salix viminalis L.) plants under limited synthetic fertilizers application. 55, 510-521.

Gärtner, G., Stoyneva-Gärtner, M. and Uzunov, B. (2021) Algal toxic compounds and their aeroterrestrial, airborne and other extremophilic producers with attention to soil and plant contamination: A review. Toxins 13(5), 322.

Hallasgo, A.M., Spangl, B., Steinkellner, S. and Hage-Ahmed, K. (2020) The fungal endophyte Serendipita williamsii does not affect phosphorus status but carbon and nitrogen dynamics in arbuscular mycorrhizal tomato plants. Journal of Fungi 6(4), 233.

Han, S.H., An, J.Y., Hwang, J., Kim, S.B. and Park, B.B. (2016) The effects of organic manure and chemical fertilizer on the growth and nutrient concentrations of yellow poplar (Liriodendron tulipifera Lin.) in a nursery system. Forest science and technology 12(3), 137-143.

Hayman, D. and Mosse, B. (1972) PLANT GROWTH RESPONSES TO VESICULAR - ARBUSCULAR MYCORRHIZA III. INCREASED UPTAKE OF LABILE P FROM SOIL. New Phytologist 71(1), 41-47.

He, W.-X., Wu, Q.-S., Hashem, A., Abd_Allah, E.F., Muthuramalingam, P., Al-Arjani, A.-B.F. and Zou, Y.-N. (2022) Effects of symbiotic fungi on sugars and soil fertility and structure-mediated changes in plant growth of Vicia villosa. Agriculture 12(10), 1523.

He, Z., Olk, D.C. and Cade-Menun, B.J. (2011) Forms and lability of phosphorus in humic acid fractions of Hord silt loam soil. Soil Science Society of America Journal 75(5), 1712-1722.

Heidarianpour, M.B., Aliasgharzad, N. and Olsson, P.A. (2020) Positive effects of co-inoculation with Rhizophagus irregularis and Serendipita indica on tomato growth under saline conditions, and their individual colonization estimated by signature lipids. Mycorrhiza 30(4), 455-466.

Henrard, A., De Morais, M. and Costa, J.A.V. (2011) Vertical tubular photobioreactor for semicontinuous culture of Cyanobium sp. Bioresource Technology 102(7), 4897-4900.

Higgins, B.T. (2011) Life-cycle Environmental and Cost Impacts of Using an Algal Turf Scrubber for Wastewater Treatment and Electricity Generation. Dissertations & Theses - Gradworks 16(3), 436–447.

Higgins, B.T. and Kendall, A. (2011) Life-cycle Environmental and Cost Impacts of Using an Algal Turf Scrubber for Wastewater Treatment. Journal of Industrial Ecology 16(3), 436-447.

Ho, S.-H., Huang, S.-W., Chen, C.-Y., Hasunuma, T., Kondo, A. and Chang, J.-S. (2013) Bioethanol production using carbohydrate-rich microalgae biomass as feedstock. Bioresource Technology 135, 191-198.

Hom-Diaz, A., Jaén-Gil, A., Bello-Laserna, I., Rodríguez-Mozaz, S., Vicent, T., Barceló, D. and Blánquez, P. (2017) Performance of a microalgal photobioreactor treating toilet wastewater: pharmaceutically active compound removal and biomass harvesting. Science of the Total Environment 592, 1-11.

Huang, J., Ying, J., Fan, F., Yang, Q., Wang, J. and Li, Y. (2016) Development of a novel multi-column airlift photobioreactor with easy scalability by means of computational fluid dynamics simulations and experiments. Bioresource Technology 222, 399-407.

Hukari, S., Hermann, L. and Nättorp, A. (2016) From wastewater to fertilisers—Technical overview and critical review of European legislation governing phosphorus recycling. Science of the Total Environment 542, 1127-1135.

IPCC (2007) Mitigation of Climate Change: Contribution of Working Group III to the Fourth Assessment Report of the Intergovernmental Panel on Climate Change. 52.

Irving, T.E. and Allen, D.G. (2011) Species and material considerations in the formation and development of microalgal biofilms. Applied microbiology biotechnology 92, 283-294.

ISO (2004) Water Quality–Determination of Phosphorus–Ammonium Molybdate Spectrometric Method.

Issarapayup, K., Powtongsook, S. and Pavasant, P. (2011) Economical review of Haematococcus pluvialis culture in flat-panel airlift photobioreactors. Aquacultural Engineering 44(3), 65-71.

Jansa, J., Finlay, R., Wallander, H., Smith, F.A. and Smith, S.E. (2011) Role of mycorrhizal symbioses in phosphorus cycling. Phosphorus in action: biological processes in soil phosphorus cycling, 137-168.

Jung, E.E., Jain, A., Voulis, N., Doud, D.F., Angenent, L.T. and Erickson, D. (2014) Stacked optical waveguide photobioreactor for high density algal cultures. Bioresource Technology 171, 495-499.

Kangas, P. and Mulbry, W. (2014) Nutrient removal from agricultural drainage water using algal turf scrubbers and solar power. Bioresource Technology 152, 484-489.

Kangas, P., Mulbry, W., Klavon, P., Laughinghouse, H.D. and Adey, W. (2017) High diversity within the periphyton community of an algal turf scrubber on the Susquehanna River. Ecological Engineering 108, 564-572.

Karimi, Z., Laughinghouse, H.D., Davis, V.A. and Blersch, D.M. (2021) Substrate properties as controlling parameters in attached algal cultivation. Applied microbiology biotechnology 105, 1823-1835.

Kebede-westhead, E., Pizarro, C., Mulbry, W.W. and Wilkie, A.C. (2003) Production and Nutrient Removal by Periphyton Grown Under Different Loading Rates of Anaerobically Digested Flushed Dairy Manure. Journal of Phycology 39(6), 1275-1282.

Kebede‐westhead, E., Pizarro, C., Mulbry, W.W. and Wilkie, A.C. (2003) Production and nutrient removal by periphyton grown under different loading rates of anaerobically digested flushed dairy manure 1. Journal of Phycology 39(6), 1275-1282.

Kesaano, M. and Sims, R.C. (2014) Algal biofilm based technology for wastewater treatment. Algal Research 5, 231-240.

Khan, S.A., Sharma, G.K., Malla, F.A., Kumar, A. and Gupta, N. (2019) Microalgae based biofertilizers: a biorefinery approach to phycoremediate wastewater and harvest biodiesel and manure. Journal of Cleaner Production 211, 1412-1419.

Kovač, D.J., Simeunović, J.B., Babić, O.B., Mišan, A.Č. and Milovanović, I.L. (2013) Algae in food and feed. Food Feed Research 40(1), 21-32-21-32.

Kube, M., Spedding, B., Gao, L., Fan, L. and Roddick, F. (2020) Nutrient removal by alginate‐immobilized Chlorella vulgaris: response to different wastewater matrices. Journal of Chemical Technology Biotechnology 95(6), 1790-1799.

Lee, E., Pruvost, J., He, X., Munipalli, R. and Pilon, L. (2014) Design tool and guidelines for outdoor photobioreactors. Chemical Engineering Science 106, 18-29.

Leong, Y.K., Huang, C.-Y. and Chang, J.-S. (2021) Pollution prevention and waste phycoremediation by algal-based wastewater treatment technologies: The applications

of high-rate algal ponds (HRAPs) and algal turf scrubber (ATS). Journal of Environmental Management 296, 113193.

Li, C.-h., Wang, Y.-k., Ye, C., Wei, W.-w., Zheng, B.-h. and Xu, B. (2019a) A proposed delineation method for lake buffer zones in watersheds dominated by non-point source pollution. Science of the Total Environment 660, 32-39.

Li, H., Smith, S.E., Holloway, R.E., Zhu, Y. and Smith, F.A. (2006) Arbuscular mycorrhizal fungi contribute to phosphorus uptake by wheat grown in a phosphorus - fixing soil even in the absence of positive growth responses. New Phytologist 172(3), 536-543.

Li, H., Zhao, Q. and Huang, H. (2019b) Current states and challenges of salt-affected soil remediation by cyanobacteria. Science of the Total Environment 669, 258-272.

Li, H., Zhu, Y., Marschner, P., Smith, F. and Smith, S. (2005) Wheat responses to arbuscular mycorrhizal fungi in a highly calcareous soil differ from those of clover, and change with plant development and P supply. Plant and Soil 277, 221-232.

Li, K., Liu, Q., Fang, F., Luo, R., Lu, Q., Zhou, W., Huo, S., Cheng, P., Liu, J. and Addy, M. (2019c) Microalgae-based wastewater treatment for nutrients recovery: A review. Bioresource Technology 291, 121934.

Li, M., Zamyadi, A., Zhang, W., Dumée, L.F. and Gao, L. (2022) Algae-based water treatment: A promising and sustainable approach. Journal of Water Process Engineering 46, 102630.

Li, Y.Q., Horsman, M., Wu, N., Lan, C.Q., Duboiscalero, N., Bhatnagar, S.K., Saxena, A. and Kraan, S. (2008) Biofuels from microalgae. Biotechnol Prog 24(4), 815-820.

Lindblad, P., Fuente, D., Borbe, F., Cicchi, B., Conejero, J.A., Couto, N., Čelešnik, H., Diano, M.M., Dolinar, M. and Esposito, S. (2019) CyanoFactory, a European consortium to develop technologies needed to advance cyanobacteria as chassis for production of chemicals and fuels. Algal Research 41, 101510.

Liu, J. and Vyverman, W. (2015) Differences in nutrient uptake capacity of the benthic filamentous algae Cladophora sp., Klebsormidium sp. and Pseudanabaena sp. under varying N/P conditions. Bioresource Technology 179, 234-242.

Liu, J.Z., Danneels, B., Vanormelingen, P. and Vyverman, W. (2016) Nutrient removal from horticultural wastewater by benthic filamentous algae Klebsormidium sp., Stigeoclonium spp. and their communities: From laboratory flask to outdoor Algal Turf Scrubber (ATS). Water Research 92, 61-68.

López-Rosales, L., García-Camacho, F., Sánchez-Mirón, A., Beato, E.M., Chisti, Y. and Grima, E.M. (2016) Pilot-scale bubble column photobioreactor culture of a marine dinoflagellate microalga illuminated with light emission diodes. Bioresource Technology 216, 845-855.

Lu, Q. and Xiao, Y. (2022) From manure to high-value fertilizer: The employment of microalgae as a nutrient carrier for sustainable agriculture. Algal Research 67, 102855.

Mackay, J., Macdonald, L., Smernik, R. and Cavagnaro, T. (2017) Organic amendments as phosphorus fertilisers: Chemical analyses, biological processes and plant P uptake. Soil Biology Biochemistry 107, 50-59.

Maity, J.P., Bundschuh, J., Chen, C.-Y. and Bhattacharya, P. (2014) Microalgae for third generation biofuel production, mitigation of greenhouse gas emissions and wastewater treatment: Present and future perspectives–A mini review. Energy 78, 104-113.

Makarov, M., Haumaier, L. and Zech, W. (2002) The nature and origins of diester phosphates in soils: a 31 P-NMR study. Biology and Fertility of Soils 35, 136-146.

Mallick, N. (2002) Biotechnological potential of immobilized algae for wastewater N, P and metal removal: a review. BioMetals 15, 377-390.

Mantzorou, A., Navakoudis, E., Paschalidis, K. and Ververidis, F. (2018) Microalgae: a potential tool for remediating aquatic environments from toxic metals. International Journal of Environmental Science Technology 15, 1815-1830.

Marella, T.K., Datta, A., Patil, M.D., Dixit, S. and Tiwari, A. (2019) Biodiesel production through algal cultivation in urban wastewater using algal floway. Bioresource Technology 280, 222-228.

Marín, D., Posadas, E., Cano, P., Pérez, V., Blanco, S., Lebrero, R. and Muñoz, R. (2018) Seasonal variation of biogas upgrading coupled with digestate treatment in an outdoors pilot scale algal-bacterial photobioreactor. Bioresource Technology 263, 58-66.

Martin, F.M. and van Der Heijden, M.G. (2024) The mycorrhizal symbiosis: research frontiers in genomics, ecology, and agricultural application. New Phytologist.

Masojídek, J. and Torzillo, G. (2008), pp. 2226-2235.

Mau, L., Junker, S., Bochmann, H., Mihiret, Y.E., Kelm, J.M., Schrey, S.D., Roessner, U., Schaaf, G., Watt, M. and Kant, J. (2022) Root growth and architecture of wheat and brachypodium vary in response to algal fertilizer in soil and solution. Agronomy 12(2), 285.

Mau, L., Kant, J., Walker, R., Kuchendorf, C.M., Schrey, S.D., Roessner, U. and Watt, M. (2021) Wheat can access phosphorus from algal biomass as quickly and continuously as from mineral fertilizer. Frontiers in plant science 12, 631314.

McGonigle, T.P., Miller, M.H., Evans, D., Fairchild, G. and Swan, J.A. (1990) A new method which gives an objective measure of colonization of roots by vesicular—arbuscular mycorrhizal fungi. New Phytologist 115(3), 495-501.

Meena, R.S., Vijayakumar, V., Yadav, G.S. and Mitran, T. (2018) Response and interaction of Bradyrhizobium japonicum and arbuscular mycorrhizal fungi in the soybean rhizosphere. Plant Growth Regulation 84, 207-223.

Mendes, M.C., Navalho, S., Ferreira, A., Paulino, C., Figueiredo, D., Silva, D., Gao, F., Gama, F., Bombo, G. and Jacinto, R. (2022) Algae as food in Europe: An overview of species diversity and their application. Foods 11(13), 1871.

Missong, A., Bol, R., Willbold, S., Siemens, J. and Klumpp, E. (2016) Phosphorus forms in forest soil colloids as revealed by liquid‐state 31P‐NMR. Journal of Plant Nutrition and Soil Science 179(2), 159-167.

Mohsenpour, S.F., Hennige, S., Willoughby, N., Adeloye, A. and Gutierrez, T. (2021) Integrating micro-algae into wastewater treatment: A review. Science of the Total Environment 752, 142168.

Molinuevo-Salces, B., García-González, M.C. and González-Fernández, C. (2010) Performance comparison of two photobioreactors configurations (open and closed to the atmosphere) treating anaerobically degraded swine slurry. Bioresource Technology 101(14), 5144-5149.

Moody, J.W., McGinty, C.M. and Quinn, J.C. (2014) Global evaluation of biofuel potential from microalgae. Proceedings of the National Academy of Sciences 111(23), 8691-8696.

Moreno-Garrido, I. (2008) Microalgae immobilization: current techniques and uses. Bioresource Technology 99(10), 3949-3964.

Moseley, J. and Grossman, A.R. (2009) The Chlamydomonas Sourcebook (Second Edition). Stern, D.B. and Witman, G.B. (eds), pp. 189-215, Academic Press, London.

Mulbry, W., Kondrad, S., Pizarro, C. and Kebede-Westhead, E. (2008) Treatment of dairy manure effluent using freshwater algae: Algal productivity and recovery of manure nutrients using pilot-scale algal turf scrubbers. Bioresource Technology 99(17), 8137-8142.

Mulbry, W.W. and Wilkie, A.C. (2001) Growth of benthic freshwater algae on dairy manures. Journal of Applied Phycology 13(4), 301-306.

Munoz, R. (2005) Algal-bacterial photobioreactors for the degradation of toxic organic pollutants, Lund University.

Mussatto, S.I., Dragone, G., Guimarães, P.M., Silva, J.P.A., Carneiro, L.M., Roberto, I.C., Vicente, A., Domingues, L. and Teixeira, J.A. (2010) Technological trends, global market, and challenges of bio-ethanol production. Biotechnology advances 28(6), 817-830.

Naidoo, S. and Olaniran, A.O. (2014) Treated wastewater effluent as a source of microbial pollution of surface water resources. International journal of environmental research public health 11(1), 249-270.

Nkebiwe, P.M., Weinmann, M., Bar-Tal, A. and Müller, T. (2016) Fertilizer placement to improve crop nutrient acquisition and yield: a review and meta-analysis. Field Crops Research 196, 389-401.

Norambuena, F., Hermon, K., Skrzypczyk, V., Emery, J.A., Sharon, Y., Beard, A. and Turchini, G.M. (2015) Algae in fish feed: performances and fatty acid metabolism in juvenile Atlantic salmon. PloS one 10(4), e0124042.

Nurdogan, Y. and Oswald, W. (1995) Enhanced nutrient removal in high-rate ponds. Water Science and Technology 31(12), 33-43.

Nurfadilah, S., Swarts, N.D., Dixon, K.W., Lambers, H. and Merritt, D.J. (2013) Variation in nutrient-acquisition patterns by mycorrhizal fungi of rare and common orchids explains diversification in a global biodiversity hotspot. Annals of Botany 111(6), 1233-1241.

Oberwinkler, F., Riess, K., Bauer, R., Selosse, M.-A., Weiß, M., Garnica, S. and Zuccaro, A. (2013) Enigmatic sebacinales. Mycological Progress 12, 1-27.

Oswald, W.J. and Gotaas, H.B. (1957) Photosynthesis in sewage treatment. Transactions of the American Society of Civil Engineers 122(1), 73-97.

Oyetunji, O., Bolan, N. and Hancock, G. (2022) A comprehensive review on enhancing nutrient use efficiency and productivity of broadacre (arable) crops with the combined utilization of compost and fertilizers. Journal of Environmental Management 317, 115395.

Ozkan, A. and Berberoglu, H. (2011) Adhesion of Chlorella vulgaris on hydrophilic and hydrophobic surfaces, pp. 169-178.

Ozkan, A., Kinney, K., Katz, L. and Berberoglu, H. (2012) Reduction of water and energy requirement of algae cultivation using an algae biofilm photobioreactor. Bioresource Technology 114, 542-548.

Pandey, A., Gupta, A., Sunny, A., Kumar, S. and Srivastava, S. (2020a) Multi-objective optimization of media components for improved algae biomass, fatty acid and starch biosynthesis from Scenedesmus sp. ASK22 using desirability function approach. Renewable Energy 150, 476-486.

Pandey, A., Srivastava, S. and Kumar, S. (2020b) Development and cost-benefit analysis of a novel process for biofuel production from microalgae using pre-treated high-strength fresh cheese whey wastewater. Environmental Science and Pollution Research 27(19), 23963-23980.

Park, D.M., Reed, D.W., Yung, M.C., Eslamimanesh, A., Lencka, M.M., Anderko, A., Fujita, Y., Riman, R.E., Navrotsky, A. and Jiao, Y. (2016) Bioadsorption of rare earth elements through cell surface display of lanthanide binding tags. Environmental science technology 50(5), 2735-2742.

Park, J., Craggs, R. and Shilton, A. (2011a) Recycling algae to improve species control and harvest efficiency from a high rate algal pond. Water Research 45(20), 6637-6649.

Park, J., Craggs, R. and Shilton, A. (2011b) Wastewater treatment high rate algal ponds for biofuel production. Bioresource Technology 102(1), 35-42.

Park, J.B.K., Montemezzani, V., Picken, C., Rendle, D. and Craggs, R.J. (2022) Effect of algal contact time and horizontal water velocity on the performance of Filamentous Algal Nutrient Scrubbers (FANS). Journal of Environmental Management 312, 114882.

Peirce, C., Smernik, R. and McBeath, T. (2013) Phosphorus availability in chicken manure is lower with increased stockpiling period, despite a larger orthophosphate content. Plant and Soil 373, 359-372.

Penn, C.J. and Camberato, J.J. (2019) A critical review on soil chemical processes that control how soil pH affects phosphorus availability to plants. Agriculture 9(6), 120.

Perez-Garcia, O., Escalante, F.M., De-Bashan, L.E. and Bashan, Y. (2011) Heterotrophic cultures of microalgae: metabolism and potential products. Water Research 45(1), 11-36.

Pfandl, K., Chatzinotas, A., Dyal, P. and Boenigk, J. (2009) SSU rRNA gene variation resolves population heterogeneity and ecophysiological differentiation within a morphospecies (Stramenopiles, Chrysophyceae). Limnology Oceanography 54(1), 171-181.

Pirdashti, H., Yaghoubian, Y., Goltapeh, E. and Hosseini, S. (2012) Effect of mycorrhiza-like endophyte (Sebacina vermifera) on growth, yield and nutrition of rice (Oryza sativa L.) under salt stress.

Pittman, J.K., Dean, A.P. and Osundeko, O. (2011) The potential of sustainable algal biofuel production using wastewater resources. Bioresource Technology 102(1), 17-25.

Pizarro, C., Mulbry, W., Blersch, D. and Kangas, P. (2006) An economic assessment of algal turf scrubber technology for treatment of dairy manure effluent. Ecological Engineering 26(4), 321-327.

Plappally, A. (2012) Energy requirements for water production, treatment, end use, reclamation, and disposal. Renewable sustainable energy reviews 16(7), 4818-4848.

Posadas, E., Muñoz, A., García‐González, M.C., Muñoz, R. and García‐Encina, P.A. (2015) A case study of a pilot high rate algal pond for the treatment of fish farm and domestic wastewaters. Journal of Chemical Technology and Biotechnology 90(6), 1094-1101.

Powell, N., Shilton, A., Chisti, Y. and Pratt, S. (2009) Towards a luxury uptake process via microalgae–defining the polyphosphate dynamics. Water Research 43(17), 4207-4213.

Priyadarshani, I. and Rath, B. (2012) Commercial and industrial applications of micro algae–A review. Journal of Algal Biomass Utilization 3(4), 89-100.

Qin, B. (2009) Lake eutrophication: control countermeasures and recycling exploitation. Ecological Engineering 35(11), 1569-1573.

Radakovits, R., Jinkerson, R.E., Darzins, A. and Posewitz, M.C. (2010) Genetic engineering of algae for enhanced biofuel production. Eukaryotic Cell 9(4), 486-501.

Ramya, S.S., Vijayanand, N. and Rathinavel, S. (2015) Foliar application of liquid biofertilizer of brown alga Stoechospermum marginatum on growth, biochemical and yield of Solanum melongena. International Journal of Recycling of Organic Waste in Agriculture 4, 167-173.

Raven, J.A., Cockell, C.S. and De La Rocha, C.L. (2008) The evolution of inorganic carbon concentrating mechanisms in photosynthesis. Philosophical Transactions of the Royal Society B: Biological Sciences 363(1504), 2641-2650.

Ray, N.E., Terlizzi, D.E. and Kangas, P.C. (2015) Nitrogen and phosphorus removal by the Algal Turf Scrubber at an oyster aquaculture facility. Ecological Engineering 78, 27-32.

Ray, P., Abraham, P.E., Guo, Y., Giannone, R.J., Engle, N.L., Yang, Z.K., Jacobson, D., Hettich, R.L., Tschaplinski, T.J. and Craven, K.D. (2019) Scavenging organic nitrogen and remodelling lipid metabolism are key survival strategies adopted by the endophytic fungi, Serendipita vermifera and Serendipita bescii to alleviate nitrogen and phosphorous starvation in vitro. Environmental microbiology reports 11(4), 548-557.

Ray, P. and Craven, K.D. (2016) Sebacina vermifera: a unique root symbiont with vast agronomic potential. World Journal of Microbiology Biotechnology 32, 1-10.

Reinecke, D., Bischoff, L.-S., Klassen, V., Blifernez-Klassen, O., Grimm, P., Kruse, O., Klose, H. and Schurr, U. (2022) Nutrient recovery from wastewaters by algal biofilm for fertilizer production Part 1: Case study on the techno-economical aspects at pilot-scale. Separation and Purification Technology, 122471.

Reinecke, D., Bischoff, L.-S., Klassen, V., Blifernez-Klassen, O., Grimm, P., Kruse, O., Klose, H. and Schurr, U. (2023) Nutrient recovery from wastewaters by algal biofilm for fertilizer production part 1: Case study on the techno-economical aspects at pilot-scale. Separation and Purification Technology 305, 122471.

Richardson, A.E., Lynch, J.P., Ryan, P.R., Delhaize, E., Smith, F.A., Smith, S.E., Harvey, P.R., Ryan, M.H., Veneklaas, E.J. and Lambers, H. (2011) Plant and microbial strategies to improve the phosphorus efficiency of agriculture. Plant and Soil 349, 121-156.

Richardson, J.W., Johnson, M.D. and Outlaw, J.L. (2012) Economic comparison of open pond raceways to photo bio-reactors for profitable production of algae for transportation fuels in the Southwest. Algal Research 1(1), 93-100.

Roy, E.D., Richards, P.D., Martinelli, L.A., Coletta, L.D., Lins, S.R.M., Vazquez, F.F., Willig, E., Spera, S.A., VanWey, L.K. and Porder, S. (2016) The phosphorus cost of agricultural intensification in the tropics. Nature plants 2(5), 1-6.

Salama, E.-S., Roh, H.-S., Dev, S., Khan, M.A., Abou-Shanab, R.A., Chang, S.W. and Jeon, B.-H. (2019) Algae as a green technology for heavy metals removal from various wastewater. World Journal of Microbiology Biotechnology 35, 1-19.

Sandefur, H.N., Matlock, M.D. and Costello, T.A. (2011) Seasonal productivity of a periphytic algal community for biofuel feedstock generation and nutrient treatment. Ecological Engineering 37(10), 1476-1480.

Santos, S.R., Silva, E.d.B., Alleoni, L.R.F. and Grazziotti, P.H. (2017) Citric acid influence on soil phosphorus availability. Journal of Plant Nutrition 40(15), 2138-2145.

Sañudo-Wilhelmy, S.A., Tovar-Sanchez, A., Fu, F.-X., Capone, D.G., Carpenter, E.J. and Hutchins, D.A. (2004) The impact of surface-adsorbed phosphorus on phytoplankton Redfield stoichiometry. Nature 432(7019), 897-901.

Sanz-Luque, E., Chamizo-Ampudia, A., Llamas, A., Galvan, A. and Fernandez, E. (2015) Understanding nitrate assimilation and its regulation in microalgae. Frontiers in Plant Science 6, 899.

Sarkar, D., Rovenich, H., Jeena, G., Nizam, S., Tissier, A., Balcke, G.U., Mahdi, L.K., Bonkowski, M., Langen, G. and Zuccaro, A. (2019) The inconspicuous gatekeeper: endophytic Serendipita vermifera acts as extended plant protection barrier in the rhizosphere. New Phytologist 224(2), 886-901.

Schnurr, P.J. and Allen, D.G. (2015) Factors affecting algae biofilm growth and lipid production: A review. Renewable and Sustainable Energy Reviews 52, 418-429.

Schreiber, C., Behrendt, D., Huber, G., Pfaff, C., Widzgowski, J., Ackermann, B., Müller, A., Zachleder, V., Moudříková, Š. and Mojzeš, P. (2017) Growth of algal biomass in laboratory and in large-scale algal photobioreactors in the temperate climate of western Germany. Bioresource Technology 234, 140-149.

Schreiber, C., Schiedung, H., Harrison, L., Briese, C., Ackermann, B., Kant, J., Schrey, S.D., Hofmann, D., Singh, D. and Ebenhöh, O. (2018) Evaluating potential of green alga Chlorella vulgaris to accumulate phosphorus and to fertilize nutrient-poor soil substrates for crop plants. Journal of Applied Phycology 30(5), 2827-2836.

Selosse, M.A., Setaro, S., Glatard, F., Richard, F., Urcelay, C. and Weiß, M. (2007) Sebacinales are common mycorrhizal associates of Ericaceae. New Phytologist 174(4), 864-878.

Shen, Y., Xu, X., Zhao, Y. and Lin, X. (2014) Influence of algae species, substrata and culture conditions on attached microalgal culture. Bioprocess Biosystems Engineering 37(3), 441-450.

Shi, J., Podola, B. and Melkonian, M. (2007) Removal of nitrogen and phosphorus from wastewater using microalgae immobilized on twin layers: an experimental study. Journal of Applied Phycology 19(5), 417-423.

Shi, J., Wang, X. and Wang, E. (2023) Mycorrhizal symbiosis in plant growth and stress adaptation: From genes to ecosystems. Annual Review of Plant Biology 74, 569-607.

Siebers, N., Hofmann, D., Schiedung, H., Landsrath, A., Ackermann, B., Gao, L., Mojzeš, P., Jablonowski, N.D., Nedbal, L. and Amelung, W. (2019) Towards phosphorus recycling for agriculture by algae: Soil incubation and rhizotron studies using 33P-labeled microalgal biomass. Algal Research 43, 101634.

Sindelar, H.R., Yap, J.N., Boyer, T.H. and Brown, M.T. (2015) Algae scrubbers for phosphorus removal in impaired waters. Ecological Engineering 85, 144-158.

Singh, A., Nigam, P.S. and Murphy, J.D. (2011) Renewable fuels from algae: an answer to debatable land based fuels. Bioresource Technology 102(1), 10-16.

Singh, S., Shrivastava, A. and Singh, V. (2014) Arsenic and cadmium are inhibitors of cyanobacterial dinitrogenase reductase (nifH1) gene. Functional integrative genomics 14, 571-580.

Singh, S. and Singh, P. (2015) Effect of temperature and light on the growth of algae species: A review. Renewable sustainable energy reviews 50, 431-444.

Slegers, P., Van Beveren, P., Wijffels, R., Van Straten, G. and Van Boxtel, A. (2013) Scenario analysis of large scale algae production in tubular photobioreactors. Applied energy 105, 395-406.

Smil, V. (2000) Phosphorus in the environment: natural flows and human interferences. Annual review of energy the environment 25(1), 53-88.

Smith, I.L., Stanton, T. and Law, A. (2021) Plastic habitats: Algal biofilms on photic and aphotic plastics. Journal of Hazardous Materials Letters 2, 100038.

Smith, S.E. and Read, D.J. (2010) Mycorrhizal symbiosis, Academic press.

Stanier, R., Kunisawa, R., Mandel, M. and Cohen-Bazire, G. (1971) Purification and properties of unicellular blue-green algae (order Chroococcales). Bacteriological Reviews 35(2), 171-205.

Stiefvatter, L., Neumann, U., Rings, A., Frick, K., Schmid-Staiger, U. and Bischoff, S.C. (2022) The microalgae Phaeodactylum tricornutum is well suited as a food with positive effects on the intestinal microbiota and the generation of SCFA: Results from a pre-clinical study. Nutrients 14(12), 2504.

Su, Y. (2020) Revisiting carbon, nitrogen, and phosphorus metabolisms in microalgae for wastewater treatment. Science of the Total Environment, 144590.

Su, Y., Mennerich, A. and Urban, B. (2011) Municipal wastewater treatment and biomass accumulation with a wastewater-born and settleable algal-bacterial culture. Water Research 45(11), 3351-3358.

Sukačová, K., Trtílek, M. and Rataj, T. (2015) Phosphorus removal using a microalgal biofilm in a new biofilm photobioreactor for tertiary wastewater treatment. Water Research 71, 55-63.

Suleiman, A.K.A., Lourenço, K.S., Clark, C., Luz, R.L., da Silva, G.H.R., Vet, L.E., Cantarella, H., Fernandes, T.V. and Kuramae, E.E. (2020) From toilet to agriculture: Fertilization with microalgal biomass from wastewater impacts the soil and rhizosphere active microbiomes, greenhouse gas emissions and plant growth. Resources, Conservation and Recycling 161, 104924.

Sun, R., Guo, X., Wang, D. and Chu, H. (2015) Effects of long-term application of chemical and organic fertilizers on the abundance of microbial communities involved in the nitrogen cycle. Applied Soil Ecology 95, 171-178.

Sun, Y., Chen, Z., Wu, G., Wu, Q., Zhang, F., Niu, Z. and Hu, H.-Y. (2016) Characteristics of water quality of municipal wastewater treatment plants in China: implications for resources utilization and management. Journal of Cleaner Production 131, 1-9.

Sutherland, D.L., Burke, J. and Ralph, P.J. (2020) Flow-way water depth affects algal productivity and nutrient uptake in a filamentous algae nutrient scrubber. Journal of Applied Phycology 32(6), 4321-4332.

Sutton, C. and Larsen, S.J.S.S. (1964) Pyrophosphate as a source of phosphorus for plants. 97(3), 196-201.

Talling, J. (2010) Potassium—a non-limiting nutrient in fresh waters? Freshwater reviews 3(2), 97-104.

Tchobanoglus, G., Burton, F. and Stensel, H.D. (2003) Wastewater engineering: treatment and reuse.

Thapa, S., Bharti, A. and Prasanna, R. (2017) Algal green chemistry, pp. 285-303, Elsevier.

Tomitani, A., Knoll, A.H., Cavanaugh, C.M. and Ohno, T. (2006) The evolutionary diversification of cyanobacteria: molecular–phylogenetic and paleontological perspectives. Proceedings of the National Academy of Sciences 103(14), 5442-5447.

Turner, B.L., Cade-Menun, B.J., Condron, L.M. and Newman, S. (2005) Extraction of soil organic phosphorus. Talanta 66(2), 294-306.

Tyagi, J., Mishra, A., Kumari, S., Singh, S., Agarwal, H., Pudake, R.N., Varma, A. and Joshi, N.C. (2023) Deploying a microbial consortium of Serendipita indica, Rhizophagus intraradices, and Azotobacter chroococcum to boost drought tolerance in maize. Environmental Experimental Botany 206, 105142.

Uduman, N., Qi, Y., Danquah, M.K., Forde, G.M. and Hoadley, A. (2010) Dewatering of microalgal cultures: a major bottleneck to algae-based fuels. Journal of renewable sustainable energy 2(1), 012701.

Valeta, J. and Verdegem, M. (2015) Removal of nitrogen by Algal Turf Scrubber Technology in recirculating aquaculture system. Aquaculture Research 46(4), 945-951.

Varma, A., Bakshi, M., Lou, B., Hartmann, A. and Oelmueller, R. (2012) Piriformospora indica: a novel plant growth-promoting mycorrhizal fungus. Agricultural Research 1, 117-131.

Venable, M.E. and Podbielski, M.R. (2019) Impact of substrate material on algal biofilm biomass growth. Environmental Science Pollution Research 26, 7256-7262.

Verbruggen, E., Rillig, M.C., Wehner, J., Hegglin, D., Wittwer, R. and van der Heijden, M.G. (2014) Sebacinales, but not total root associated fungal communities, are affected by land-use intensity. New Phytologist 203(4), 1036-1040.

Vierheilig, H., Coughlan, A.P., Wyss, U. and Piché, Y. (1998) Ink and vinegar, a simple staining technique for arbuscular-mycorrhizal fungi. Applied and Environmental Microbiology 64(12), 5004-5007.

Vo, H.N.P., Ngo, H.H., Guo, W., Nguyen, T.M.H., Liu, Y., Liu, Y., Nguyen, D.D. and Chang, S.W. (2019) A critical review on designs and applications of microalgae-based photobioreactors for pollutants treatment. Science of the Total Environment 651, 1549-1568.

Vymazal, J. (2011) Constructed wetlands for wastewater treatment: five decades of experience. Environmental science technology 45(1), 61-69.

Walter, M., Shannon, K., Carolina, P. and Elizabeth, K.W. (2008) Treatment of dairy manure effluent using freshwater algae: algal productivity and recovery of manure

nutrients using pilot-scale algal turf scrubbers. Bioresource Technology 99(17), 8137-8142.

Wan, J., Gu, J., Zhao, Q. and Liu, Y. (2016) COD capture: a feasible option towards energy self-sufficient domestic wastewater treatment. Scientific reports 6(1), 1-9.

Wang, H.-M.D., Chen, C.-C., Huynh, P. and Chang, J.-S. (2015) Exploring the potential of using algae in cosmetics. Bioresource Technology 184, 355-362.

Wang, H., He, P., Shen, C. and Wu, Z. (2019a) Effect of irrigation amount and fertilization on agriculture non-point source pollution in the paddy field. Environmental Science Pollution Research 26, 10363-10373.

Wang, J.-H., Zhuang, L.-L., Xu, X.-Q., Deantes-Espinosa, V.M., Wang, X.-X. and Hu, H.-Y. (2018a) Microalgal attachment and attached systems for biomass production and wastewater treatment. Renewable sustainable energy reviews 92, 331-342.

Wang, L., Amelung, W. and Willbold, S. (2021) 18O isotope labeling combined with 31P nuclear magnetic resonance spectroscopy for accurate quantification of hydrolyzable phosphorus species in environmental samples. Analytical Chemistry 93(4), 2018-2025.

Wang, M., Keeley, R., Zalivina, N., Halfhide, T., Scott, K., Zhang, Q., van der Steen, P. and Ergas, S.J. (2018b) Advances in algal-prokaryotic wastewater treatment: A review of nitrogen transformations, reactor configurations and molecular tools. Journal of Environmental Management 217, 845-857.

Wang, X., Fan, X., Chang, W., Li, K., Zhang, M., Ping, Y. and Song, F. (2023) Combining the advantages of Rhizophagus intraradices and Serendipita indica to reduce the risk of Cd on soybean safety and environmental pollution. Rhizosphere 25, 100669.

Wang, Y. and Lambers, H. (2020) Root-released organic anions in response to low phosphorus availability: recent progress, challenges and future perspectives. Plant and Soil 447, 135-156.

Wang, Z., Gui, H., Luo, Z., Zhen, Z., Yan, C. and Xing, B. (2019b) Dissolved organic phosphorus enhances arsenate bioaccumulation and biotransformation in Microcystis aeruginosa. Environmental Pollution 252, 1755-1763.

Webster, N. (1981) Webster's third new international dictionary of the English language, unabridged, Merriam-Webster.

Wegahita, N.K., Ma, L., Liu, J., Huang, T., Luo, Q. and Qian, J. (2020) Spatial Assessment of Groundwater Quality and Health Risk of Nitrogen Pollution for Shallow Groundwater Aquifer around Fuyang City, China. China Water 12(12), 3341.

Wei, J., Gao, L., Shen, G., Yang, X. and Li, M. (2020) The role of adsorption in microalgae biological desalination: salt removal from brackish water using Scenedesmus obliquus. Desalination 493, 114616.

Weiß, M., Waller, F., Zuccaro, A. and Selosse, M.A. (2016) Sebacinales–one thousand and one interactions with land plants. New Phytologist 211(1), 20-40.

Wells, M.L., Potin, P., Craigie, J.S., Raven, J.A., Merchant, S.S., Helliwell, K.E., Smith, A.G., Camire, M.E. and Brawley, S.H. (2017) Algae as nutritional and functional food sources: revisiting our understanding. Journal of Applied Phycology 29, 949-982.

Wicker, R.J., Kwon, E., Khan, E., Kumar, V. and Bhatnagar, A. (2023) The potential of mixed-species biofilms to address remaining challenges for economically-feasible microalgal biorefineries: A review. Chemical Engineering Journal 451, 138481.

Wilkie, A.C. and Mulbry, W.W. (2002) Recovery of dairy manure nutrients by benthic freshwater algae. Bioresource Technology 84(1), 81-91.

Witzenberger, A. and Hack, H. (1989) Erlaeuterungen zum BBCH-Dezimal-Code fuer die Entwicklungsstadien des Getreides-mit Abbildungen. Gesunde Pflanzen 41.

Xia, Y., Zhang, M., Tsang, D.C., Geng, N., Lu, D., Zhu, L., Igalavithana, A.D., Dissanayake, P.D., Rinklebe, J. and Yang, X. (2020) Recent advances in control technologies for non-point source pollution with nitrogen and phosphorous from agricultural runoff: current practices and future prospects. Applied Biological Chemistry 63(1), 1-13.

Xiao, R. and Zheng, Y. (2016) Overview of microalgal extracellular polymeric substances (EPS) and their applications. Biotechnology Advances 34(7), 1225-1244.

Xie, H., Li, J., Zhu, P., Peng, C., Wang, J., He, H. and Zhang, X. (2014) Long-term manure amendments enhance neutral sugar accumulation in bulk soil and particulate organic matter in a Mollisol. Soil Biology and Biochemistry 78, 45-53.

Xie, Y., Zhao, X., Chen, J., Yang, X., Ho, S.-H., Wang, B., Chang, J.-S. and Shen, Y. (2017) Enhancing cell growth and lutein productivity of Desmodesmus sp. F51 by optimal utilization of inorganic carbon sources and ammonium salt. Bioresource Technology 244, 664-671.

Xin, L., Hong-Ying, H., Ke, G. and Ying-Xue, S. (2010) Effects of different nitrogen and phosphorus concentrations on the growth, nutrient uptake, and lipid accumulation of a freshwater microalga Scenedesmus sp. Bioresource Technology 101(14), 5494-5500.

Xu, M., Bernards, M. and Hu, Z. (2014) Algae-facilitated chemical phosphorus removal during high-density Chlorella emersonii cultivation in a membrane bioreactor. Bioresource Technology 153, 383-387.

Ye, Y., Ngo, H.H., Guo, W., Chang, S.W., Nguyen, D.D., Zhang, X., Zhang, J. and Liang, S.J.B.t.r. (2020) Nutrient recovery from wastewater: From technology to economy. 11, 100425.

Zang, C., Huang, S., Wu, M., Du, S., Scholz, M., Gao, F., Lin, C., Guo, Y. and Dong, Y. (2011) Comparison of relationships between pH, dissolved oxygen and chlorophyll a for aquaculture and non-aquaculture waters. Water, Air and Soil Pollution 219(1), 157-174.

Zhang, L., Fan, J., Ding, X., He, X., Zhang, F. and Feng, G. (2014) Hyphosphere interactions between an arbuscular mycorrhizal fungus and a phosphate solubilizing bacterium promote phytate mineralization in soil. Soil Biology and Biochemistry 74, 177-183.

Zhang, Y., Duan, P., Zhang, P. and Li, M. (2018) Variations in cyanobacterial and algal communities and soil characteristics under biocrust development under similar environmental conditions. Plant and Soil 429, 241-251.

Zhou, Y., Kiely, P.D., Kibbee, R. and Ormeci, B. (2021) Effect of polymeric support material on biofilm development, bacterial population, and wastewater treatment performance in anaerobic fixed-film systems. Chemosphere 264, 128477.

Zhou, Y., Nguyen, B.T., Zhou, C., Straka, L., Lai, Y.S., Xia, S. and Rittmann, B.E. (2017) The distribution of phosphorus and its transformations during batch growth of Synechocystis. Water Research 122, 355-362.

Zhu, C., Ji, Y., Du, X., Kong, F., Chi, Z. and Zhao, Y. (2022) A smart and precise mixing strategy for efficient and cost-effective microalgae production in open ponds. Science of the Total Environment 852, 158515.

Zhu, C., Xi, Y., Zhai, X., Wang, J., Kong, F. and Chi, Z. (2021) Pilot outdoor cultivation of an extreme alkalihalophilic Trebouxiophyte in a floating photobioreactor using bicarbonate as carbon source. Journal of Cleaner Production 283, 124648.

Zhu, C., Zhai, X., Xi, Y., Wang, J., Kong, F., Zhao, Y. and Chi, Z. (2019) Progress on the development of floating photobioreactor for microalgae cultivation and its application potential. World Journal of Microbiology Biotechnology 35(12), 1-10.

Zorofchian Moghadamtousi, S., Karimian, H., Khanabdali, R., Razavi, M., Firoozinia, M., Zandi, K. and Abdul Kadir, H. (2014) Anticancer and antitumor potential of fucoidan and fucoxanthin, two main metabolites isolated from brown algae. The Scientific World Journal 2014.

Zou, Y., Zeng, Q., Li, H., Liu, H. and Lu, Q. (2021) Emerging technologies of algae‐based wastewater remediation for bio‐fertilizer production: a promising pathway to sustainable agriculture. Journal of Chemical Technology & Biotechnology 96(3), 551-563.